

ANALYSIS OF VASCULAR RESPONSE TO SYSTEMIC HEATING USING THE  
PALLID BAT WING

A Thesis

by

TANYA MENDEZ

Submitted to the Office of Graduate Studies of  
Texas A&M University  
in partial fulfillment of the requirements for the degree of

MASTER OF SCIENCE

December 2007

Major Subject: Mechanical Engineering

ANALYSIS OF VASCULAR RESPONSE TO SYSTEMIC HEATING USING THE  
PALLID BAT WING

A Thesis

by

TANYA MENDEZ

Submitted to the Office of Graduate Studies of  
Texas A&M University  
in partial fulfillment of the requirements for the degree of  
MASTER OF SCIENCE

Approved by:

Chair of Committee, Obdulia Ley  
Committee Members, N.K. Anand  
Christopher Quick

Head of Department, Dennis O'Neal

December 2007

Major Subject: Mechanical Engineering

## ABSTRACT

Analysis of Vascular Response to Systemic Heating Using the Pallid Bat Wing.

(December 2007)

Tanya Mendez, B.S., University of California, Davis

Chair of Advisory Committee: Dr. Obdulia Ley

The objective of this research is to analyze the relationship between environmental heat exchange and vascular response in the pallid bat wing during systemic heating and to develop a simplified model of heat transfer for theoretical analysis. During heating experiments, metabolic activity, body temperature and alterations in vessel diameter and blood flow were monitored. This research is very significant, as it will correlate thermoregulation and vascular response in a way that has not been studied before.

The wing of the pallid bat is selected because the microvascular bed performs similar functions as that of the human skin in terms of thermoregulation; understanding vascular response to heat or cold allows to analyze vascular function, or arterial health, a response that is altered at early stages of several diseases in humans. At high body temperatures, bats can dissipate heat through their wings; the bat wing serves as a *thermal window* where heat exchange is determined by local blood flow and vascular response in the wing.

For this study, a lumped mathematical model to calculate body and skin temperature alterations in response to changes in environmental conditions has been developed. In order to formulate this model, experiments have been proposed where the pallid bat is subjected to dynamic systemic heating with and without the wing extended. By having the wing extended outside a metabolic chamber during heating, the bats were able to maintain an equilibrated body temperature; having the wing en-

closed caused body temperature to increase rapidly. The experiments were designed to obtain correlations between systemic and vascular responses and therefore learn about the thermoregulatory mechanisms of the pallid bat.

Results from experiments following Animal Use Protocols 2006-253 and 2007-110 indicate that vascular responses to environmental temperature changes (changes in  $T_{chamber}$ ) maintain or reduce body temperature to basal conditions. Vessel diameter, centerline velocity, blood flow and heat flux increase with  $T_{chamber}$  therefore delivering a greater volume of blood to the bat wing and increasing heat exchange with the environment. The positive responses in the wing to  $T_{chamber}$  signify that the pallid bat is regulating its body temperature as had been expected.



To my loving parents: Salvador Juan and Maria Trinidad Mendez

## ACKNOWLEDGMENTS

There are many people that have been involved in this research that I would like to show my appreciation to. First of all, I would like to thank Melissa F. Young for handling the bats during the experiments and being open-minded about our research. Thanks to Dr. Vincent Gresham for all the veterinary support. Thank you to Dr. Christopher Quick for allowing us to use his lab and resources for our research. I need to thank Alex and Karl Gephart who began to create the first prototype for the metabolic chamber; and Julia Buck, Michael Goffredo, Brittney Mott, Kelly Lazo, Paul Guevarra and Toni Lafferty for assisting in the collection of data and results presented in this research.

Most importantly I would like to thank my advisor, Dr. Obdulia Ley, for her patience and understanding throughout these last two years and for giving me free rein in this research and therefore allowing me to grow to my utmost potential. For that, I am extremely grateful.

## TABLE OF CONTENTS

CHAPTER		Page
I	INTRODUCTION . . . . .	1
	A. Summary of Research and Objectives . . . . .	1
II	THERMOREGULATION . . . . .	4
	A. General Concepts on Thermoregulation . . . . .	4
	B. Diseases That Affect Thermoregulation . . . . .	6
	C. Environmental Energy Exchange . . . . .	8
	D. Effects of Cutaneous Blood Flow on Heat Exchange . . . . .	11
	E. Thermal Windows and Their Effect on Thermoregulation . . . . .	15
	F. Theoretical Study of Thermoregulation . . . . .	17
	G. Tissue Heat Transfer . . . . .	21
	1. Consideration of Vascular Geometry . . . . .	26
III	THE PALLID BAT AS AN ANIMAL MODEL . . . . .	28
	A. Thermoregulation in Bats . . . . .	29
	B. Energy Saving and Expenditure of Bats . . . . .	35
	C. Circulation in the Bat Wing . . . . .	40
IV	EXPERIMENTAL METHODS . . . . .	44
	A. Proposed Experiments . . . . .	44
	B. Animals . . . . .	45
	C. Experimental Set-Up . . . . .	46
	D. Open Flow Respirometry . . . . .	48
	1. Metabolic Rate Calculations . . . . .	49
	E. Protocol . . . . .	50
	F. Effects on Wing Vasculature . . . . .	53
V	ANALYSIS AND DISCUSSION OF EXPERIMENTAL RESULTS . . . . .	55
	A. Basal Conditions . . . . .	56
	B. Systemic Heating . . . . .	57
	C. Analysis of Vascular Response to Systemic Heating . . . . .	71
	D. Correlations . . . . .	76
	E. Conclusions . . . . .	84

CHAPTER	Page
VI	THEORETICAL ANALYSIS OF THERMOREGULATION
	IN BATS . . . . . 88
	A. Model Implementation . . . . . 97
	B. Numerical Results . . . . . 100
	C. Conclusions . . . . . 106
VII	CONCLUSIONS . . . . . 109
	REFERENCES . . . . . 110
	VITA . . . . . 122

## LIST OF TABLES

TABLE		Page
I	Properties of Vascular Compartments . . . . .	23
II	Different Species of Bats in Texas . . . . .	32
III	Table Indicating Parameters Involved in the Thermoregulation Model Described by Equations 6.14 to 6.16 . . . . .	98

## LIST OF FIGURES

FIGURE	Page
1	Schematic of peripheral circulation in a tissue considering three layer anatomical model [42]. . . . . 12
2	Schematic diagram of vascular structure showing capillary bed and arterio-venous anastomoses. . . . . 14
3	Schematic of heat exchange at the cutaneous tissue layer (skin). . . . . 15
4	Factors affecting thermoregulation are divided into local and central nervous system control. This figures is modified from Ref. [67]. . . . . 19
5	A cross-sectional view of the block model of a squirrel monkey; this study is the only that uses mathematical models to analyze thermoregulation in an animal model. Taken from Ref. [69]. . . . . 21
6	Schematic drawing of capillary supply and anastomoses at edge of wing [80]. . . . . 29
7	Schematic of microvasculature of the cutaneous layer [42]. . . . . 30
8	Anatomy of a typical bat [81]. . . . . 31
9	Heat loss as a function of body weight [80]. . . . . 33
10	Alterations in body temperature of bats during torpid and euthermic conditions [80]. . . . . 34
11	Relationship between metabolic rate and ambient temperature during normothermia (open circles) and torpor (filled circles) for <i>Vespadelus vulturnus</i> (4g) [2]. . . . . 37
12	Relationship between ambient temperature and body temperature for torpid (filled circles) and normothermic (open circles) bats ( <i>V. vulturnus</i> , 4g) [2]. . . . . 37

FIGURE	Page
13	Relationship between ambient temperature and wet thermal conductance for torpid (filled circles) and normothermic (open circles) <i>V. vulturinus</i> [2]. . . . . 38
14	Relationship between body mass (g) and basal metabolic rate for 18 species of bats, including <i>V. vulturinus</i> (4g). The plots are shown in base 10 log [2]. . . . . 38
15	Relationship between metabolic rate and ambient temperature for euthermic (filled circles), torpid (open circles) and torpid but thermoregulating (gray circles) bats ( <i>Chalinolobus gouldii</i> , 17.5g)[3]. 40
16	Relationship between wet and dry thermal conductance and ambient temperature of euthermic (filled circles), torpid (open circles) and torpid but thermoregulating (gray circles) bats ( <i>C. gouldii</i> ) [3]. . 41
17	Percentages of blood volumes in different vessels of the bat wing [83]. 42
18	General shape of vasculature in bat wings, specifically pallid bat ( <i>Antrozous pallidus</i> ). Figure created by Missy F. Young. . . . . 43
19	Diagram showing experimental setup. . . . . 47
20	Schematic of Protocols: <b>A)</b> dynamic heating, <b>B)</b> constant temperature, and <b>C)</b> dynamic cooling. . . . . 51
21	Placement of heat flux sensors and thermocouples in the pallid bat wing. Modified figure created by Missy F. Young. . . . . 52
22	Body temperature from twenty-nine experiments where the pallid bat ( <i>Antrozous pallidus</i> ) is completely enclosed inside the metabolic chamber; average basal body temperature is $T_{body,o} = 30.4 \pm 1.6^{\circ}\text{C}$ . . 57
23	Oxygen ( $\text{O}_2$ ) content and carbon dioxide ( $\text{CO}_2$ ) content for two different bats during normal ambient conditions. <b>A)</b> B11, Female, 24.41g; at the points where carbon dioxide increases due to movement, oxygen values are reduced. Bat B11 never reached a steady state as indicated by the oscillations in $\text{CO}_2$ . <b>B)</b> B13, Female, 24.07g; plots show that bat B13 was at a metabolic steady state throughout experiment. Initial peak in $\text{CO}_2$ indicates that the bat was stressed when first placed inside the metabolic chamber. . . 58

FIGURE	Page
24	Changes in body temperature during experiments at <b>higher</b> ambient temperatures <b>A)</b> <i>without</i> wing extended (B12, Female, 17.51g), and <b>B)</b> <i>with</i> wing extended (B23, Female, 21.3g). . . . . 61
25	Changes in body temperature during experiments at <b>higher</b> ambient temperatures <i>with</i> wing extended for <b>A)</b> B23, Female, 21.3g, and <b>B)</b> B16, Male, 24.8g. . . . . 63
26	Three stages observed during systemic heating experiments that correspond to: <b>A)</b> $T_{body} \geq T_{chamber}$ , <b>B)</b> $T_{chamber} \geq T_{body}$ and $T_{body}$ <u>decreases then increases</u> , and <b>C)</b> $T_{chamber} \geq T_{body}$ and $T_{body}$ <u>decreases</u> . 64
27	Temperature at three different locations in the wing during experiments at <b>higher</b> ambient temperatures <i>with</i> wing extended (B23, Female, 21.3g). $T_{wing}$ increases at a slow rate until the heating system is stopped at minute 72, after this time $T_{wing}$ still increases but at an even slower rate. . . . . 66
28	Changes in wing temperature during experiments at <b>higher</b> ambient temperatures <i>with</i> wing extended: <b>A)</b> B23, Female, 21.3g; <b>B)</b> B16, Male, 24.8g. . . . . 68
29	Changes in heat flux in the wing at normal ambient conditions (B12, Female, 17.51g). Heat flux in both locations of the wing is fairly constant throughout the entire experiment. . . . . 69
30	Changes in heat flux in the wing during systemic heating for <b>A)</b> pallid bat (B23, Female, 21g) and <b>B)</b> pallid bat (B16, Male, 24.8g). Heat flux in Location #2 increases as heating progresses while in Location #1, the same pattern is not observed. . . . . 70
31	Arteriole diameter and centerline velocity in the wing during normal ambient conditions (B14, Female, 25.98g). The last part shows a larger variation in diameter due to movement of bat wing and loss of focus in the diameter tracking software. . . . . 72



FIGURE	Page	
32	Changes in arteriole diameter and centerline velocity in the wing during systemic heating (B16, Male, 24.8g). Data shows that diameter increases at a constant rate up to minute 88 which corresponds to the time when the heating stops; the diameter then continues to increase but at a slower rate. Average values of velocity are higher at the end of the experiment when $T_{chamber}$ is 32.4°C than the beginning when $T_{chamber}$ is 25.5°C. . . . .	73
33	Blood flow and wall shear stress with respect to time during systemic heating; (B16, Male, 24.8g). After the metabolic chamber has reached a maximum temperature of 36°C blood flow and wall shear stress increase about 0.2 ml/min (300%) and about 4 dyne/cm <sup>2</sup> (166.6%), respectively. . . . .	75
34	Results for <b>Stage A</b> ( $T_{body} \geq T_{chamber}$ ), shows that as $T_{body}$ increases the pallid bat responds through vasodilation, indicated by an increase in vessel diameter and centerline velocity (B23, Female, 21.3g). . . . .	78
35	Results for <b>Stage A</b> ( $T_{body} \geq T_{chamber}$ ), shows that as $T_{body}$ increases blood flow also increases in order for heat exchange to take place in the wing and therefore assist in thermoregulation (B23, Female, 21.3g). . . . .	79
36	Results for <b>Stage B</b> ( $T_{chamber} \geq T_{body}$ and $T_{body}$ <u>decreases then increases</u> ) show that when $T_{chamber}$ increases, the pallid bat responds through vasodilation (increase in vessel diameter and centerline velocity) which then causes $T_{body}$ to decrease to basal values (B23, Female, 21.3g). . . . .	80
37	Results for <b>Stage B</b> ( $T_{chamber} \geq T_{body}$ and $T_{body}$ <u>decreases then increases</u> ) show that when $T_{chamber}$ increases, there is an increase in blood flow which then allows $T_{body}$ to return to basal values (B23, Female, 21.3g). . . . .	81
38	Results for <b>Stage C</b> ( $T_{chamber} \geq T_{body}$ and $T_{body}$ <u>decreases</u> ) show that when $T_{chamber}$ increases, the pallid bat responds through vasodilation (increase in vessel diameter and centerline velocity) which then causes $T_{body}$ to decrease to basal values (B16, Male, 24.8g). . . . .	82

FIGURE	Page
39	Results for <b>Stage C</b> ( $T_{chamber} \geq T_{body}$ and $T_{body}$ <u>decreases</u> ) show that when $T_{chamber}$ increases, due to vasodilation, there is an increase in blood flow which then allows $T_{body}$ to return to basal values because more heat exchange is taking place in the wing (B16, Male, 24.8g). . . . . 83
40	Heat flux remains constant during experiments at normal ambient conditions; since there is no increase in $T_{chamber}$ , there is no need for the bat to release heat from the wing to the environment. . . . . 83
41	During systemic heating, $q_{wing}$ responds the same during the three different stages ( <b>Stages A, B and C</b> ). $q_{wing}$ increases proportional to <b>A)</b> $T_{chamber}$ , <b>B)</b> $T_{body}$ , and <b>C)</b> $T_{wing}$ due to the need for the bat to dissipate heat from to body through the wing. . . . . 84
42	For the last systemic heating experiment, temperature measurements began before the heating system was turned on. $T_{wing}$ begins to increase 22 minutes after heating was turned on which indicates a positive response to changes in $T_{chamber}$ (B14, Female, 25.98g). . . . . 85
43	Relationship between metabolic rate and $T_a$ for <i>V. vulturinus</i> . Values included in the regression analysis are indicated by dark circles, and open triangles are $T_a$ values below the minimum set-point during which bats increased metabolic rate to maintain body temperature [2]. . . . . 90
44	Mass-specific evaporative water loss of male and female <i>L. cinereus</i> as a function of air temperature ( $T_a$ ). Closed symbols represent normothermic individuals, open symbols are torpid bats [89]. . . . . 93
45	Calculated time variation of both body temperature and wing temperature during a heating experiment for the case of different values of the initial body temperature. The initial wing temperature $T_{wing}^o$ is considered constant in all the cases. . . . . 102

FIGURE	Page
46	Calculated time variation of both body temperature and wing temperature during a heating experiment for the case of different combinations of the values associated to coefficients $A$ and $B$ used in Equation 6.17 to estimate the contribution of body temperature and wing temperature signals to the wing perfusion $\beta_{wing}$ . . . . . 104
47	Calculated time variation of both body temperature and wing temperature during a heating experiment for the case of different value of basal metabolic heat production. The plot shows three different values: corresponding to: $2Q_{met,o}$ , $Q_{met,o}$ and $Q_{met,o}/2$ , where $Q_{met,o}$ is calculated at baseline body temperature and for a mass of 22g using Equation 6.5. In the figure, the tim variation of $T_{chamber}$ is presented as reference. . . . . 105
48	Calculated time variation of both body temperature and wing temperature during two heating experiment where two different heating rates are considered: <i>slow heating</i> and <i>rapid heating</i> . . . . . 107

## CHAPTER I

### INTRODUCTION

#### A. Summary of Research and Objectives

The bat wing provides an arterial bed actively involved in thermoregulation, where a large amount of environmental heat exchange can take place by controlled alterations of vessel diameter and blood flow. Previous studies in local heating in the pallid bat wing show that percentile diameter dilation depends on arteriole size. Arterioles between 40 and 60  $\mu\text{m}$  respond actively and follow a bi-phasic response, while arterioles of 25  $\mu\text{m}$  do not show a bi-phasic response and present diminished dilation [1]. This bi-phasic behavior to local heat is also observed in vasculature in the human skin; given the importance of vascular control and thermoregulation in humans, an animal model to study such interactions is very desirable. The fact that the wing of the pallid bat is actively involved in thermoregulation, makes the pallid bat a suitable model to study thermoregulation and vascular response.

**The objective of this research is to analyze the relationship between environmental heat exchange and vascular response in the pallid bat wing during both systemic heating and local heating.** These studies can provide information about vascular response, as well as the mechanisms controlling blood flow and heat exchange; factors that allow mammals to regulate their body temperature.

Thermoregulation studies, like the one proposed herein, analyze factors that trigger changes in mechanisms that control heat exchange. During these studies, metabolic rate and body temperature are usually observed, as well as evaporative water loss due to respiration. **In our research, we will monitor metabolic**

---

The journal model is *IEEE Transactions on Biomedical Engineering*.

**activity and body temperature during alterations in ambient conditions; simultaneously, we will observe vascular response in the microvasculature of the wing and estimate correlations between systemic and vascular response.** This is a novel approach, as common studies of thermoregulation focus on either measurement of single systemic quantities, such as metabolism, respiration and body temperature, or analysis of vascular response (blood vessel diameter and blood flow).

The pallid bat wing is being used as animal model because it provides a membrane where the microvasculature is easily accessed and non-destructive measuring techniques can be used to monitor vessel diameter and centerline velocity, without the need for anesthesia which has a negative effect on thermoregulation. Previous thermoregulation studies in bats of similar body mass have focused on energy conservation at low temperatures when bats respond by entering a state of torpor (Chapter III) [2, 3, 4, 5, 6, 7, 8]. In this novel research, we will look at the change of energy (heat) responses of the pallid bat at higher ambient temperatures.

Understanding thermoregulation and the mechanisms controlling vascular response and heat exchange is important because there exist several conditions that affect thermoregulation, such as cardiovascular disease (CVD) [9, 10], diabetes [11, 12, 13], and Raynaud's phenomenon [14, 15] among others which will be explained in greater detail in Chapter II. Alterations in skin vasculature occur at early stages of such diseases and therefore, learning about vascular responses to systemic heating will help improve treatment, early detection and non-invasive monitoring of such diseases.

To achieve the objectives of this study, a metabolic chamber was built which allows control of internal ambient temperature and determination of metabolic activity by using open flow respirometry [2, 3, 4]. This research was conducted at the Cardiovascular Systems and Dynamics Laboratory directed by Dr. C. Quick. The

experiments were performed under the Animal Use Protocols: AUP 2006-253 and AUP 2007-110. The experiments proposed and discussed in Chapter IV, will study alterations in body temperature, arm temperature, wing tissue temperature, wing heat flux, vessel diameter and centerline red blood cell velocity at different arterial segments of the wing vasculature (60  $\mu\text{m}$  and 45  $\mu\text{m}$ ), and their correlation to different protocols of systemic heating, such as: **1)** dynamic body heating, **2)** constant ambient temperature, and **3)** dynamic effects of ambient temperature reduction.

Experiments performed under the two different protocols (AUP 2006-253 and AUP 2007-110) include: **1)** analysis of body temperature and basal metabolic activity of the pallid bat at **normal** ambient temperatures *without* the wing extended; **2)** analysis of body temperature through the use of a rectal probe and metabolic activity ( $\text{CO}_2$  production) of the pallid bat at **higher** ambient temperatures *without* the wing extended; **3)** analysis of body temperature, wing temperature and vascular response in the wing (blood vessel diameter and blood flow) at **normal** ambient temperatures *with* wing extended; and **3)** analysis of body temperature, wing temperature and vascular response of the pallid bat at **higher** ambient temperatures *with* wing extended.

The results from the experiments provided the information necessary to study correlations between metabolic chamber temperature ( $T_{chamber}$ ), body temperature ( $T_{body}$ ), wing temperature ( $T_{wing}$ ), wing heat flux ( $q_{wing}$ ) and arm temperature ( $T_{arm}$ ) during systemic heating. In Chapter V, analysis of experimental findings will be discussed and modifications to the procedures will be proposed. The analysis will help to estimate how blood perfusion to the wing changes in response to systemic and environmental changes. The culmination of this analysis will be presented in Chapter VI with a simple thermoregulatory model for the bat.

## CHAPTER II

### THERMOREGULATION

#### A. General Concepts on Thermoregulation

Thermoregulation is the ability of an organism to maintain a fairly constant body or core temperature through continuous alterations in environmental conditions; such constancy is achieved through changes in internal heat production and physiological parameters controlling environmental heat exchange, such as cutaneous blood flow, among others. Thermoregulation is critical for survival, as optimal organ function occurs within a specific temperature range for many species. Organisms that have the ability to maintain body temperature regulated within a narrow range ( $\pm 2^{\circ}C$ ) are called homeotherms, and include mammals and birds among others. The average body temperature of homeotherms is within the range of  $36^{\circ}C$  to  $40^{\circ}C$  and varies with species. On the other hand, poikilotherms are organisms that do not regulate their temperature, such as insects, fish and reptiles. In these animals, their core or body temperature is almost equal to that of the environment. In homeotherms, body temperature is maintained within a controlled range due to energy conservation mechanisms that alter the rate of body heat production to match the energy being exchanged with the environment [16].

The study of thermoregulation in homeotherms is paramount, as the increase or decrease of temperature beyond the optimal range can cause detrimental effects to life. If the temperature falls slightly below the functional temperature (hypothermia) then metabolic activity and oxygen consumption are reduced. If the temperature then continues to decrease, a body can go into cardiac arrest and die. During hyperthermia, or abnormal temperature increase, oxygen demands increase and protein

break-down occurs after  $42^{\circ}\text{C}$ , killing cells or affecting the membrane stability and other processes. Because hyperthermia and hypothermia can affect organ function and produce death, the study of the mechanisms responsible for thermoregulation or temperature control is fundamental to optimize hypothermic or hyperthermic therapies, as well as to further understand diseases where thermoregulation or the vascular response mechanisms associated to it are affected, such as diabetes which affects a large amount of the population worldwide [17, 18, 19].

Thermoregulatory responses can be divided into two categories: behavioral responses and physiological responses [20, 21]. Behavioral responses denote responses where an organism consciously acts or responds to the environment; some of these responses are environmental selection or migration, and change in posture and environmental exposure [20].

Physiological responses include thermogenesis, evaporative heat loss and alterations in cutaneous perfusion or vasomotor activity among others. Thermogenesis is a physiological response where shivering takes place to increase heat generation. An organism who is shivering produces about five times additional metabolic heat than a non-shivering organism [22]. Evaporative heat loss is found in the form of sweating for humans and some animals and in panting for others. Sweating is a special activity of the sympathetic nervous system and allows for cooling of the skin when the sweat is evaporated [22]. In humans, evaporative heat loss from the skin is about 14% of total body heat loss [23]. Panting also allows for cooling in some animals through evaporation from the mouth, tongue and upper airways [22].

Vasomotor activity or vasomotion, is described as the variations in vessel diameter, also known as vasoconstriction or vasodilation, respectively. Alterations in vascular diameter occur in response to different stimuli, and help provide the necessary amount of blood to a particular tissue.



For thermoregulatory purposes, vasoconstriction (VC) and vasodilation (VD) take place at the cutaneous vasculature and help increase (VD) and reduce (VC) environmental heat exchange. Vasoconstriction occurs when an organism is subjected to low ambient temperatures (hypothermia) where heat needs to remain inside the body in order to protect deep or core organs from the changes in the external environment. At high temperatures, when body temperature increases above normal conditions (hyperthermia), vasodilation occurs to augment the blood volume in the cutaneous vessels (i.e. skin) and therefore increasing heat exchange with the environment. Vasoconstriction and vasodilation serve a major role in determining volume and volume rate of blood available at the skin, which affects thermophysical factors of the cutaneous layer such as thermal conductivity and temperature. During active vasodilation, skin blood volume is about 60% of the cardiac output as opposed to 5% under normal conditions [13]. Vasomotor activity together with other factors, such as heart rate and respiration are controlled by a site in the hypothalamus [24].

It is important to note that even though there are different physiological responses to changes in the external environment, in this research, vasomotor activity in the cutaneous layer (skin) is the response that will be taken into consideration.

## B. Diseases That Affect Thermoregulation

It has been recognized that vascular function alterations start developing at the early stages of cardiovascular disease (CVD) [9, 10], endothelial dysfunction [25, 26, 27, 28], diabetes [18, 19, 11, 29, 12, 13], kidney failure [30], and are present in other conditions such as pain syndrome [31], menopause [13], scleroderma [15], and Raynaud's phenomenon [14, 15]. The skin serves a number of vital functions, such as nutritional support for tissues, heat regulation, a means of metabolic exchange and tissue home-

ostasis; its main function though, is to ensure the nutrition of tissue [32]. The study of vascular responses (skin blood flow) is necessary to understand diseases where thermoregulation is affected because when blood flow is affected in the skin, then tissue nutrition is adversely affected and certain diseases are manifested.

Diabetes has been known to compromise vascular function at different levels. There is a reduction in heat tolerance due to impairment of cutaneous vasomotion when exposed to heat [12, 29, 19, 18, 13] that increases the risk of heat stroke and heat exhaustion [13]. Under thermal stimulation inadequate small blood vessel perfusion inhibits the healing of small wounds [12]. The nervous system (neuropathy) is affected causing numbness in limbs among other things. Also, in diabetic patients the reduction of blood flow to capillaries causes them to rupture, therefore causing the formation of ulcers.

During menopause, control of skin blood flow is altered by changes in reproductive hormone levels [13]. These alterations inhibit heat transfer to the environment by affecting cutaneous blood flow and therefore cause an increase in body temperature.

Raynaud's syndrome is a condition in which the smaller arteries that carry blood to the fingers or toes constrict when exposed to extreme cold temperatures or from shock. When this happens, the fingers or toes become pale, cold and numb because blood remains trapped in the capillaries [14].

Finally, scleroderma [15] is a progressive disease that leads to the hardening and tightening of the skin and connective tissues also affecting vasomotor response. If scleroderma is not treated, it can lead to organ failure.

Learning about thermoregulation and the mechanisms controlling vascular response and heat exchange will help to improve treatment and early detection of some diseases. This is possible because the alterations in vascular response are observed in the beginning stages of these diseases.

### C. Environmental Energy Exchange

The study of vascular response in the cutaneous layer is important because of its involvement in thermoregulation [13, 33, 20, 16], neural stimulation [34, 35] and mental stress [36]. The microvasculature geometry and blood flow distribution at the skin have a profound effect on heat exchanged between blood, tissue and the external environment. The vasculature in the cutaneous tissue layer, or the skin, is formed mostly by small arterioles and venules ranging from 20 - 30  $\mu\text{m}$  in diameter and capillaries whose diameters are about 8  $\mu\text{m}$  [37, 38]. The skin tissue is about 2 mm thick and can essentially be represented as a two-dimensional vascular sheet.

Heat exchange taking place between skin surface and the environment depends on different factors including physical as well as physiological factors. There are four different mechanisms that control heat exchange between the skin and the environment and correspond to: conduction, convection, radiation and evaporation. Heat is transferred to the environment when there is a temperature difference between ambient temperature and skin temperature. In a resting person, about 3% of heat loss is through conduction, 27% from convection, 40% through radiation and 30% by evaporation [39]. These percentages are affected by the geometry of an organism; heat capacity of an organism; conduction of heat due to thermal gradients; heat production due to metabolic processes; the role of blood flow in heat transfer; thermoregulatory mechanisms in the organism and their functions; thermophysical and physiological properties of various organs and tissues; and the interaction with the environment and its condition. These factors will be discussed later on with more detail, as they are important in thermoregulatory models. Because mammals maintain their body temperatures at a fairly constant level, there is a continuous exchange of energy between the organism with its environment [40].

Applying the principle of conservation of energy to an organism gives the following equation:

$$\dot{Q}_{metabolism} = \dot{Q}_{stored} + W + \dot{Q}_{lost}. \quad (2.1)$$

In Equation 2.1, the terms from the left to the right are usually expressed in terms of body surface area ( $\text{W}/\text{m}^2 \cdot \text{s}$ ) or body mass ( $\text{W}/\text{kg} \cdot \text{s}$ ) and are: the rates of energy production through metabolism ( $\dot{Q}_{metabolism}$ ), energy storage in body tissues and fluids ( $\dot{Q}_{stored}$ ), the rate of work performed ( $W$ ) by the body, and the heat loss to the environment through different methods of heat transfer ( $\dot{Q}_{lost}$ ) [40], respectively.

The external source of energy ( $\dot{Q}_{metabolism}$ ) comes from the food that is ingested. Food is made up of three major energy-carrying constituents - carbohydrates, lipids and proteins. They are synthesized chemically in the body so they can be converted into useful compounds from where energy can be extracted, a process called anabolism. The sum of the biochemical process by which food is broken down into these compounds is called *metabolism*. The major result of metabolism is the production of ATP (adenosine triphosphate). This is the main internal energy source of the body. When ATP is produced, about 60% of the energy involved in the process becomes heat. When energy is transferred from ATP to the functional system there is an additional release of heat. Total heat generation depends on the activity level of an individual among other factors. There is also a significant difference in metabolic rates of different organs and organisms depending on the tissue [40]; for example, children have greater metabolic rates than adults [41].

$\dot{Q}_{lost}$  is a sum of the different methods of heat transfer to the environment; these include conduction through the tissue,  $\dot{Q}_{conduction}$ ; convection through the circulatory system and the surface  $\dot{Q}_{convection}$ ; radiation,  $\dot{Q}_{radiation}$  and evaporation through

sweating or the respiratory airways,  $\dot{Q}_{evaporation}$  (Equation 2.2);

$$\dot{Q}_{lost} = \dot{Q}_{conduction} + \dot{Q}_{convection} + \dot{Q}_{radiation} + \dot{Q}_{evaporation}. \quad (2.2)$$

$\dot{Q}_{convection}$  describes the overall convective exchange between an organism and its environment and is dependent on  $h_c$  and  $A_d$ , where  $h_c$  is the convective heat transfer coefficient and is dependent on the type of convection and on geometrical factors. For example, for a nude, standing human the convection coefficient is  $2.7 \text{ W/m}^2 \text{ }^\circ\text{C}$  while for a nude, seated human it is  $2.3 \text{ W/m}^2 \text{ }^\circ\text{C}$  [40] which means that a standing person will lose more heat through convection.  $A_d$  is the total surface area and for humans the body surface area is determined by the following DuBois equation,

$$A_d = 0.202W^{0.425}z^{0.725}, \quad (2.3)$$

where  $W$  is the body weight in kilograms and  $z$  is the height in centimeters [40].  $\dot{Q}_{radiation}$  is energy exchange by thermal radiation, where  $\sigma$  is the Stefan-Boltzman constant and  $\varepsilon$  is the emittance of the body surface,  $f_r$  is the effective radiation area factor determined as 0.696 for the sedentary body posture and 0.725 for standing posture for humans, and  $T_s$  and  $T_a$  are surface and air temperature, respectively;

$$\dot{Q}_{radiation} = \sigma\varepsilon A_d f_r (T_s^4 - T_a^4). \quad (2.4)$$

Equations 2.1 through 2.4 show that in order to have a realistic model for heat transfer in a tissue, many different factors must be taken into consideration [40]. In bats, even though the mechanisms of heat transfer are the same, their contribution to heat exchange is different, as will be discussed in Chapter VI.

#### D. Effects of Cutaneous Blood Flow on Heat Exchange

When classified by function, there are different types of blood vessels. There are blood vessels that feed core organs (i.e. heart, kidney, liver, brain) and there are peripheral blood vessels that feed the rest of the body. Internal or core organs count with autoregulatory mechanisms capable of matching organ blood flow to metabolic need and to changes in tissue temperature and local pH [16]. The cutaneous circulatory system is a group of peripheral blood vessels that feed the skin.

The cutaneous circulation allows for convective heat transfer from the body core to the skin surface. The cutaneous circulation contains resistance vessels that are capable of controlling blood flow by varying vessel diameter.

Changes in vessel diameter are controlled by neural mechanisms capable of integrating, among other signals, temperature signals from different parts of the body, such as core organs like the brain, and skin temperature at different locations around the body. These physiological mechanisms provide a way to maintain internal body temperature within a narrow range by varying the volume rate of blood delivered to the cutaneous layer (skin), where environmental heat exchange takes place. Maintaining different volumes of blood in the cutaneous circulation is possible by the presence of capacitance vessels veins and veno-plexuses<sup>1</sup> which are major blood reservoirs capable of storing about 80% of blood volume.

Some important physical factors in the skin (cutaneous tissue layer) deal with the structure of tissue and blood vessels; vessels in the skin are arranged into superficial and deep horizontal plexuses and are involved in thermoregulation, oxygen and nutritional support [32]. Blood flow greatly affects skin temperature and heat transfer from the core to the environment and therefore, the structure of the vasculature in the

---

<sup>1</sup>Plexus is a network of blood vessels.

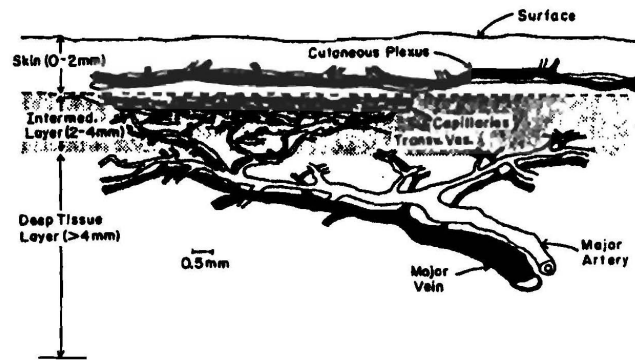


Fig. 1. Schematic of peripheral circulation in a tissue considering three layer anatomical model [42].

tissue will also have a great effect on heat exchange. Blood flow into the cutaneous layer is dependent on the arterial distribution in the tissue and the type of vessels that are present; this is because different types of vessels can hold different volumes of blood. Also, because one of the functions of blood is to transfer heat from the core to the environment, the proximity of blood vessels to the surface is an important factor for heat exchange. The vessels in the deep plexus (lying between the dermal and cutaneous layer) run parallel to the surface of the skin and this constitutes a large surface area for blood flowing through this bed to exchange heat with the external environment [32]. A schematic showing the location of these vessels can be seen in Figure 1. Blood flow is the only controllable way to distribute internal heat (from the core) to the skin [20].

Skin blood flow is affected by the ambient temperature; it ranges from about 20 ml/min in the cold to 8 l/min during maximal heating [43]. Skin blood flow responds differently when a human is subjected to either hyperthermia, hypothermia [11, 44, 45, 46, 47, 48] or local heating [44, 49, 50, 51]. During heat exposure and exercise, vasodilation and increased blood flow are very important to heat dissipation.

During cold exposure vasoconstriction in the skin helps decrease heat loss from the body [13].

The volume of blood entering the venous side of the vascular system depends on the physiological regulatory mechanisms. Blood flows from the arterial side to the venous side by two possible directions; one possibility is blood flow through the capillary bed, which connects the arterial side to the venous side. Another possibility is blood flow through arterio-venous anastomoses (AVAs) which provide a low resistance pathway for blood from the arteries to the veins [16, 52, 53, 54] (Figure 2); in other words, AVAs are structures that connect the arteries and veins and allow arterial blood to enter the venous side without having to pass through the capillaries. These AVAs play an important role in heat transfer through the skin and are maintained in a constricted state by peripheral sympathetic constriction under normal conditions and at lower temperatures [32, 43]. As blood passes from arteries to veins through capillaries, its velocity is reduced and the blood has ample time to thermally equilibrate and reach tissue temperature (i.e. heat exchange increases). If blood flows from arteries to veins without passing through the capillary bed (i.e. passes through AVAs) the blood returning through the veins will not be as cold due to the fact that thermal equilibration has not been achieved. In addition, in the presence of high arterial blood volumes (VD), the blood is pooled at the venous plexus<sup>2</sup> increasing its residency time near the surface and therefore increasing heat exchange.

At higher body temperatures, AVA vasodilation will allow for larger volumes of blood at high arterial temperatures to be transferred to the venous side for greater heat exchange with the environment due to the closer proximity to the external environment of the venous side of the vascular system. It is estimated that in a thermally

---

<sup>2</sup>Venous pooling indicates that the veins accommodate a greater volume of blood.



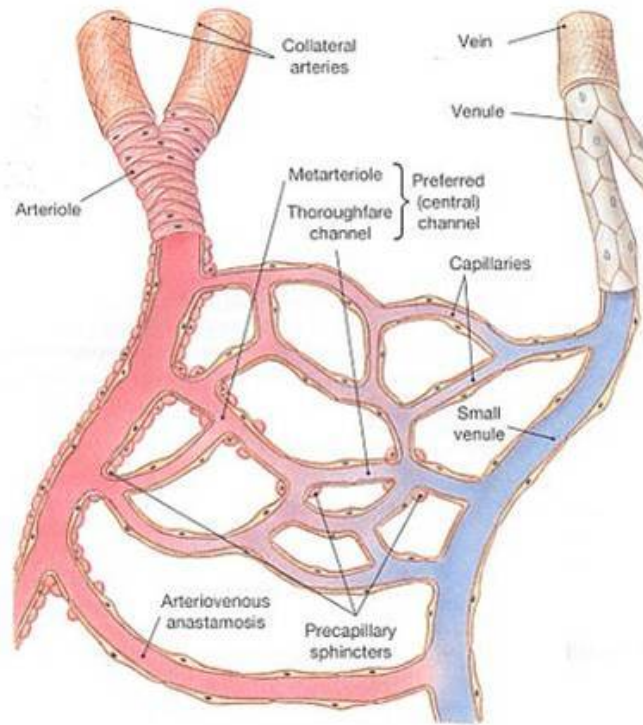


Fig. 2. Schematic diagram of vascular structure showing capillary bed and arterio-venous anastomoses.

comfortable subject nearly one-half of skin blood flow is distributed to regions with arterio-venous anastomoses [55].

Figure 3 shows a schematic of how blood flow through the skin helps release heat to the environment; blood enters at arterial temperature which is about equal to the core temperature; it flows either through the capillary bed or through the arterio-venous anastomoses into the superficial venous plexus. Because the venous plexus is able to maintain large volumes of blood, this is where the greatest heat exchange takes place. After the blood has been cooled down, it flows back to the core at a lower temperature, therefore also cooling the core temperature or maintaining it at a desirable temperature.

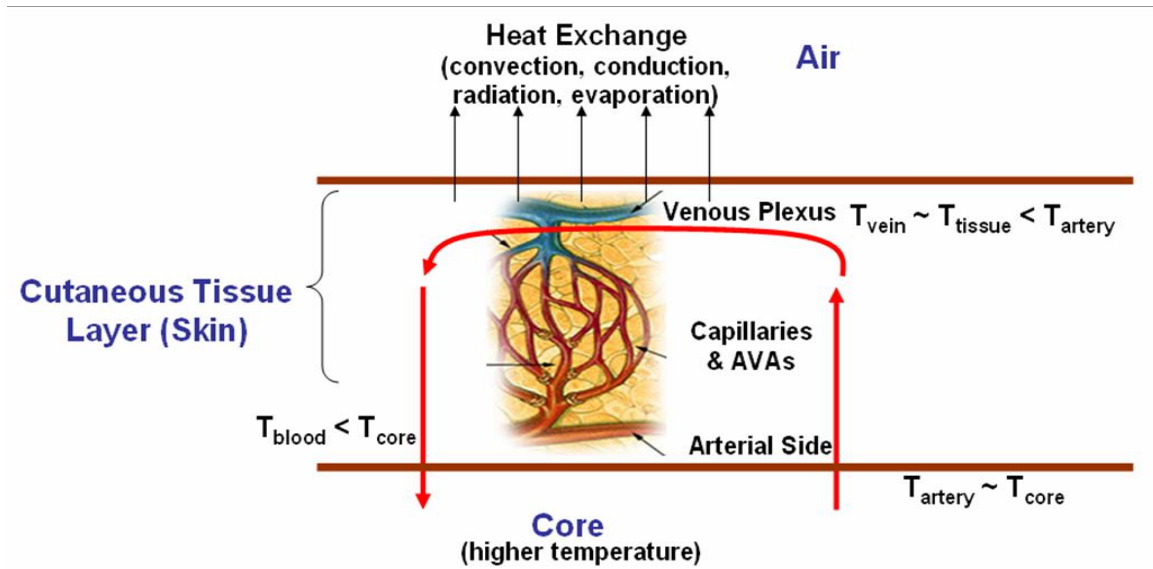


Fig. 3. Schematic of heat exchange at the cutaneous tissue layer (skin).

#### E. Thermal Windows and Their Effect on Thermoregulation

The amount of heat lost to the environment from a body depends greatly on the surface area. For example, heat loss through convection is dependent on the convective transfer coefficient,  $h$ , the temperature difference between the ambient temperature and the surface temperature and the area. If the convection coefficient and the temperature difference remains the same but the area changes, then heat loss will change proportionately. Having a larger surface area means that more heat will be lost to the environment. In cold ambient temperatures animals try to reduce their surface area so that heat will not be lost to the surroundings.

Appendages, including fingers, ears, fins and wings among others, are structures with large surface areas compared with tissue volume; the presence of such structures helps the animal release more heat in a hot environment. These thermal windows have a potential rate of heat dissipation to the environment which is determined by

local skin blood flow [16] or perfusion, meaning that blood flow in the skin greatly determines how much heat is exchanged with the environment. One example of a thermal window is the wing of a bat; bats have very large wings that account for about 80% of the total surface area. The wings are very important in maintaining homeothermy because blood vessels in the thin membranes are exposed to the environment. In these thermal windows, the presence of AVAs increase heat exchange with the environment because of the characteristics that AVAs possess.

Heat exchange across a tissue is also dependent on the thermal conductance of the tissue which in itself is affected by the vasculature. Thermal conductance is the rate of heat flow across the temperature gradient between the core and either the air or skin, per unit of temperature difference [16] and is described by:

$$conductance = \frac{heat\ flow}{temperature\ gradient} \left[ \frac{W \cdot m^{-2}}{^{\circ}C} \right]. \quad (2.5)$$

Thermal conductance is used as a way to measure a species' adaptation to a cold or hot environment [16]. If the thermal conductance of any organism is large, then there is more heat lost to the environment; if it is small, then the organism can be better protected against the cold. There are two different definitions for thermal conductance: dry thermal conductance ( $C_{dry}$ ) and wet thermal conductance ( $C_{wet}$ ).  $C_{wet}$  and  $C_{dry}$  are determined as:

$$C_{wet} = \frac{\dot{V}_{O_2}}{T_c - T_a}, \text{ and} \quad (2.6)$$

$$C_{dry} = \frac{MHP - EHL}{T_c - T_a}. \quad (2.7)$$

In Equations 2.6 and 2.7,  $\dot{V}_{O_2}$  is the rate of oxygen consumption,  $MHP$  is the metabolic heat production,  $EHL$  is the evaporative heat loss and  $T_c$  and  $T_a$  are the core temperature and ambient temperature, respectively [3]. The definitions of

thermal conductance show that metabolic heat production (determined by the rate of oxygen consumption in  $C_{wet}$ ) has an effect on heat flow from the core to the surface of an organism. The difference between the wet thermal conductance and dry thermal conductance is that for the dry thermal conductance, the evaporative heat loss is subtracted from the metabolic heat production in the calculations, therefore giving a value for the thermal conductance at dry conditions.

Just like humans and other organisms, bats use peripheral blood flow to remove excess heat; bats use their wings which provide a large vascularized tissue surface (thermoregulatory bed) to transfer heat from the body to the environment. In the pallid bat, the microvasculature in the wing plays an important role in thermoregulation. The pallid bat provides a good thermal window that can be studied and therefore is a good animal model for this research. The small arteries in the pallid bat wing can easily be studied using the same methods that have been previously used for larger arteries in different organisms [24, 32, 56].

#### F. Theoretical Study of Thermoregulation

Understanding thermoregulation in mammalian tissue has mostly been achieved through experiments involving core and skin temperature measurement inside climate controlled chambers in individuals or animals resting or performing specific exercise tasks [57, 58, 59, 60]. Given the important effect of cutaneous blood perfusion on temperature control, studies involving different levels of flow visualization have been performed [52, 23]. Most studies involving blood flow and temperature monitoring are of invasive nature and can be performed only with the use of anesthetics which are known to affect the thermal response of organisms.

When anesthesia is introduced into an organism, core temperature will typically

drop rapidly [61]. This core temperature drop is a result of a combination of negative heat balance and core-to-peripheral redistribution of internal heat [62]. The negative heat balance results from losing heat to the environment while the body is unable to produce metabolic heat, ultimately reducing core temperature.

*Theoretical* models based on heat transfer analysis have been developed and used since the sixties, when the interest in understanding hibernation and its clinical applications, as well as the interest in improving thermal comfort began [20, 23, 63, 64, 65, 66]; the thermoregulation models are limited due to the difficulty in achieving model validation [67]. In the literature there are two main models of thermoregulation from which all others derive: one for humans first proposed by Stolwijk [68], and one for the squirrel monkey proposed by Spiegel [69]. These models are necessary for understanding integrated biological systems.

Nelson et al [67] developed an anatomically-based model to incorporate active and passive thermoregulation mechanisms. Their thermoregulation model includes local and central nervous system (CNS) control. Local regulation is based on the  $Q_{10}$  model and includes metabolism, sweating and blood flow as affected by local temperature. The  $Q_{10}$  law is commonly used in physiology to estimate alterations in tissue metabolism, blood flow and  $O_2$  consumption due to alterations in body temperature [70]. Figure 4 also shows that CNS regulation includes sweating, vasoconstriction, vasodilation and skin blood flow.

Spiegel et al [69] created a three-dimensional model of a squirrel monkey to simulate the flow of heat into and out of the body. In their model, Spiegel et al considered heat flow through heat generation (metabolism), cooling and distribution of heat by blood, thermal conduction throughout the body, evaporative heat loss from sweating, and radiation and convection from the outer surface of the body. The model also considers active mechanisms of thermoregulation such as vasodilation, vasocon-

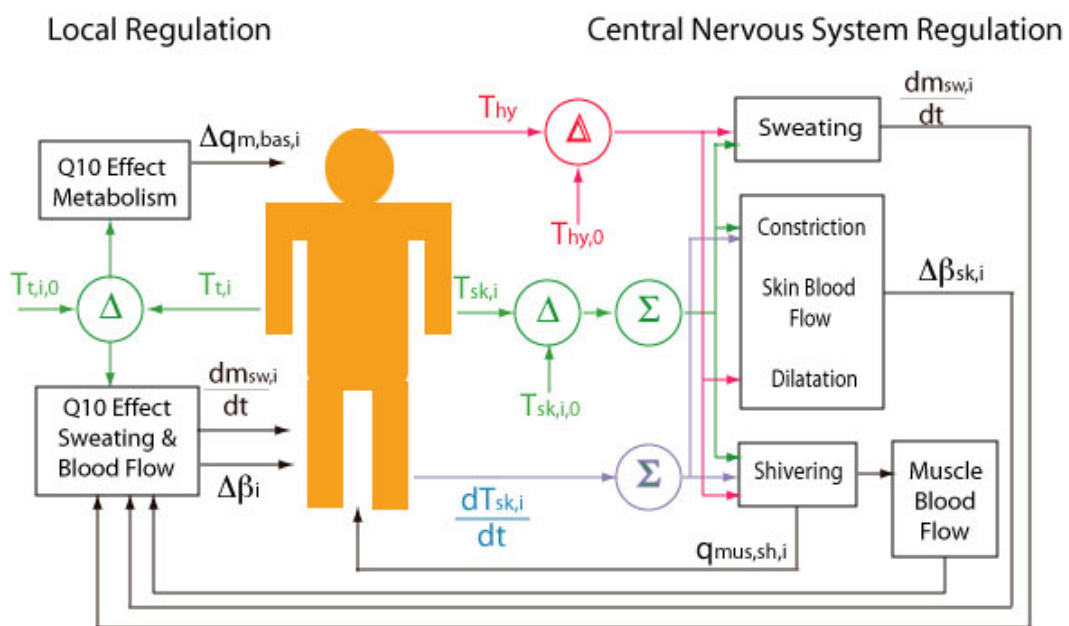


Fig. 4. Factors affecting thermoregulation are divided into local and central nervous system control. This figure is modified from Ref. [67].

striction, and sweating, as well as the passive modes of heat transfer (conduction, convection, and radiation). Vasoconstriction and vasodilation are mechanisms that modulate blood flow delivered to the skin following equation:

$$BF = \frac{[BF_o + VD]2^{(T_{skin} - T_{skin,set})/10}}{1 + VC}, \quad (2.8)$$

where  $BF_o$  is the local basal blood flow rate,  $T_{skin}$  is the local skin temperature,  $T_{skin,set}$  is the local skin set point temperature,  $VD$  is the total controller command for skin vasodilation, and  $VC$  is the total controller command for skin vasoconstriction.  $VD$  and  $VC$  correspond to sigmoidal relationships and do not act simultaneously, rather, when vasodilation occurs,  $VC = 0$  and when vasoconstriction occurs,  $VD = 0$  [69]. The functions for  $VD$  and  $VC$  follow sigmoidal curves that express their activation as  $T_{body}$  or  $T_{skin}$  change or deviate from a set value or threshold.

The squirrel monkey model was created by using rectangular blocks of various sizes to represent the different parts of the body. Figure 5 shows the different layers (core, composite layer of fat and muscle, skin, fur) that were considered in the squirrel monkey model. This model is the only animal model available that has taken into consideration thermoregulatory mechanisms; but, because detailed anatomical information is lacking, the tissue distribution and the fractional volume for the core and outer layers of the model are based on information from the human model in [71].

The main difficulty associated with these models is the lack of anthropometric and thermophysical data ( $k$ ,  $c$ ,  $w_b$ ) required for their implementation; however, they help provide **1)** useful insight to factors affecting heat exchange, **2)** a way to compare simulation results with experimental results, and **3)** tools for learning about the interactions that are difficult to control experimentally. In this study we will use energy balance to establish a simplified or lumped model of thermoregulation for the

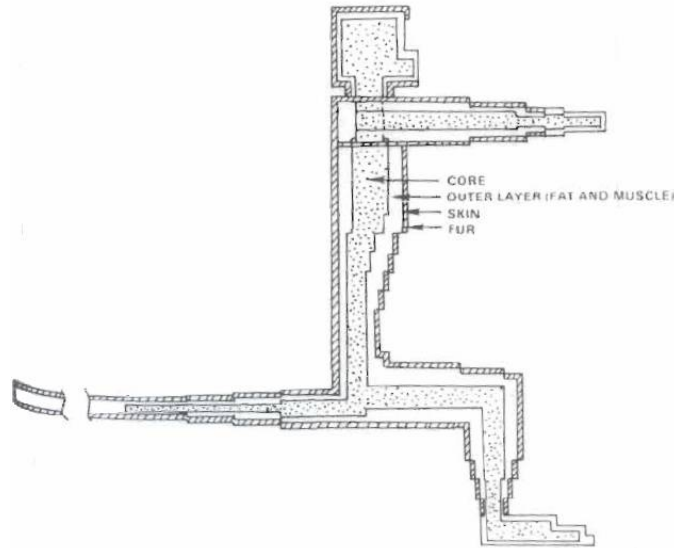


Fig. 5. A cross-sectional view of the block model of a squirrel monkey; this study is the only that uses mathematical models to analyze thermoregulation in an animal model. Taken from Ref. [69].

pallid bat based on the models indicated above; this will be presented in Chapter VI.

### G. Tissue Heat Transfer

To advance in the understanding of heat and mass transfer processes that occur in a living organism, several *mathematical* models have been proposed [72, 73, 74, 75, 38, 52, 42, 76, 77, 78, 63]; these models are based on the energy conservation at the tissue level and the application of constitutive laws. However, thermal energy transport in living tissue is extremely difficult to model, due to tissue heterogeneity; convective effect added by the vasculature; simultaneous heat transfer processes occurring in the tissue, such as conduction, convection, radiation, and evaporation; species variability of tissue thermal properties; as well as the difficulty encountered in the in-vivo measurement of tissue thermal properties. Among the factors to be considered when



developing a basic model to describe the thermal state of an organism are:

1. Geometry of the organ or tissue in consideration
2. Heat capacity or thermal inertia of the tissues involved
3. Conduction of heat due to temperature gradients in the tissue
4. Heat production due to metabolic processes
5. Role of blood flow in the transfer of heat between tissues and between tissue and environment
6. Thermoregulatory mechanisms and physiological responses of an organism to different thermal stresses
7. Thermophysical properties of tissues and their variations with temperature
8. The interaction with the environment

Consideration of organ anatomy and physiology are essential characteristics in the development of thermal models because anatomy and physiology define blood flow and metabolic activity. The presence of the circulatory system is the most important characteristic of a biological tissue because it adds convective heat transport to the other thermal characteristics governing tissue heat transfer, such as conduction and heat capacitance. Blood circulation is strongly dependent on physiology, organ anatomy and vasculature, and when including the effects of blood flow in the thermal modeling of tissue, two different factors should be considered: blood vessels change in diameter size as they branch out; and second, there are fundamental vascular structures which appear in tissues or organs.

Heat transfer in living tissues differs from inert materials because of the existence of vasculature. Given the complexity of the vascular structure, it is very difficult

Table I. Properties of Vascular Compartments

Generation	Vessel	$r_i$ ( $\mu m$ )	$x_{e_j}$ (m)	$l_j/x_{e_j}$
1	Aorta	5000	190	0.002
2	Large artery	1500	4	0.05
3	Arterial branch	500	0.3	0.3
4	Terminal branch	300	0.08	0.1
5	Arteriole	10	$5 \times 10^{-6}$	400
6	Capillary	4	$2 \times 10^{-8}$	6000
7	Venules	15	$2 \times 10^{-6}$	800
8	Terminal vein	750	0.1	0.1
9	Venous branch	1200	0.3	0.3
10	Large vein	3000	5	0.04
11	Vena Cava	6250	190	0.002

Note: For a blood vessel in the  $j$ -th branching generation,  $r_j$  and  $l_j$  represent the vessel radius and length, respectively; and  $x_{e_j}$  denotes the thermal equilibration length [38].

to account for the contribution of all the blood vessels. Thermally, blood vessels are divided into thermally significant and thermally equilibrated vessels, depending on their diameter as indicated in Table I, which shows the vessel radius, thermal equilibration length  $x_{e_j}$  and the ratio between vessel length  $l_j$  and  $x_{e_j}$ . The thermal relaxation length,  $x_{e_j}$ , represents the distance inside the vessel that the blood needs to travel in order to equilibrate its temperature to that of the tissue. The thermal equilibration is complete when the temperature difference between blood and tissue is reduced to  $1/e$  of its initial value. The thermal equilibration begins at the terminal arteries and veins, and it is widely accepted that equilibration takes place at the arteriole and venule levels (before entering capillary beds) [38].

In one of the most frequently used equations for bio-heat transfer, the Pennes' bio-heat equation, thermal effects of vessels with different diameters and different geometrical configurations are described. In Pennes' bio-heat equation (Equation 2.9), all effects from blood perfusion are approximated with a heat sink term as follows:

$$\rho c \frac{\partial T}{\partial t} = \nabla \cdot k_i \nabla T + S \omega_b \rho_b c_b (T_a - T) + \dot{Q}_1, \quad (2.9)$$

where  $\rho$  and  $c$  are the mean density and mean specific heat of the tissue, respectively.  $\omega_b$  is the volumetric blood perfusion,  $\rho_b$  and  $c_b$  are the density and specific heat of the blood, respectively.  $\dot{Q}_1$  is a heat sink or source, and  $T_a = T_a(x, y, z, t)$  and  $T = T(x, y, z, t)$  are the arterial and continuum tissue temperatures, respectively. The coefficient  $S$  ( $0 \leq S \leq 1$ ) depends on the way in which the temperature of the capillary blood equilibrates to the surrounding tissue temperature and is used to reduce the strength of the heat sink due to blood perfusion. If  $S = 1$  as it is in the Pennes equation, all heat exchange between tissue and blood takes place in the capillary bed. The Pennes equation reflects the overall energy balance in a tissue when

the veins do not thermally interact with the arteries [63]. Pennes' bio-heat equation includes a term that represents the contribution of flowing blood to the overall energy balance. Pennes assumption was that energy exchange between blood vessels and the surrounding tissue occurs mainly across the wall of capillaries (blood vessels with 0.005-0.015 mm in diameter), where blood velocity is very low. In the equation, it is suggested that blood enters the capillary bed at the temperature of major supply vessels,  $T_a$ , and immediately equilibrates thermally with the surrounding tissue. It then exits the capillary bed and enters the venous circulation at tissue temperature,  $T$ . Pennes' equation suggests that total energy exchange by flowing blood is proportional to the volumetric blood flow and the difference between local tissue and major supply arterial temperatures [79]. Although other literature [63, 79] deduces that thermal equilibration of the blood with the tissue occurs not in the capillaries, but in vessels with diameters in the range of 0.2-0.5 mm, Pennes' equation is still commonly used.

A different model, the Weinbaum, Jiji and Lemons (WJL) model, is applied to thermally significant small vessels and not major supply blood vessels. The basic configuration for the model consists of a control volume of tissue surrounding a pair of thermally significant blood vessels directly connected by capillaries. Based on anatomical observations, Weinbaum et. al. [52] concluded that the main contribution of the local blood perfusion to heat transfer in the tissue is associated with an incomplete countercurrent heat exchange mechanism between pairs of arteries and veins, and not with heat exchange at the level of the capillaries as in Pennes' bio-heat equation. Heat transfer between countercurrent vessels depends not only on the difference between temperature at an artery and vein ( $T_a - T_v$ ) but also on the difference between the tissue temperature,  $T$ , and the average blood temperature  $(T_a + T_v)/2$ . Based on all the studies on heat transfer in a perfused tissue, not one single equation can be applied to all tissues. A combination of models may be used to better describe

heat transfer [79].

Weinbaum and Jiji [76] also derived a new simplified bioheat equation to describe the effect of countercurrent exchange and capillary bleed off on local tissue heat transfer. They derived an expression for tensor conductivity in terms of the number density, flow velocity and geometry of the local thermally significant countercurrent vessels. In the new bioheat equation the blood-tissue heat transfer can be directly related to the local vascular ultrastructure and flow. A fundamental assumption used allows the local blood-tissue energy equation to be expressed in terms of only a single temperature variable, the local tissue temperature.

### 1. Consideration of Vascular Geometry

Detailed microvasculature geometry and blood flow distribution have a major effect on heat exchange between blood and tissue and the heat exchange between tissue near the surface and the external environment. A model of the vascular geometry must include length, diameter, orientation, and position in space for each vessel that participates significantly in heat transfer. The vessels should have numbers, sizes and branching characteristics typical of the tissue being modeled. Some algorithms have been developed to construct a vascular tree but they are not entirely accurate because the bifurcation angles are usually at right angles whereas vessels in real vascular trees tend to form different angles [63]. Therefore, in the model of the vasculature in the pallid bat wing all these different factors can be measured in order to have a realistic model. Even though the model is only two-dimensional, it can provide a lot of information as to how the vessels branch out from one another. Analyzing heat exchange in a two-dimensional tissue with a simplified vascular structure was the original objective of this work, however, given the importance of understanding the relationship between systemic parameters and vascular response, the direction of the

project was changed.

The new Weinbaum and Jiji model is a feasible model to use in this research as geometrical information about the vasculature in the pallid bat wing can eventually be obtained. This would consist of taking scans of the wing and measuring the lengths of each blood vessel, the angles of bifurcations and vessel diameters along the branches. Although the bat wing only has two main vascular structures, creating a correct representation of the vasculature can be very complicated and time consuming.

## CHAPTER III

## THE PALLID BAT AS AN ANIMAL MODEL

As described in the previous chapter, thermoregulation is highly affected by heat transfer through the skin. Heat transfer in the skin is controlled by the arrangement of the micro-vasculature as well as by the vascular response due to changes in body and skin temperature. In humans, studies have been carried out in an unanesthetized, thermoregulatory bed (i.e. skin) but direct measurements of vessel diameter or arterial blood flow have not been performed [1]. Introducing the pallid bat as an animal model allows for the direct visualization of a thermoregulatory bed (i.e. pallid bat wing) and for direct measurement of microvascular diameters and arterial blood velocity (vascular response) [1] in a controlled environment. The microvasculature in their wings is easily seen through a microscope and there is no need for destructive measuring techniques. The bats are trained to sleep or be still with one of their wings open which allows for observation without the need for anesthesia, which is known to have an effect on body thermoregulation in animals. Research shows that induction of anesthesia decreases metabolic heat production about 20% [48].

The wing of the pallid bat is being studied because the microvascular bed performs similar functions as that of the human skin in terms of thermoregulation. Research shows that there are several behaviors of the bat wing microvasculature that are analagous to those reported in human skin blood flow studies as described in [1]. Even though the vasculature in human skin and the pallid bat wing perform similar functions, it is important to note that the structure is very different. Figures 6 and 7 show the vascular structures in the wing of a bat and human skin, respectively. As shown in Figure 7, the larger countercurrent vessels (artery-vein pair) lie in a horizontal plane in the deeper portions of the cutaneous plexus. These larger vessels are

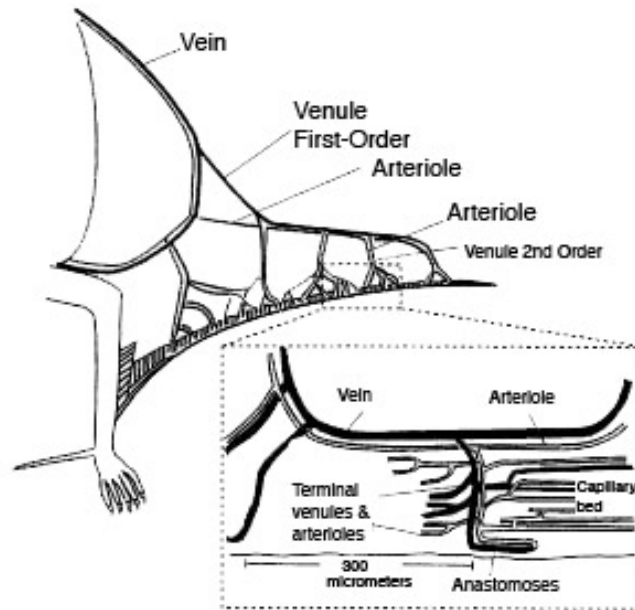


Fig. 6. Schematic drawing of capillary supply and anastomoses at edge of wing [80].

connected by arteriovenous anastomoses to the more superficial arterial and venous plexes just beneath and parallel to the surface of the skin. While the microvasculature in human skin is arranged at different depths, in the bat wing the microvasculature branches out across the wing on a horizontal plane. Because the ratio of surface area to volume of an organism is critical in thermoregulation the thermoregulatory capabilities in the pallid bat wing are likely to be different than those of human skin [1] because of the difference in magnitude of this ratio.

#### A. Thermoregulation in Bats

Bats are mammals that possess all the characteristic features of homeotherms, but also have the ability to fly which makes them very susceptible to the level of stored energy reserves. To maintain such reserves, bats undergo behavioral and metabolic changes that will be described in this section.



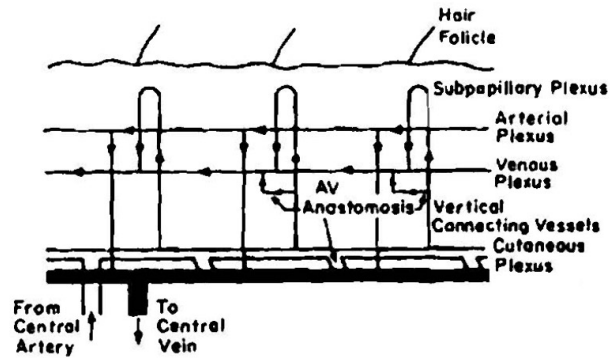


Fig. 7. Schematic of microvasculature of the cutaneous layer [42].

Bats are highly specialized for flight and therefore have difficulty with other forms of locomotion [81]. The anatomy of a typical bat is shown in Figure 8. The upper arm, or humerus, is shorter than the forearm. All bats have a short, clawed thumb, used to move around roosts, and four long fingers that serve to spread and manipulate the wing. The hind limbs of the bats are small and are attached at the hip in a reverse manner from other mammals. The hind foot has five toes which are all about the same length and used to hang upside down. The wing membrane consists of an upper and lower skin layer and is attached along the sides of the body and hind legs and is braced by the elongated finger bones, arms and legs [81].

Bats have body masses that range from 2 g to over 1,000 g [81]. Table II shows several species of bats in Texas and their corresponding sizes. It has been stated that body size exerts a great influence on most aspects of animal physiology including basal metabolic rate, minimum thermal conductance and propensity for heterothermy [2]. Since bats are small, they have a large relative surface area compared to the volume of their body which increases the energy losses and causes them to be very sensitive to changes in their environment [81]. The energy costs for keeping a constant

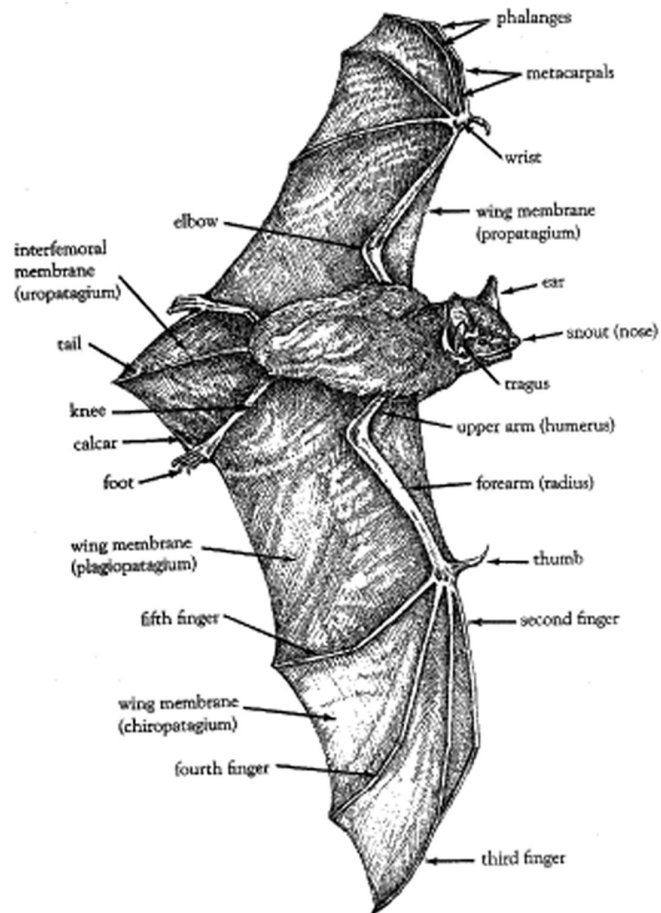


Fig. 8. Anatomy of a typical bat [81].

Table II. Different Species of Bats in Texas

Species	Weight ( <i>grams</i> )	Wingspan ( <i>mm</i> )	Wing area ( <i>cm</i> )
<i>D. ecaudata</i>	30-40	326	110
<i>E. fuscus</i>	13-20	325	162
<i>M. californicus</i>	3-5	220	77
<i>A. pallidus</i>	12-17	353	228
<i>E. perotis</i>	65	550	322

Note: Different species of bats have different body mass and different size wingspans. [81]

body temperature are high and can be problematic for small endotherms in various habitats [3]. Figure 9 shows that small animals have to sacrifice a large proportion of their energy intake in order to compensate for heat loss [80]. Flight is energetically expensive; bats have been able to compensate for the energy required in different forms including the evolution of a lung to procure the large amounts of oxygen needed for flight [82] and the ability to go into torpor in order to save energy [16]. Although bats increase their oxygen uptake by a factor of 20- to 30-fold during flight, and their energy demands increase, active flight is the most cost-effective form of locomotion [82].

In order to conserve energy bats respond with different behavioral and physiological strategies to changes in the environmental conditions. In cold temperatures, bats can cluster in different ways and move to different locations to receive sun radiation. Bats also respond to changes in the seasons by moving to more favorable areas, or

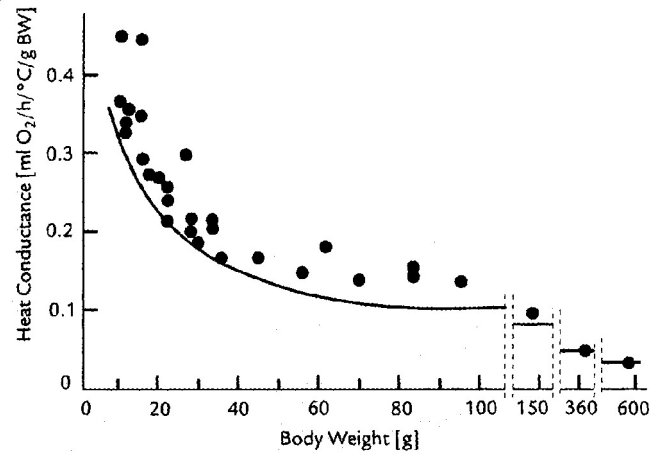


Fig. 9. Heat loss as a function of body weight [80].

migrating [81]. They migrate to warmer latitudes at the beginning of winter. Migration is not well studied in bats, and destinations and distances traveled are poorly known [81].

In areas with favorable conditions, bats use roosting sites to rest, groom, and interact with other bats. Since bats are very sensitive to factors such as temperature, relative humidity or light intensity, they will occupy only sites where variation of such factors is controlled within a specific range [81]. Bats may roost alone or in small groups. Some bats, like the pallid bat (*Antrozous pallidus*), use roosting sites to hibernate in tightly packed clusters. Although this behavior is not well understood, it probably helps bats stabilize their body temperature when environmental conditions change. Bats near the center are better protected against changes, and are probably better able to conserve their supply of body fat [81].

Roosting sites of bats differ and vary according to the species of bats. The major environmental conditions that determine bat distribution and abundance are climate, roosts, food and other animals-predators and competitors [81]. Climate and

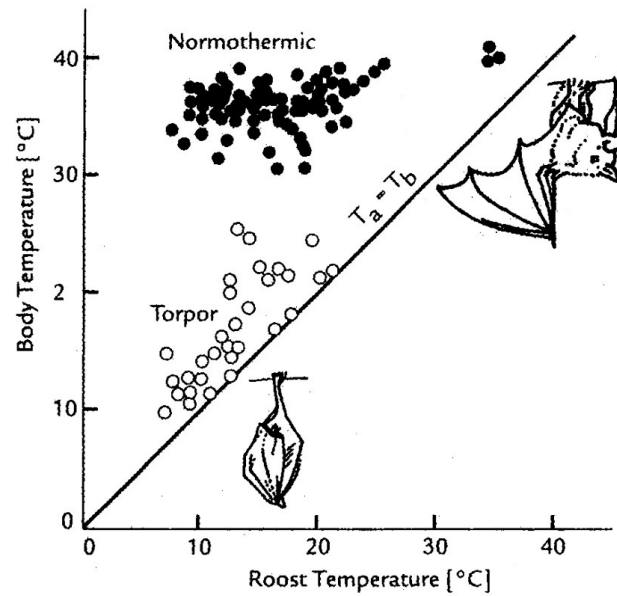


Fig. 10. Alterations in body temperature of bats during torpid and euthermic conditions [80].

roosts are the most important factors in determining where the bats live due to the expenses correlated to temperature regulation and its importance for the survival of bats. They mostly reside in tropical areas, but live nearly everywhere on earth except in the polar regions, highest mountains, and some remote islands [81]. Figure 10 shows that the temperature range of roosts falls between about  $5^{\circ}\text{C}$  to about  $40^{\circ}\text{C}$ . In cold temperatures below  $20^{\circ}\text{C}$  some bats may become torpid to conserve energy without the need to maintain their body temperature within the normal range.

All organisms have a *thermoneutral zone*; this is the ambient temperature range, bounded by upper and lower critical temperatures, where a resting animal can maintain a constant body temperature without the need to produce additional energy to survive [80]. When the ambient temperature is lower than the critical point, or the lower limit of the thermoneutral zone, bats can generate heat and maintain their body

temperature by increasing metabolic activity. This can be achieved through shivering [80]; but since generating heat consumes energy, the best solution to maintain sufficient energy reserves for take off and other actions is to enter a state of torpor.

*Torpor* is a state of diurnal lethargy, where bats allow their body temperature to drop close to or equal to the ambient temperature allowing them minimize their metabolic needs [80]. This decision is based not only on the ambient temperature but also on the availability of food and on reproductive condition; it is possible to find both active and lethargic animals in the same colony on the same day (Figure 10) [80]. The ability to enter a state of torpor is also influenced by the basal metabolic rate; a low metabolic rate is correlated with the ability to go into torpor. It is critical that bats remain in a state of torpor for a limited amount of time because if their body temperatures remain low for a long period of time they might not have the ability to return to their normal body temperature and will die [80].

Bats that have a larger body mass do not necessarily have to enter a state of torpor to conserve energy. Since the ability to become torpid is influenced by the basal metabolic rate and the basal metabolic rate is dependent on body weight, therefore, larger bats may not go into torpor at all [80]. Also, as was mentioned before, surface area plays an important role in thermoregulation in small animals. Larger bats have a lower surface area to volume ratio and therefore lose less heat than smaller bats at a given temperature.

## B. Energy Saving and Expenditure of Bats

Different researchers have investigated different areas of bat behavior dealing with temperature regulation. Torpor use and thermal energetics were studied in one of the smallest (4 g) Australian vespertilionids, *Vespadelus vulturnus* [2]. Researchers

found that bats showed a high propensity for torpor and typically aroused for only brief periods. Values for upper and lower critical temperatures of the thermoneutral zone, basal metabolic rate, resting metabolic rate, torpid metabolic rate, and wet thermal conductance over a range of ambient temperatures were measured. Body temperature was also measured during torpor and normothermia. The results indicate that the *V. vulturnus* is adapted to minimizing heat loss at low ambient temperatures. This shows that vespertilionid bats have evolved energy-conserving physiological traits, such as low basal metabolic rate and propensity for torpor [2]. Figures 11, 12, 13, and 14 show the results from [2]. Figure 11 shows that torpid bats maintain a very low metabolic rate throughout the entire temperature range while normothermic bats have a higher metabolic rate at lower temperatures and it decreases as the ambient temperature increases. Figure 12 shows that while bats are in a state of torpor, their bodies are at a temperature almost equal to that of the environment. Figure 13 shows that wet thermal conductance of normothermic bats below the thermoneutral zone was higher than the wet thermal conductance for torpid bats. Lastly, Figure 14 shows that vespertilionids usually have lower basal metabolic rate relative to other bats and have therefore evolved energy-conserving physiological traits.

During reproduction, torpor behavior changes in female bats. The use of torpor during reproduction is relatively uncommon presumably because of the costs associated with a lowered metabolic rate [5]. Pregnant and lactating female *E. fuscus* use torpor to the same extent overall (degree-min), but pregnant bats used torpor less frequently and with more time in deep torpor. During post-lactation, females reached significantly lower minimum skin temperature than during lactation, even though they were in the same ambient temperatures [5]. During post-lactation, greater use of torpor reduced the energy lost to the surroundings, and females saved energy as

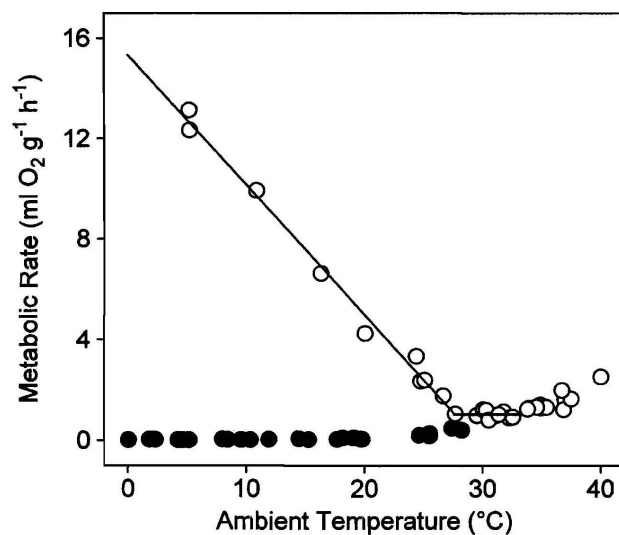


Fig. 11. Relationship between metabolic rate and ambient temperature during normothermia (open circles) and torpor (filled circles) for *Vespardelus vulturnus* (4g) [2].

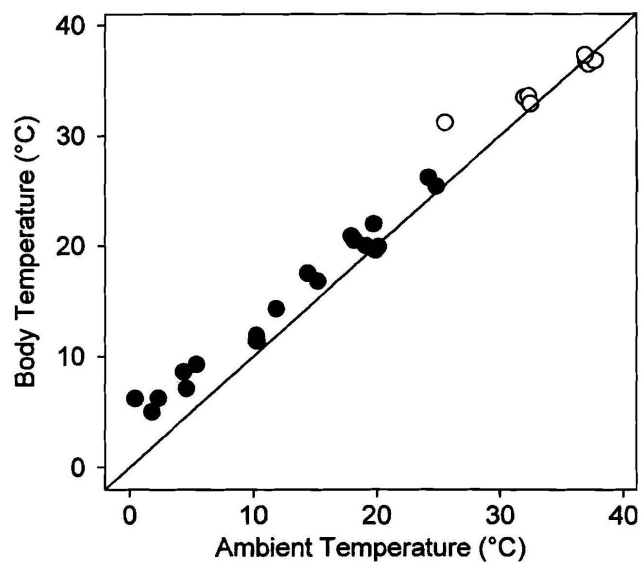


Fig. 12. Relationship between ambient temperature and body temperature for torpid (filled circles) and normothermic (open circles) bats (*V. vulturnus*, 4g) [2].



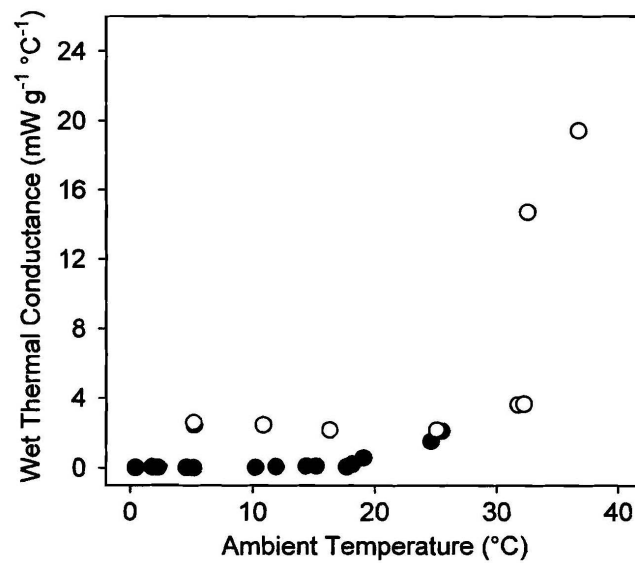


Fig. 13. Relationship between ambient temperature and wet thermal conductance for torpid (filled circles) and normothermic (open circles) *V. vulturnus* [2].

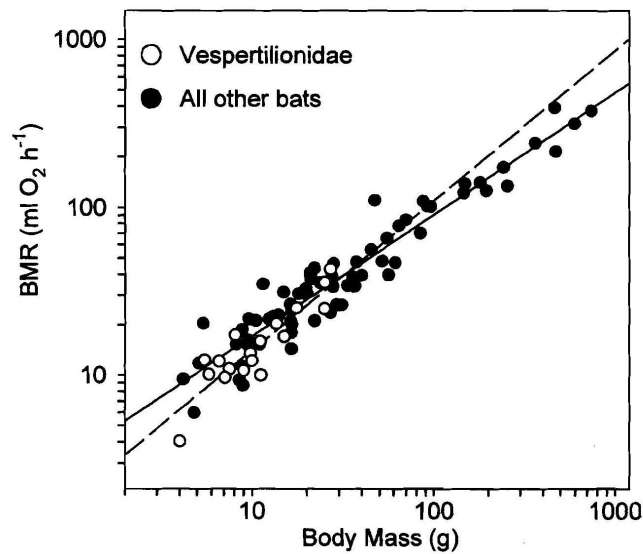


Fig. 14. Relationship between body mass (g) and basal metabolic rate for 18 species of bats, including *V. vulturnus* (4g). The plots are shown in base 10 log [2].

they prepared for hibernation. This shows that while pregnant and lactating female bats will not go into torpor as often as post-lactating females because it can affect the survival of their young.

Hosken et al [3], studied the *Chalinolobus gouldii* to investigate the thermal and metabolic physiology over a range of ambient temperature. They found the rate of oxygen consumption, ( $\dot{V}_{O_2}$ ) and the rate of carbon dioxide production, ( $\dot{V}_{CO_2}$ ), respiratory quotient, evaporative water loss (EWL), and thermal conductance at various ambient temperatures and compared euthermic and torpid bats [3].

The ability to lower body temperature and energy use is very important, especially for small animals, to survive in cold and unproductive habitats [3]. Use of torpor in the *C. gouldii* leads to significant energy savings. The *C. gouldii* is able to enter into torpor and spontaneously arouse at ambient temperatures as low as  $5^{\circ}C$ . At low ambient temperature ( $\leq 10^{\circ}C$ ), torpid *C. gouldii* begin to regulate their body temperature by increasing metabolic heat production; the evaporative water loss is reduced during torpor; the thermal conductance, which was explained in the previous chapter, is considerably lower for torpid bats at intermediate body temperature and ambient temperature, but increases to euthermic values for torpid bats at low ambient temperatures [3]. It is important to recall that thermal conductance is used as a way to measure an organism's ability to adapt to a cold or hot environment [16].

Figure 15 shows the relationship between the metabolic rate and ambient temperature for bats when euthermic, passively torpid, and torpid but thermoregulating. The metabolic rate for passively torpid bats is almost non-existent but for torpid but thermoregulating bats, the metabolic rate can be very high at lower ambient temperatures.

The changes in thermal conductance for an Australian bat are shown in Figure 16. The wet conductance increases as the ambient temperature approaches the body

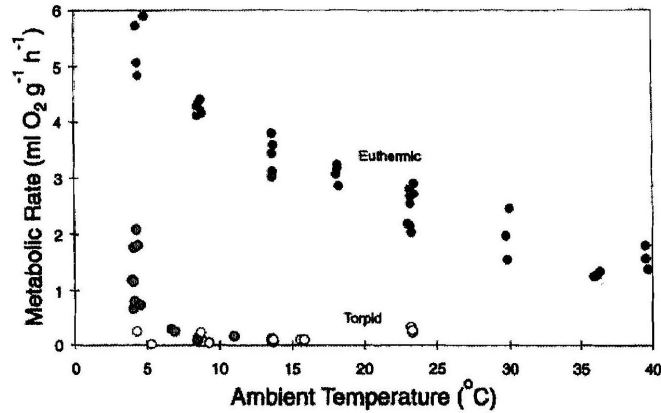


Fig. 15. Relationship between metabolic rate and ambient temperature for euthermic (filled circles), torpid (open circles) and torpid but thermoregulating (gray circles) bats (*Chalinolobus gouldii*, 17.5g)[3].

temperature and grows significantly if the ambient temperature is equal to the body temperature. The dry conductance followed the same pattern as the wet conductance. The mean dry conductance for euthermic bats was  $3.41 \text{ J} \cdot ^\circ\text{C}/\text{g}\cdot\text{h}$  and for torpid bats it was  $0.65 \text{ J} \cdot ^\circ\text{C}/\text{g}\cdot\text{h}$  [3].

### C. Circulation in the Bat Wing

Bats are less able to protect themselves from overheating than from overcooling. The only means of lowering the body temperature in a hot environment is through evaporative cooling and the creation of convection currents by movement of air [80] and through effective blood volume in the wing. The bat wing is a thermoregulatory bed and therefore the circulation in the wing plays an important factor on heat exchange with the environment.

During flight, about 86% of the metabolic heat load is lost through the surface by evaporation, conduction-convection, and radiation [4]. It is well known that the

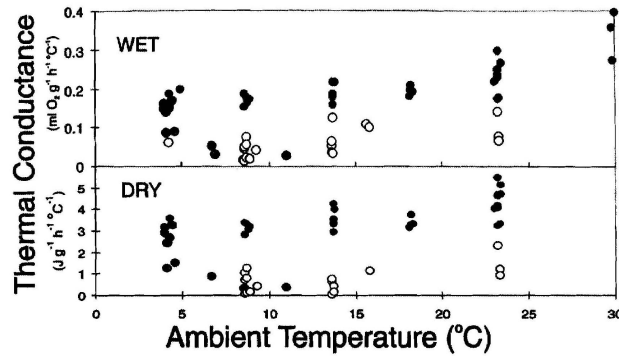


Fig. 16. Relationship between wet and dry thermal conductance and ambient temperature of euthermic (filled circles), torpid (open circles) and torpid but thermoregulating (gray circles) bats (*C. gouldii*) [3].

cardiovascular system is important in regulating heat transfer and that during heat stress, blood is shunted to the surfaces that are best suited for effective heat loss [4]; in the case of the bat, the surface best suited for heat loss is the wing because it corresponds to about 80% of the total surface area and consists of two main vascular structures. Therefore, studying blood flow in the wing vasculature can give information about thermoregulation of these animals and peripheral vascular control.

The large surface area of the wing membrane requires good circulation. The large vessels in the flight membrane branch out to first-order venules and arterioles, which in turn branch out to secondary branches as shown in Figure 6. The arteries of the wing membrane show capillary networks and anastomoses which are shunts formed by the direct connection of arteries with the elastic venous system. Some researchers say that anastomoses open during flight because at high heart rates more blood is pumped into the flight membrane than is necessary [83, 4]. When the bat is resting, the anastomoses close so that blood flows through the highly branched capillary network. The regulation of anastomoses plays a role in thermoregulation,

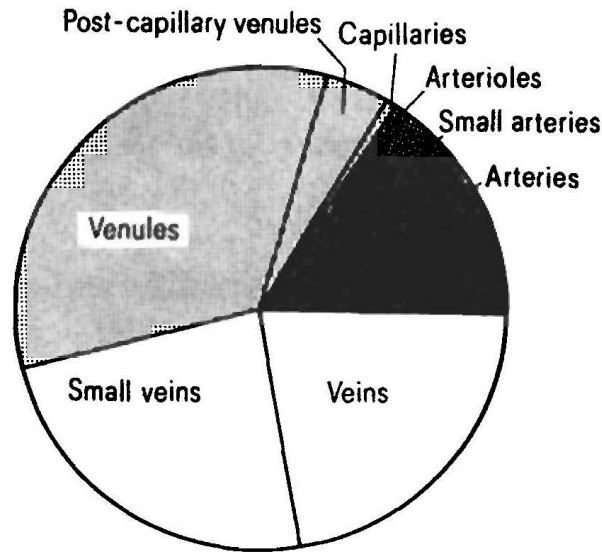


Fig. 17. Percentages of blood volumes in different vessels of the bat wing [83].

but there have been no experiments on this subject [80].

Figure 17 shows the percentages of blood volumes contained in various portions of vascular beds in the bat wing. Venules are part of the low pressure side of the vascular exchange bed, and therefore have a greater blood volume than the rest of the vessels. Also, a greater proportion of the venous volume of the bat wing is in small veins as opposed to larger ones [83].

Blood vessels in the bat wings follow a general pattern in many different species of bats. Figure 18 shows the vascular structure in a bat wing. Although this is a figure of the vasculature of the species *Antrozous pallidus*, most bat wings have a very similar structure but vary greatly. The branching of the major artery-vein pairs are necessary in order to accomplish good circulation in the entire area of the wing membrane [80].

Wing blood vessels studied in this research range from about 25  $\mu\text{m}$  to about

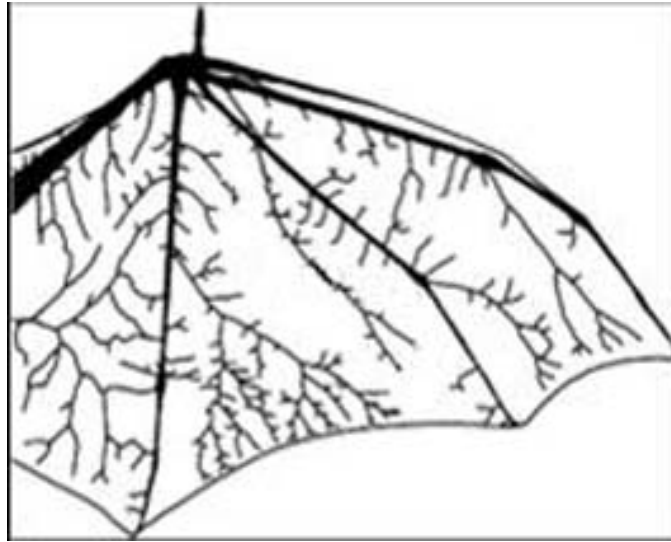


Fig. 18. General shape of vasculature in bat wings, specifically pallid bat (*Antrozous pallidus*). Figure created by Missy F. Young.

60  $\mu\text{m}$  in diameter. The diameter of such vessels as well as their length are an indication that when blood travels through the wing it reaches a state of thermal equilibrium where the temperature of the blood is equal to that of the tissue. Thermal equilibration of blood vessels allows blood at higher temperatures (from the core) to cool down as it passes through the circulatory system in the wing and return to the core at lower temperatures, therefore also cooling the body.

## CHAPTER IV

### EXPERIMENTAL METHODS

#### A. Proposed Experiments

Using the pallid bat as the animal model to study different aspects of thermoregulation is useful because different non-invasive experiments can be performed. The pallid bat colony that is used in this research has been trained to remain calm during experimental procedures. In this project, there were two different objectives; one was the study of thermoregulation through metabolic activity of the pallid bat at different ambient temperatures; the second was the effect of total body or systemic heating on the wing vasculature. These objectives and experimental procedures will be explained in the next paragraphs and sections. Experiments for this research were conducted under the Animal Use Protocol (AUP 2007-110) approved by the Institutional Animal Care and Use Committee.

Metabolic activity was studied in the pallid bat by the use of open flow respirometry [3, 2, 8, 7, 6] as done in previous studies involving thermoregulation of bats.  $O_2$  consumption and  $CO_2$  production were measured during the experiments in order to find metabolic activity. At the same time, changes in the wing vasculature at different ambient temperatures were observed; as it has been previously stated, the wing vasculature has a great effect on thermoregulation of the bat. As the ambient temperature changes, so does the body temperature, thus requiring the use of thermoregulatory mechanisms such as vasomotion to diminish the effects of external temperature variations. Changes in the wing vasculature were monitored by observing changes in vessel diameter and blood velocity and heat flux was measured in the wing in order to quantify the heat released to the environment from the wing at different ambient

temperatures. From these experiments, it is possible to obtain correlations between ambient temperature, body temperature, metabolic activity, heat flux from the wing and vascular response in the wing and therefore learn about the thermoregulatory mechanisms of the pallid bat.

## B. Animals

Metabolic rate, body temperature and vascular response were investigated in 10 pallid bats, 8 females and 2 males. The bats were captured from the wild from western Texas (Scientific Research Permit Number SPR-0503-308) and were taken to College Station, Texas where they were cared for in the comparative medicine building at Texas A&M University. They were kept in a flight room specially designed to allow roosting, feeding and flight/exercise. The room was kept at a stable temperature and was constantly maintained in terms of cleanliness, feeding, and habitat. The bats were kept in a light-dark cycle of 7 hours of light (during which they were sleeping) and 17 hours of dark (during which they were feeding). After they learned how to eat in captivity, the bats were offered unrestricted access to meal worms, wax worms and crickets. The bats were identified by means of a dot system dyed into the fur on the back of each bat.

Experiments on the bats were allowed after six months of captivity. Since the experiments were conducted in a different building to that which they were housed in, they were transported between the two buildings via a small, woven cloth cage with blankets to ensure their safety and minimal exposure to light.



### C. Experimental Set-Up

Rates of  $O_2$  consumption ( $\dot{V}_{O_2}$ ) and  $CO_2$  production ( $\dot{V}_{CO_2}$ ) were determined using open flow respirometry in a controlled environment; these measurements served to estimate basal metabolic activity of the pallid bat. The experimental set-up for determining the bats' metabolic activity at different ambient temperatures consists of an air pump, a 5850E Brooks Mass Flow Controller, the Brooks Microprocessor Control & Read Out Unit Model 0152, a variable power supply (Agilent E3615A) that is used to power up a peltier cell (TECH1-12705) inside a heating box, the metabolic chamber, Vernier oxygen and carbon dioxide gas sensors and the Vernier data acquisition system. In addition, OMEGALUX silicone rubber fiberglass insulated flexible heaters (Omega) were placed under the bottom surface of the metabolic chamber when needed to set the bottom surface at a temperature higher than the ambient temperature to avoid heat loss to the environment; also, a digital ceramic heater was used in the vicinity of the metabolic chamber to increase ambient temperature outside of the chamber (Figure 19).

Temperatures and heat fluxes of the bats and the metabolic chamber were monitored and collected using heat flux and temperature sensors connected to an Omega USB Data Acquisition Module (OMB-DAQ-56). Changes in the wing vasculature of the bat were monitored with the use of an OLYMPUS BX61WI microscope equipped with a Sony Color Video Camera, which allows for tracking of vessel diameter through the LabView software and changes in blood velocity using an optical doppler velocimeter in addition to the software. Laser doppler velocimetry (LDV) is a technique used to make instantaneous velocity measurements of red blood cells in order to determine an average centerline velocity.

For the experiments, the air pump was turned on and provided air directly to

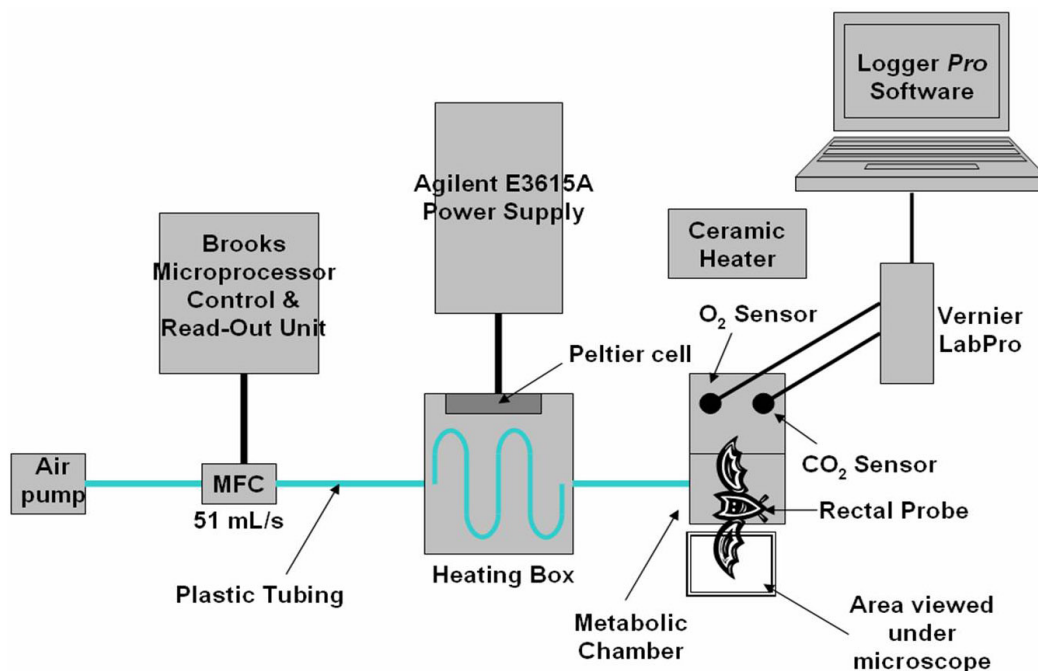


Fig. 19. Diagram showing experimental setup.

the 5850E Brooks Mass Flow Controller; the flow of air was controlled at a rate of 51 mL/s by the Brooks Microprocessor Control & Read Out Unit Model 0152. From the 5850E Brooks Mass Flow Controller, air flowed inside a long plastic tube through the heating box and coiled around a base constructed to allow for the air inside the tube to be heated as it flowed through the heating box. This heating box had a peltier cell in place that was heated using the variable power supply (Agilent E3615A) and could reach temperatures of up to about  $100^{\circ}\text{C}$ . The temperature in the heating box was controlled by varying the voltage and current from the power supply. In order to achieve the desired temperature of the air inside the tube, the voltage was turned on at maximum capacity and changed according to need. Air temperature ranged from between  $26^{\circ}\text{C}$  and  $36^{\circ}\text{C}$  after passing through the heating box. This temperature range was chosen so that the bat would not be in danger of overheating, as  $36^{\circ}\text{C}$

is below the maximum temperature reported in calorimetric studies which deal with bats of different species but of similar size [3, 2, 6, 8, 7].

After the air passed through the heating box it flowed into the metabolic chamber. The metabolic chamber was built and characterized specifically for this research; it is divided into two sections, one section is where the bat is placed and the other section houses the  $\text{CO}_2$  and  $\text{O}_2$  gas sensors (Vernier). The two sections are separated by a plastic mesh to prevent the bat from damaging the sensors. Air enters into the metabolic chamber in the side where the bat is located and exits through the side where the gas sensors are placed. The gas sensors are connected to a laptop through the Vernier LabPro interface; data is collected using the Logger *Pro* software.

In order to avoid temperature losses once the air is inserted in the metabolic chamber, when needed, OMEGALUX silicone rubber fiberglass insulated flexible heaters (Omega) were placed under the chamber in the side where the bat is located. These heating strips are controlled by a Watlow Series SD PID Controller via a Solid State Relay of Carlo Gavazzi and are maintained at a maximum temperature of about  $32^\circ\text{C}$  so that the lower surface of the chamber did not overheat, therefore avoiding the possibility of damage to the bats.

#### D. Open Flow Respirometry

Open flow respirometry consists of pumping fresh air of known oxygen ( $\text{O}_2$ ) and carbon dioxide ( $\text{CO}_2$ ) concentrations into a metabolic chamber with an organism in place. Air flows from the inlet to the exit through the metabolic chamber; the concentrations of  $\text{O}_2$  and  $\text{CO}_2$  at the exit of the metabolic chamber are determined and the difference between the levels of oxygen and carbon dioxide from the air going in and the air going out help determine metabolic activity. In the metabolic chamber

constructed for this experiment, the changes in O<sub>2</sub> and CO<sub>2</sub> levels were monitored using Vernier gas sensors.

The measurements were used to find the rate of carbon dioxide production ( $\dot{V}_{CO_2}$ ) and the rate of oxygen consumption ( $\dot{V}_{O_2}$ ); this then determined metabolic rate because the rate of carbon dioxide production and metabolic rate are proportional to each other. The measurements were also used to determine dry and wet conductance (defined in Chapter II, Section E) of the pallid bat which are necessary to characterize the bat's environmental energy exchange.

### 1. Metabolic Rate Calculations

$\dot{V}_{CO_2}$  and  $\dot{V}_{O_2}$  were determined from the information obtained with the oxygen and CO<sub>2</sub> gas sensors.  $\dot{V}_{CO_2}$  [mL CO<sub>2</sub>/g·h] was determined by:

$$\dot{V}_{CO_2} = \frac{ppmCO_{2_{produced}} \cdot \dot{m} \cdot 3600}{10^6 \cdot W \cdot h}, \quad (4.1)$$

where ppmCO<sub>2<sub>produced</sub></sub> is defined as ppmCO<sub>2<sub>bat</sub></sub> - ppmCO<sub>2<sub>air</sub></sub>; ppmCO<sub>2<sub>air</sub></sub> is the amount of CO<sub>2</sub> in the metabolic chamber without the presence of the bat and ppmCO<sub>2<sub>bat</sub></sub> is the amount of CO<sub>2</sub> in the metabolic chamber with the bat in it.  $\dot{m}$  is the air flow rate into the chamber in mL/s,  $W$  is the mass of the bat in grams and  $h$  is the unit of time, hour.  $\dot{V}_{O_2}$  [mL O<sub>2</sub>/g·h] was determined as:

$$\dot{V}_{O_2} = \frac{\%O_{2_{consumed}} \cdot \dot{m} \cdot 3600}{100 \cdot W \cdot h}, \quad (4.2)$$

where %O<sub>2<sub>consumed</sub></sub> is % O<sub>2<sub>air</sub></sub> - % O<sub>2<sub>bat</sub></sub> and the variables are the same as before.

From this information, we were able to calculate  $C_{wet}$ ,  $C_{dry}$ ,  $MHP$ , and  $EHL$  ( $C_{wet}$  and  $C_{dry}$  were defined in Chapter II, Section E, Equations 2.6 and 2.7).  $C_{wet}$  [mL O<sub>2</sub>/g·h·°C] was calculated as  $C_{wet} = \dot{V}_{O_2}/T_b - T_a$ , where  $T_b$  is body temperature and  $T_a$  is ambient temperature.  $C_{dry}$  [J/g·h·°C] was determined as  $C_{dry} = MHP -$

$EHL/T_b - T_a$ , where  $MHP$  is metabolic heat production [J/g·h] calculated from  $\dot{V}_{O_2}$  assuming 20.1 J per mL  $O_2$  and  $EHL$  is evaporative heat loss [J/g·h] calculated from evaporative water loss assuming a latent heat of vaporization of 2300 J/g [3].

#### E. Protocol

This research consisted of three different protocols; the protocols are almost identical except for the time when the bat is placed inside the metabolic chamber. The first step of all three protocols consisted of assembling the entire system as described in the Experimental Set-Up section. Two temperature sensors were placed inside the metabolic chamber as follows: one thermocouple was placed near the plastic mesh in the chamber to measure air temperature inside the chamber ( $T_{chamber}$ ); and the other was placed to measure air temperature at the inlet of the metabolic chamber ( $T_{Air\ in}$ ).

Next, the Omega USB Data Acquisition Module (OMB-DAQ-56) and the Vernier LabPro were connected to a laptop through an USB cable. The laptop was then turned on and was prepared to begin acquiring data at any given point in time. Once the system was prepared to begin taking measurements, the bat was also prepared for placement inside the chamber. This consisted first of deadening the tissue in the rectum by inserting a rectal probe covered in 2% lidocaine gel for about 15 seconds. After the tissue was deadened and in order to monitor body temperature ( $T_{body}$ ) throughout the entire experiment, the rectal probe (Phsyitemps Instruments, Inc.) designed for mice, which has a smooth ball tip of 0.065" in diameter and a 0.75" long stainless steel shaft of 0.028" diameter was reinserted and left in the bat. Previous calorimetric research shows that body temperature was obtained in this manner [3, 2, 6, 8, 7].

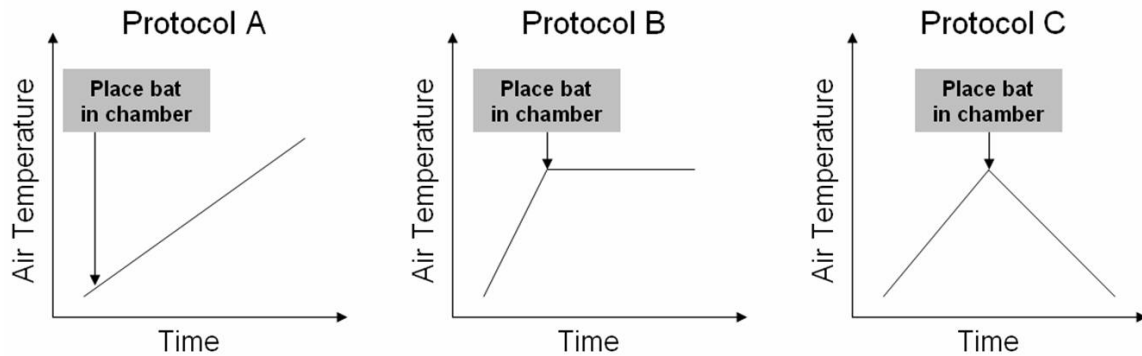


Fig. 20. Schematic of Protocols: **A)** dynamic heating, **B)** constant temperature, and **C)** dynamic cooling.

In the first protocol, the bat was placed inside the chamber at the same time that the heating box was turned on; this allowed for observation of responses while heating (Figure 20A). Figure 20B shows that the air going into the metabolic chamber is first heated to a desired temperature before the bat is placed inside the metabolic chamber (second protocol). Figure 20C shows that the air is first heated to a maximum temperature and when the bat is placed into the metabolic chamber, the heating box is then turned off in order to observe the effects that cooling has on the bat (third protocol).

For each protocol, the bat was placed inside the metabolic chamber with one wing spread out to be viewed under the microscope (OLYMPUS BX61WI). The wing was restrained with Playdough and q-tips so as not to disturb the bat with hard restraints that could produce vascular damage. In order to maintain the chamber as airtight as possible, the area around the wing was covered with silicone plastic clay (Silly Putty) to seal any possible spaces between the wing and the chamber. At this time, the data acquisition systems (Omega USB Data Acquisition Module and *LoggerPro*) began collecting data.

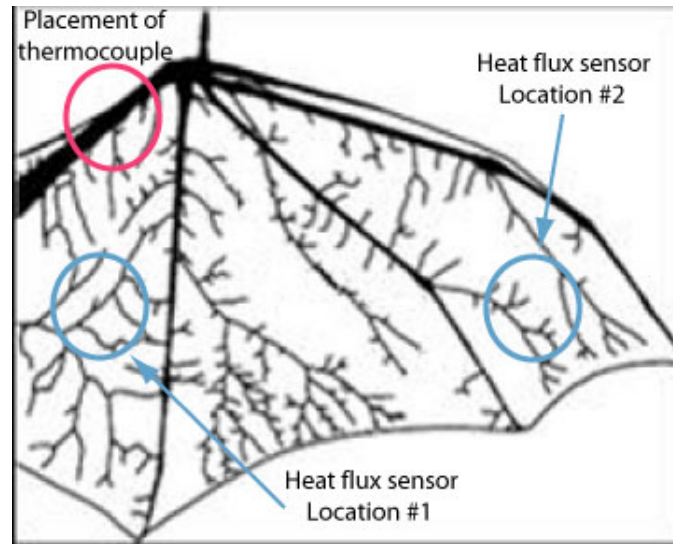


Fig. 21. Placement of heat flux sensors and thermocouples in the pallid bat wing. Modified figure created by Missy F. Young.

Other sensors were then placed on the bat as follows: two heat flux sensors embedded with thermocouples were placed on the wing ( $T_{wing}$  and  $q_{wing}$ ); and, a thermocouple was placed in the arm of the bat ( $T_{arm}$ ) (Figure 21). The heat flux sensors were manufactured by Concept Engineering, CT. They are flat plate transducers designed to measure heat flow through a surface where the plate is applied. The flow of heat from or to the surface in consideration creates a small temperature difference between the upper and lower surfaces of the meter. These surfaces are in thermal contact with a special, miniature, high temperature thermopile, which generates a direct current signal from the temperature difference and serves to estimate the surface heat flux.

During the time while and after the bat was placed inside the metabolic chamber, if the room was too cold, the digital ceramic heater was turned ON for about 15 minutes during which the wing was being positioned under the microscope in order to minimize heat loss to the environment. After temperature stabilization, the digital

ceramic heater was then turned OFF and data acquisition continued for up to 2 hours. Data was collected from the O<sub>2</sub> and CO<sub>2</sub> gas sensors through the *LoggerPro* software in % and ppm, respectively. Data from all the heat flux sensors and thermocouples was collected through the Omega USB Data Acquisition Module. Vessel diameter and blood velocity of sections of the two main vascular structures of the wing were tracked using the Sony Color Video Camera and the LabView software. After about 1 and 1/2 hours of measurements, the sensors were removed from the bat, the bat was then removed from the metabolic chamber and placed in the woven cloth cage ; each bat was only used one time per week in order to avoid misuse of the animals.

#### F. Effects on Wing Vasculature

The two main vascular structures of the wing were defined as vascular structure A (VSA) and vascular structure B (VSB). Each vessel segment is considered a vector quantity that has a length and direction following the format in [84]. Lengths and angles of each branch were measured in order to accurately describe each vessel. The lengths and angles were measured manually from wing scans of different bats that were filtered in Adobe Photoshop in order to better observe only the two main vascular structures.

By studying the vasculature, it is possible to find a relationship between temperature and blood flow as well as the thermal response of the bat to hot environments. The parameters obtained were helpful in determining how much heat was transferred from the wing to its surroundings from the effect of higher ambient temperatures inside the chamber where the body of that bat was located. These measurements also helped to: **1)** quantify the amount of heat exchange with the environment when the body and wing were kept at different temperatures, and **2)** create correlations



between skin temperature and body temperature to allow for the possible elimination of body temperature measurements in future experiments.

## CHAPTER V

## ANALYSIS AND DISCUSSION OF EXPERIMENTAL RESULTS

Experiments of systemic heating were performed under two different protocols (AUP 2006-253 and AUP 2007-110) approved by the Institutional Animal Care and Use Committee of Texas A&M University. These experiments provided the information necessary to study correlations between metabolic chamber temperature ( $T_{chamber}$ ), body temperature ( $T_{body}$ ), wing temperature and heat flux ( $T_{wing}$  and  $q_{wing}$ ), and arm temperature ( $T_{arm}$ ) during systemic heating. Different experimental protocols were used in order to estimate the heat exchange that takes place between the body and the environment through the wing and to analyze responses of the pallid bat due to systemic heating. In this Chapter, analysis of the experimental findings will be discussed and modifications to the procedures will be proposed.

Experiments under the two protocols include:

- Analysis of body temperature and basal metabolic activity (basal or normal ambient conditions) of the pallid bat at **normal** ambient temperatures *without* the wing extended;
- Analysis of body temperature through the use of a rectal probe and metabolic activity by monitoring CO<sub>2</sub> production of the pallid bat at **higher** ambient temperatures *without* wing extended;
- Analysis of body temperature, wing temperature, metabolic activity and vascular response in the wing (blood vessel diameter and blood flow) at **normal** ambient temperatures *with* wing extended; and
- Analysis of body temperature, wing temperature, metabolic activity and vascular response of the pallid bat at **higher** ambient temperatures *with* wing extended.

### A. Basal Conditions

Twenty-nine experiments (AUP 2006-253) were performed while the bats were completely enclosed inside the metabolic chamber under normal ambient conditions; the response of some bats was recorded more than one time, depending on the day the experiment was scheduled, but bats were not used more than once a week per protocol. Body masses of the pallid bats used in these experiment ranged between 17.2g and 27.18g with an average of  $22.17 \pm 2.86$ g. All experiments were performed between 10:00 in the morning and 4:00 in the afternoon, so circadian rhythms might have an effect on body temperature and metabolic activity measured. Figure 22 shows the recorded body temperature; the average basal body temperature for the pallid bat (*Antrozus pallidus*) recorded is  $T_{body,o} = 30.4 \pm 1.6^{\circ}\text{C}$ , which is in a similar range to other bat species of comparable size; however, this information for the pallid bat cannot be found in existing literature. Also, the average metabolic rate for the 29 bats, following Equation 4.2 in Chapter IV, was observed to be  $4.092 \pm 3.3$  mL O<sub>2</sub>/g·h. The large variation is due to the fact that some bats never reached a metabolic state as observed in Figure 23.

As discussed in Chapter IV, metabolic activity was determined through the use of open flow respirometry (Equations 4.1 and 4.2). Oxygen (O<sub>2</sub>) and carbon dioxide (CO<sub>2</sub>) content for two different bats at normal ambient conditions is shown in Figure 23. Figure 23 shows that when CO<sub>2</sub> levels inside the metabolic chamber go up, then O<sub>2</sub> levels go down. Metabolic activity from the bat while inside the metabolic chamber is monitored by looking at CO<sub>2</sub> production; any movement due to either stress or discomfort, as indicated in Figure 23A, causes the carbon dioxide levels to increase rapidly and a reduction of oxygen content in the metabolic chamber. These changes in carbon dioxide and oxygen levels indicate an increase in metabolic

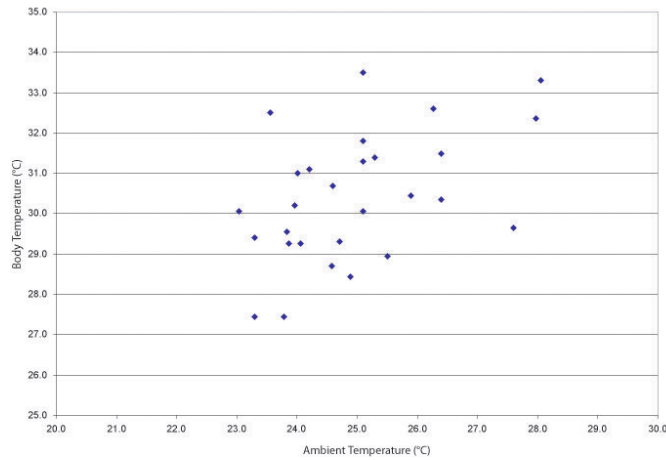


Fig. 22. Body temperature from twenty-nine experiments where the pallid bat (*Antrozus pallidus*) is completely enclosed inside the metabolic chamber; average basal body temperature is  $T_{body,o} = 30.4 \pm 1.6^\circ\text{C}$ .

activity. In Figure 23B, the reduction in oxygen and increase in carbon dioxide levels inside the metabolic chamber best describe the initial stress of the pallid bat when located inside the metabolic chamber. In order to stop a constant increase in  $\text{CO}_2$  levels ( $\text{CO}_2$  saturation can harm the animal), a hole in the metabolic chamber was unplugged following Animal Use Protocol 2006-253, to allow a greater amount of fresh air inside while the bat was able to calm down. The pallid bat used in Figure 23B was able to reach a metabolic steady state.

## B. Systemic Heating

During systemic heating experiments, the metabolic chamber was heated by inserting warm air into it at temperatures higher than  $26^\circ\text{C}$ . The bat was placed inside the metabolic chamber at the same time that the heating system was turned on; however, tracking of diameter and centerline velocity was not started until after anywhere from 30 minutes to 1 hour depending on how long it took to locate and focus on an arteriole.

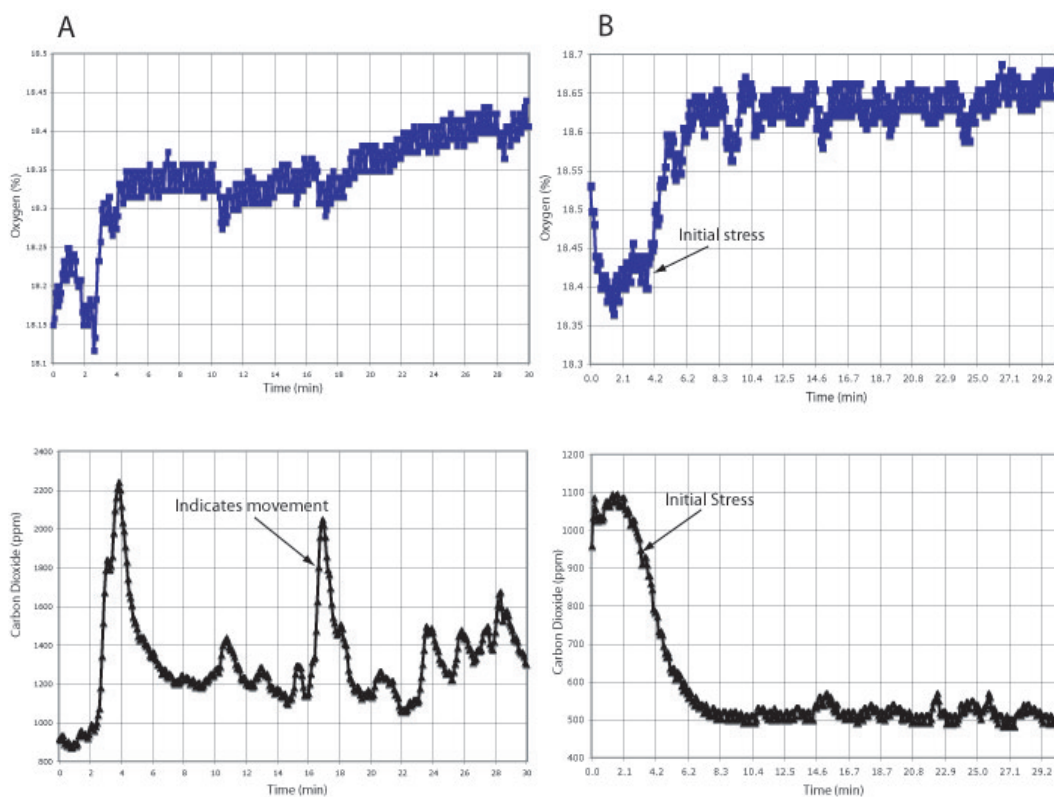


Fig. 23. Oxygen ( $O_2$ ) content and carbon dioxide ( $CO_2$ ) content for two different bats during normal ambient conditions. **A)** B11, Female, 24.41g; at the points where carbon dioxide increases due to movement, oxygen values are reduced. Bat B11 never reached a steady state as indicated by the oscillations in  $CO_2$ . **B)** B13, Female, 24.07g; plots show that bat B13 was at a metabolic steady state throughout experiment. Initial peak in  $CO_2$  indicates that the bat was stressed when first placed inside the metabolic chamber.

After  $T_{chamber}$  reached the maximum temperature of  $36^{\circ}\text{C}$ , the heating system was shut off to let the metabolic chamber cool down as indicated in Figure 20C. In the analysis presented hereafter for systemic heating experiments, the temperature inside the metabolic chamber will show both the protocol for dynamic heating (Figure 20A) and for dynamic cooling (Figure 20B). In our experiments, dynamic cooling does **not** indicate that the temperature falls below normal ambient conditions, but decreases from the maximum  $T_{chamber} = 36^{\circ}\text{C}$  to a value of 32 to  $33^{\circ}\text{C}$  depending on the amount of time allotted for the experiment in the lab. In some figures, we will analyze these two periods separately while in others they will be presented simultaneously.

Monitoring body temperature in the pallid bat during systemic heating experiments was critical to avoid heat stroke or any other situation that could compromise the health of the animals as required by the animal use protocol (AUP 2007-110); in addition  $T_{body}(t)$  gives information about metabolic activity, evaporative water loss, and thermoregulation, so its knowledge is important to estimate the heat exchanged by the animal during stressing conditions produced by dynamic heating in this case. The maximum  $T_{body}$  allowed was  $39^{\circ}\text{C}$  (AUP 2007-110), this value was selected because reported studies in bats of similar body mass show that systemic temperatures can reach values of  $40^{\circ}\text{C}$  without harming the bats [2, 3, 8, 7, 6]. If at any point in time during the experiment  $T_{body}$  exceeded  $39^{\circ}\text{C}$ , the experiment would be terminated and the bat extracted from the metabolic chamber. Body temperatures in the experiments (AUP 2006-253 and AUP 2007-110) for the pallid bat ranged from about  $27^{\circ}\text{C}$  to about  $36^{\circ}\text{C}$ . To make sure  $T_{body}$  did not increase over  $39^{\circ}\text{C}$ ,  $T_{chamber}$  was not allowed to surpass  $36^{\circ}\text{C}$ ; this value was selected also by comparison with metabolic studies with similar size animals, where ambient temperature  $T_{chamber}$  ranged between  $10^{\circ}\text{C}$  to  $42^{\circ}\text{C}$  [2, 3, 8, 7, 6].

Body temperature of the pallid bat responds differently between the experiments

where the bat is completely enclosed inside the metabolic chamber and the experiments where the bat is inside the metabolic chamber while the wing is extended. Figure 24A shows how body temperature ( $T_{body}$ ) of the pallid bat changes with time when the bat is fully enclosed (*without* wing extended) inside the metabolic chamber; body temperature can increase about  $2.8^{\circ}\text{C}$  ( $33^{\circ}\text{C} \leq T_{body} \leq 35.8^{\circ}\text{C}$ ) in just 10 minutes due to a combination of stress<sup>1</sup> and whole body heating when ambient temperature ( $T_{chamber}$ ) increases only about  $1^{\circ}\text{C}$  ( $26^{\circ}\text{C} \leq T_{chamber} \leq 27^{\circ}\text{C}$ ). This shows that heat produced while the bat is stressed is not being dissipated effectively from the body. In a separate experiment (Figure 24B) a bat was placed inside the metabolic chamber *with* one wing extended outside the chamber. Figure 24B shows that even though body temperature increased rapidly in the beginning, it then levels off because heat can be exchanged through the extended wing. Also, initial  $T_{body}$  is lower in the experiment with the wing extended and therefore drops faster as a result of the heat exchange that takes place. Initial body temperature is different in bats depending on whether they are slightly torpid or wide awake. When bats are slightly asleep, their body temperatures are lower than normal conditions [2, 3, 5]. Since body temperature is already lower than normal and the wing helps dissipate heat, then  $T_{body}$  will decrease even more.

Comparing results from Figures 24A and 24B indicates that having the wing extended in hot environments reduces the rate of body temperature increase in the pallid bat and assists in body cooling as expected. Assuming a specific heat value for the bat wing membrane ( $C_p = 3200 \text{ J/kg } ^{\circ}\text{C}$ ) given in [16], and knowing that the change in energy depends on the change in temperature ( $\Delta U = C_p \Delta T$ ), we

---

<sup>1</sup>Stress on the animal is due not only to handling, but due to the placement of the rectal probe in the bat. The protocol includes topical anesthetic to alleviate or reduce such sensation.

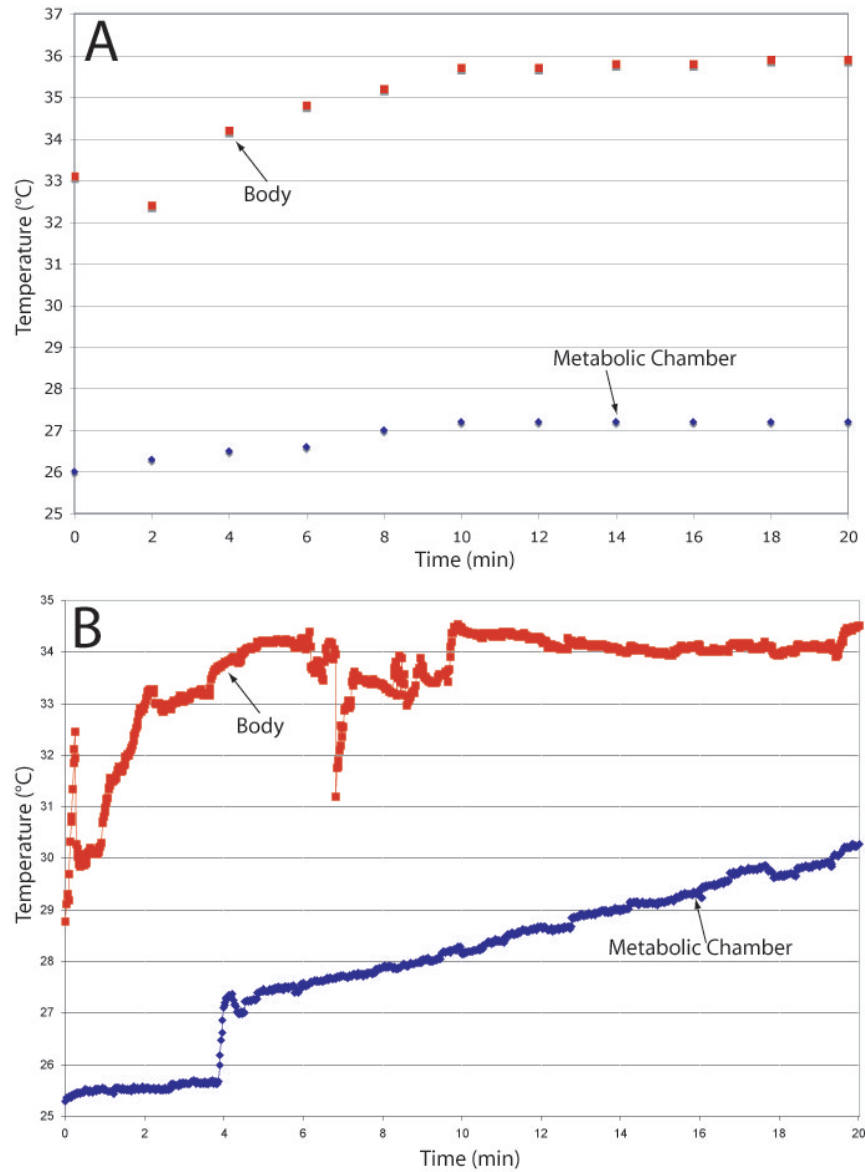


Fig. 24. Changes in body temperature during experiments at **higher** ambient temperatures **A)** *without* wing extended (B12, Female, 17.51g), and **B)** *with* wing extended (B23, Female, 21.3g).



can estimate that the wing helped release about 1600 J/kg in a matter of about 18 minutes, or about 88.8 J/kg per minute. This estimation was determined from results in Figure 24B where temperature dropped about 0.5°C from minute 10 to minute 18, whereas in Figure 24A, temperature did not drop at all. In experiments (AUP 2006-253) where the bat was completely enclosed inside the metabolic chamber, body temperature increased rapidly and remained at a constant high value as seen in Figure 24A. On the contrary, heating experiments (AUP 2007-110) with the wing extended show that heat dissipation from the body to the environment is possible after the effects of stress are diminished after about 10 minutes. Figure 25 shows two systemic heating experiments for two different pallid bats on two separate days. In Figure 25A, even when  $T_{chamber}$  increased 6°C in a span of 55 minutes,  $T_{body}$  decreased. After the heating system was turned off as indicated in the figure, body temperature also decreased at a slightly faster rate.

The two experiments for systemic heating in Figure 25 show that there is a similar trend in how  $T_{body}$  responds to changes in  $T_{chamber}$ . The different responses can be categorized into three different stages, shown in Figure 26 and denoted as:

- **Stage A:** where  $T_{body}$  is greater than  $T_{chamber}$ ,
- **Stage B:** characterized by  $T_{chamber}$  greater than  $T_{body}$ , and  $T_{body}$  showing a rapid increase followed by a rapid reduction, and finally
- **Stage C:** where  $T_{chamber}$  is greater than  $T_{body}$  and  $T_{body}$  decreases as time passes.

During **Stage A**, body temperature begins to decrease in response to vasodilation (Figure 25). During **Stage B**,  $T_{body}$  continues to decrease but then slightly increases because the pallid bat is beginning to experience the effects of high  $T_{chamber}$ ; this response can be seen in the small peak of  $T_{body}$  after  $T_{body}$  and  $T_{chamber}$  intersect for

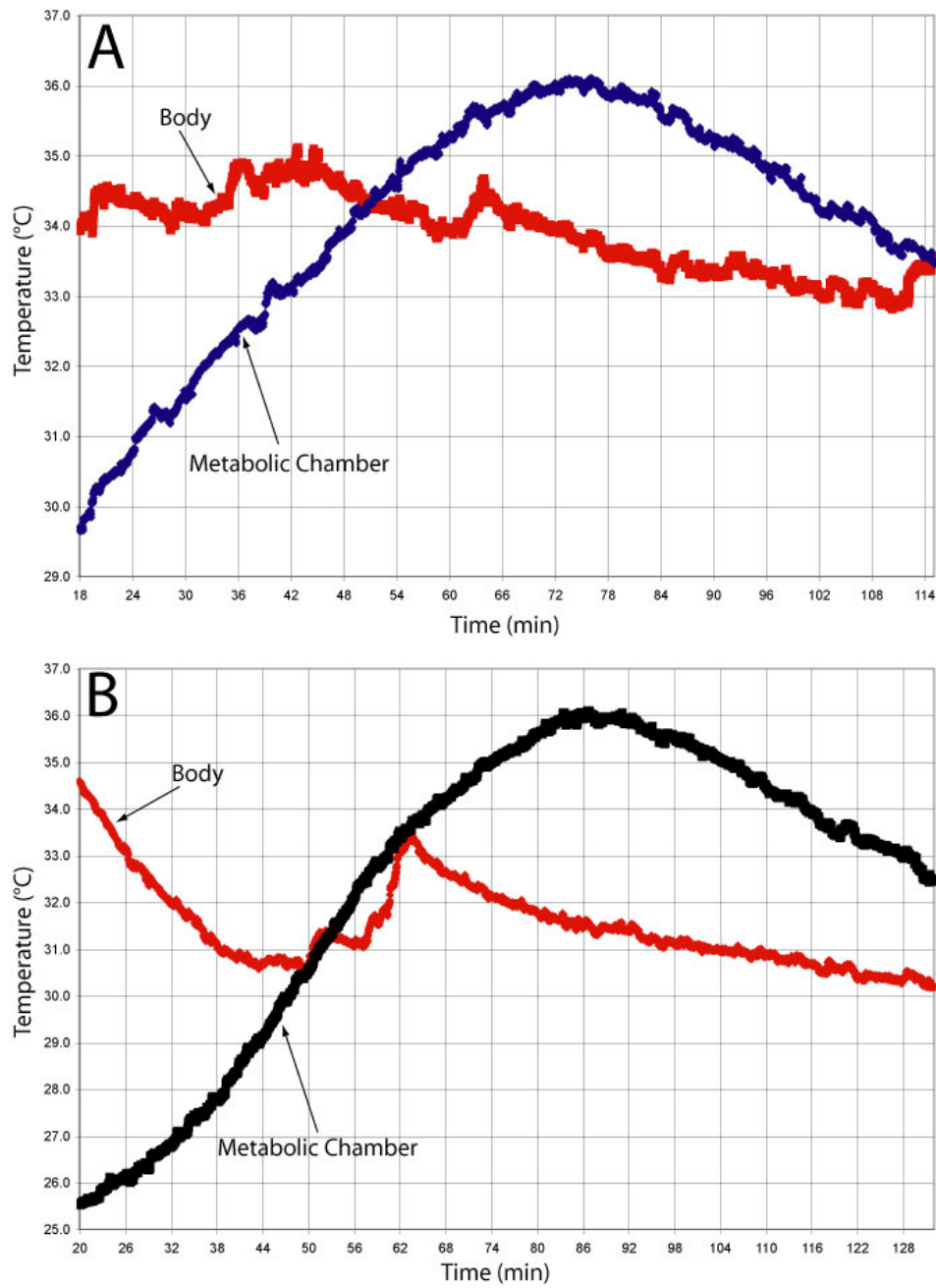


Fig. 25. Changes in body temperature during experiments at **higher** ambient temperatures *with* wing extended for **A)** B23, Female, 21.3g, and **B)** B16, Male, 24.8g.

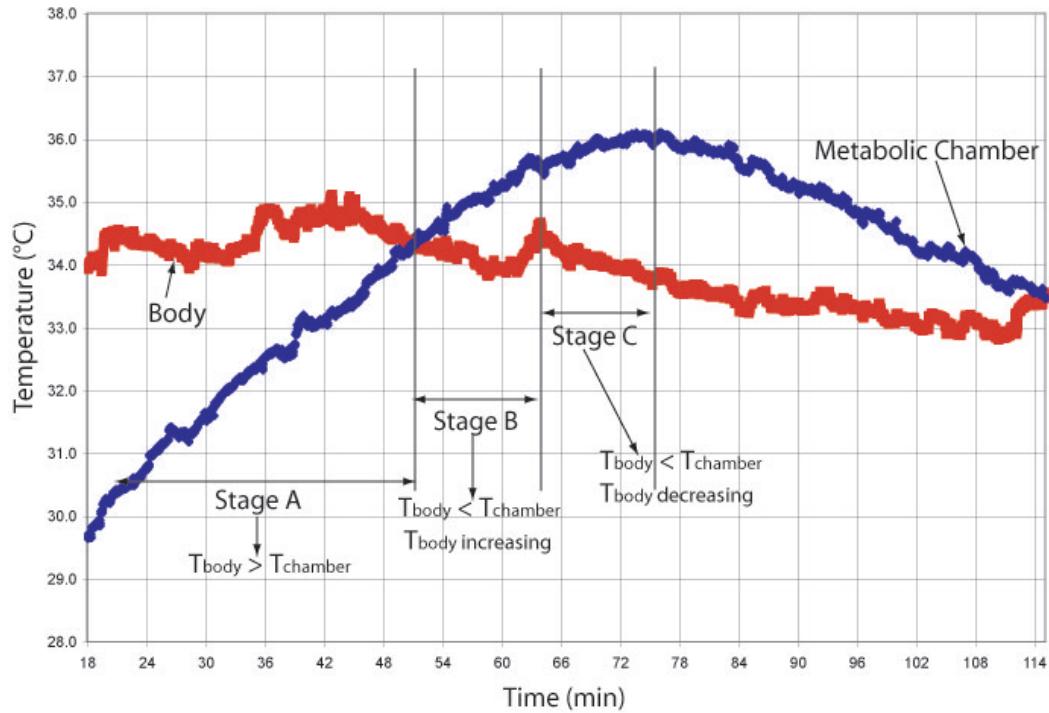


Fig. 26. Three stages observed during systemic heating experiments that correspond to: **A)**  $T_{body} \geq T_{chamber}$ , **B)**  $T_{chamber} \geq T_{body}$  and  $T_{body}$  decreases then increases, and **C)**  $T_{chamber} \geq T_{body}$  and  $T_{body}$  decreases.

both systemic heating experiments shown in Figure 25. During systemic heating experiments, when the temperature difference  $T_{body} - T_{chamber}$  changes sign, there is a different vascular response, as will be discussed later in this chapter.

After the peak in  $T_{body}$ , it then begins to reduce in value, this means that the thermoregulatory mechanisms begin to take effect; these mechanisms include, among others, dynamic alterations in vessel diameter, centerline velocity and blood flow. The thermoregulatory mechanisms then help dissipate heat from the body as observed in **Stage C**. In the experiments presented herein, body temperature never reaches baseline values because the time limit placed on experiments inhibits complete cooling of the metabolic chamber to normal ambient conditions.

The heating experiments also show that when temperature inside the metabolic chamber increases, wing and arm temperatures increase at a very slow rate. In Figure 27,  $T_{wing}$  increases from 25.8°C to 27.2°C (change of 1.4°C) in a time span of about 94 minutes. This indicates a rate of change of 0.0148°C per minute. In a separate heating experiment not shown in this case (B16, Male, 24.8g), there is a rate of change in wing temperature of 0.0156°C per minute; values from both experiments are very similar and indicate that with more data, a valid average value can be determined. The change in wing temperature is due to the fact that a larger volume of blood is entering the wing (due to both an increase in diameter and velocity); since the blood is delivered from the body, it arrives at the wing at temperature close to  $T_{body}$  as mentioned in Chapter II, Section G where mechanisms of heat transfer in tissue were discussed. Figure 27 shows three different temperatures measured in the wing, two of them are on the wing tissue and a third is a measurement at the arm as described in Figure 21 (Chapter IV). Figure 27 shows that during heating, all three temperature measurements follow a similar pattern with a variation of about 0.2°C. After heating stops, the variation is reduced to half that amount; for simplicity, in figures presented hereafter, only one of the temperatures will be shown.

As  $T_{chamber}$  increases, so does  $T_{wing}$  and  $T_{arm}$ . This response is due to active vasodilation and consequently, an increase in blood volume in the wing. After  $T_{chamber}$  reaches a maximum of 36°C (maximum allowed temperature) the heating system is turned OFF; the time in which such event takes place is indicated in the figure. After the heating is turned OFF, temperature inside the metabolic chamber begins to decrease because the room temperature is cooler than that of the metabolic chamber. At this point,  $T_{wing}$  is still increasing but the rate at which it is increasing begins to slow down. Depending on the magnitude of the body temperature during this process, wing temperature reaches an equilibrium state. When the difference between basal

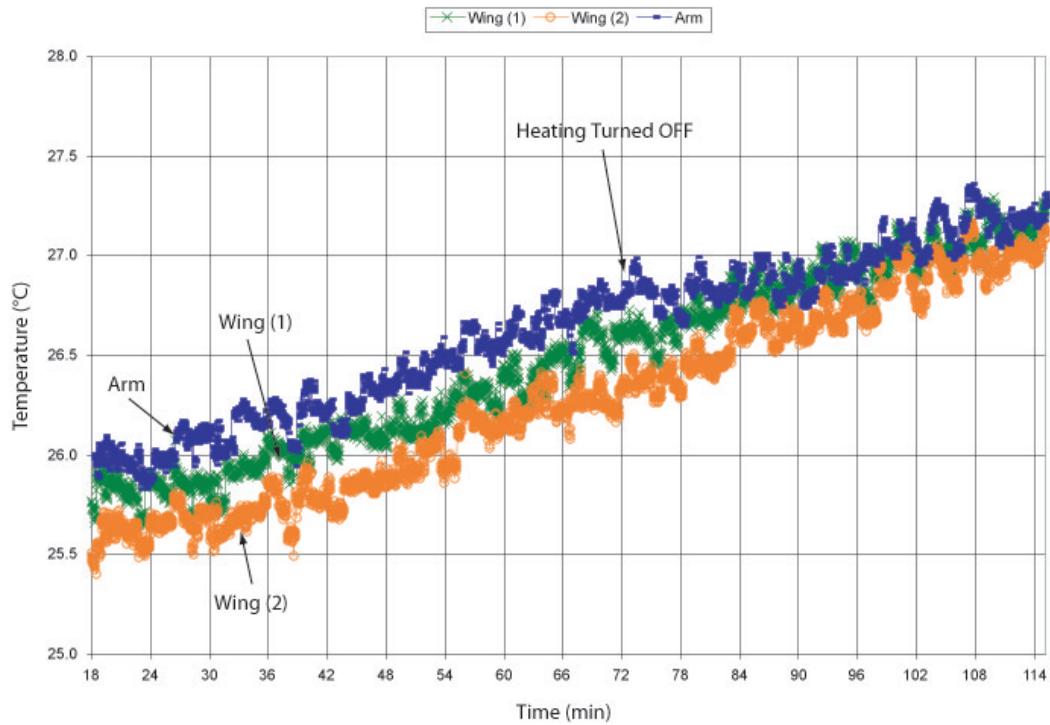


Fig. 27. Temperature at three different locations in the wing during experiments at **higher** ambient temperatures *with* wing extended (B23, Female, 21.3g).  $T_{wing}$  increases at a slow rate until the heating system is stopped at minute 72, after this time  $T_{wing}$  still increases but at an even slower rate.

body temperature and body temperature during systemic heating ( $T_{body} - T_{body,o}$ ) is small, then  $T_{wing}$  levels off, and as  $T_{body} - T_{body,o}$  increases because  $T_{body}$  is high then the slope of  $T_{wing}$  also changes to compensate for the changes in body temperature.

This change in rate of temperature increase is more obvious in Figure 28B where the slope of the temperature line is  $0.0004 \alpha/\text{min}$  during dynamic heating and then decreases to  $0.0001 \alpha/\text{min}$  after the heating system is turned off. Figures 28A and 28B show that it is necessary to continue measurements until  $T_{chamber}$  reaches the initial value in order to observe the changes in wing temperature. We expect that as heat is removed from the system and  $T_{body}$  returns to basal values,  $T_{wing}$  will equilibrate and arrive to a temperature very close to room temperature (outside metabolic chamber). Temperature will drop because blood flow to the wing will be reduced as the need for maintaining the vessels dilated is reduced.

Figures 29 and 30 show the temporal changes in wing heat flux ( $q_{wing}$ ) at normal ambient conditions and during systemic heating, respectively. Figure 29 shows that during the experiment at normal ambient conditions, the heat flux is fairly constant at both locations in the wing during the entire duration of the experiment. In all experiments (normal ambient conditions and systemic heating),  $q_{wing}$  either increases or remains constant over time. The dark solid lines in Figures 29 and 30, represent data analyzed using the Empirical Mode Decomposition (EMD) method.

The EMD method was used to remove the high frequency oscillations commonly found in dynamic biological signals which are usually produced by heart rate and respiration rate [85]. EMD was selected to filter the signals, as this algorithm allows to analyze non-linear and non-stationary signals without leaving the time domain, it decomposes the signal into a series of Intrinsic Mode Functions (IMF) that are nearly orthogonal. More importantly, the EMD method is a self contained method that does not use any predetermined filters or transforms [85, 86, 87]. The EMD method has

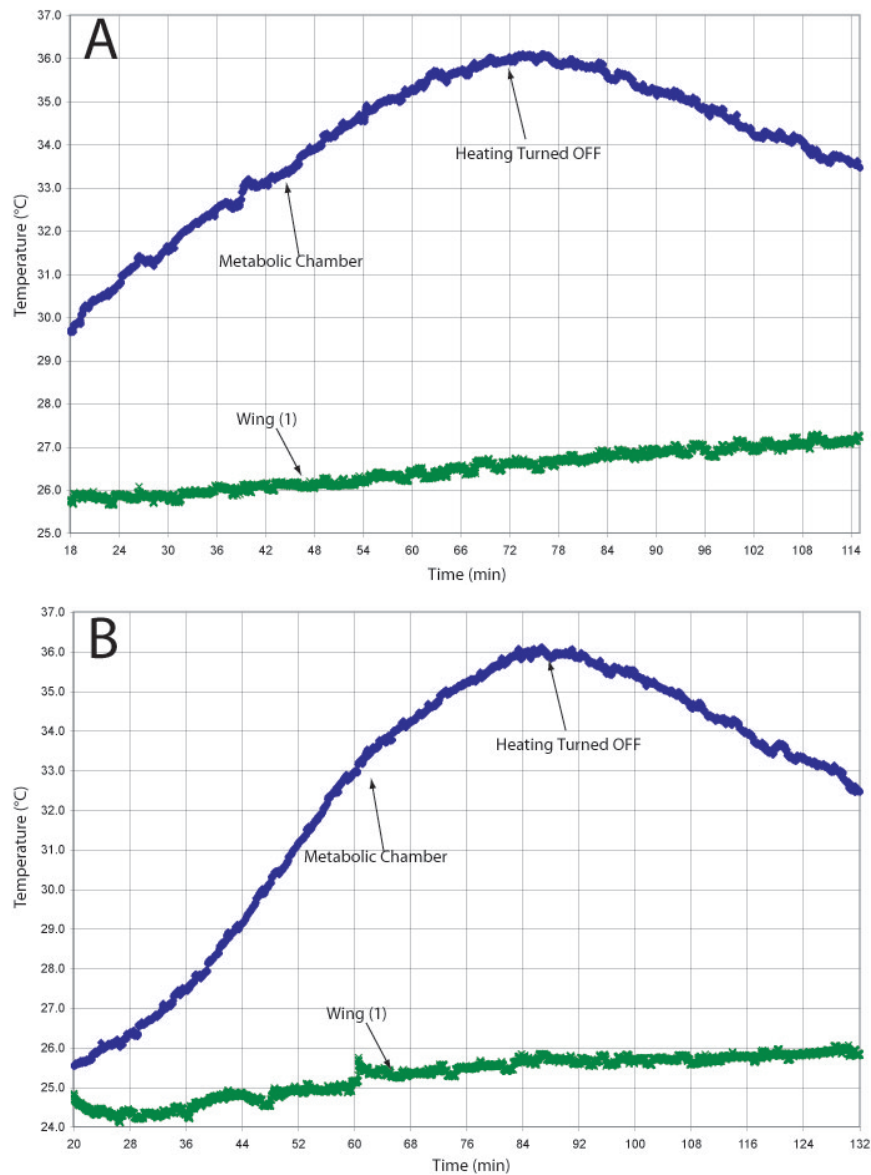


Fig. 28. Changes in wing temperature during experiments at **higher** ambient temperatures *with* wing extended: **A)** B23, Female, 21.3g; **B)** B16, Male, 24.8g.

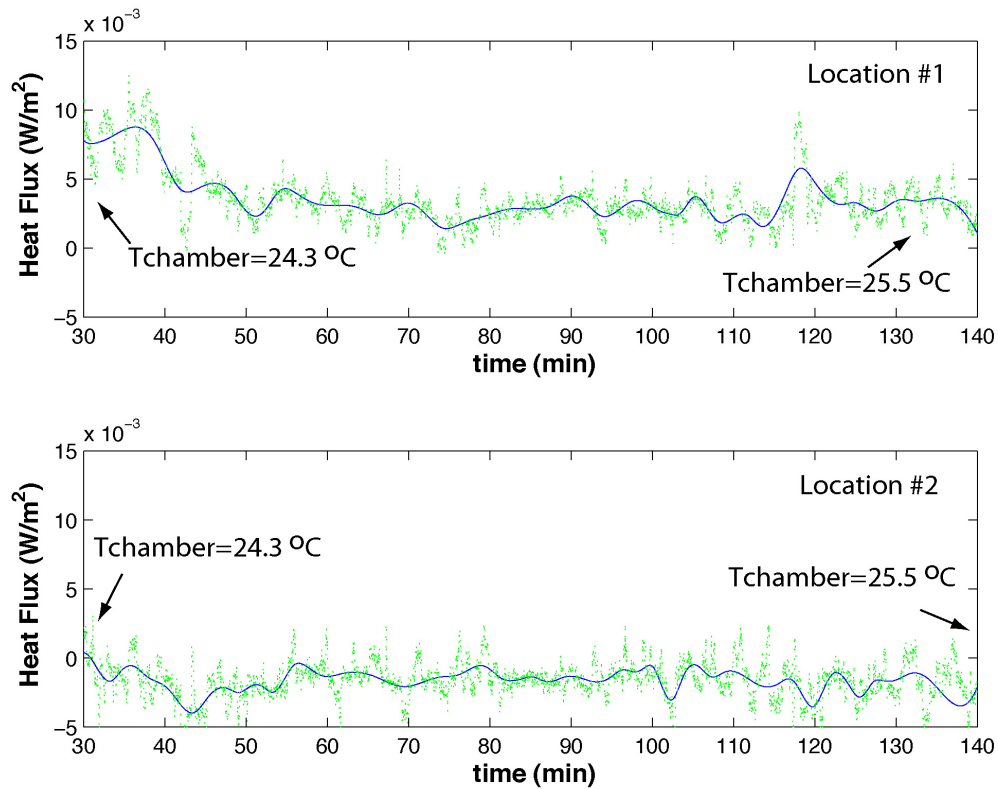


Fig. 29. Changes in heat flux in the wing at normal ambient conditions (B12, Female, 17.51g). Heat flux in both locations of the wing is fairly constant throughout the entire experiment.

been successfully applied to study results of neuroscience experiments, electrocardiograms, gastroelectrograms, and Laser Doppler Flowmetry (LDF) signals. Studies of LDF signals acquired during hyperemia indicate that accurate LDF parameters are determined from the fifth IMF component [85]. Five IMFs are sufficient to filter the high frequency oscillations, and 10 IMFs provide a considerable damping of the signal. In our case, 5 IMF signals were used to analyze the heat flux, and 8 IMF signals were used to analyze, diameter, centerline velocity, blood flow and wall shear stress that will be presented in the next section.



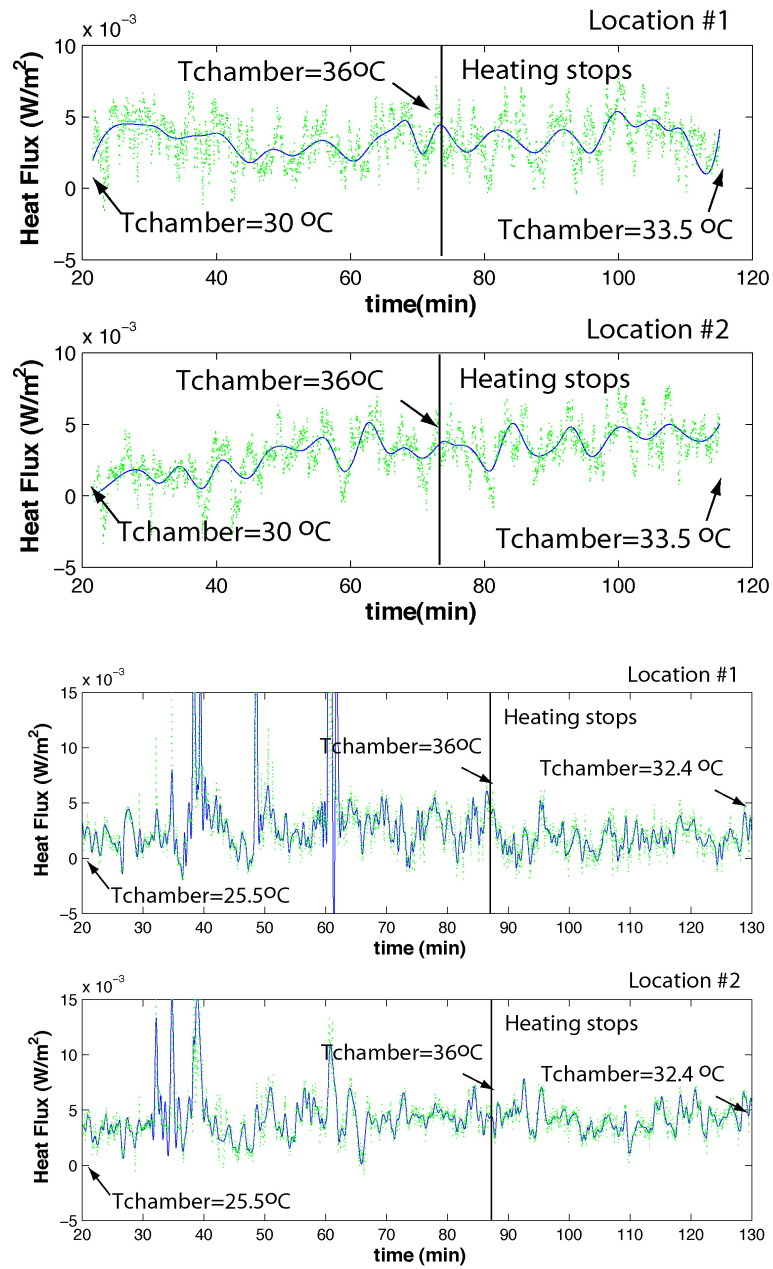


Fig. 30. Changes in heat flux in the wing during systemic heating for **A)** pallid bat (B23, Female, 21g) and **B)** pallid bat (B16, Male, 24.8g). Heat flux in Location #2 increases as heating progresses while in Location #1, the same pattern is not observed.

The heating experiments show that heat flux at Location #2 (indicated in Figure 21) increases with  $T_{wing}$  as heating progresses. In the first heating experiment (top portion of Figure 30), heating was stopped at minute 72; at this moment the slope of the heat flux begins to decrease. In the second heating experiment (bottom portion of Figure 30) the heating system was stopped at minute 88 and similar trends were observed for Location #2 in the wing. Heat flux at Location #1 is larger in magnitude than in Location #2; this might be due to the proximity of the location of sensor #1 to the bat's body. More experiments are needed to verify these observations.

The large peaks in  $q_{wing}$  at Locations #1 and #2 in the second heating experiment in Figure 30 are the result of several factors, for instance bad contact between the wing and the surface of the heat flux sensor, contact from an external object (i.e. someone's finger), or bat wing movement. In this second heating experiment (Figure 30), the slope of the heat flux decreases after the heating system was turned off indicating that  $T_{chamber}$  affects the rate of heat flux from the wing. Heat flux ( $\text{W}/\text{m}^2$ ) measurements show that the heat lost by the wing is correlated to  $T_{wing}$  and  $T_{chamber}$  and changes in the same manner.

### C. Analysis of Vascular Response to Systemic Heating

Vascular response to systemic heating will be studied by observing transient changes in vessel diameter, centerline velocity, blood flow (BF) and wall shear stress (WSS). The variations of these quantities with time, body temperature, wing temperature, and chamber temperature need to be analyzed, as they provide information about the behavior of arterial beds to both systemic and local stimuli. In addition, these are the same parameters that were studied in experiments with local heating [1]. Figure 31 shows that baseline values for diameter ( $\mu\text{m}$ ) and centerline velocity ( $\text{mm}/\text{s}$ ) are

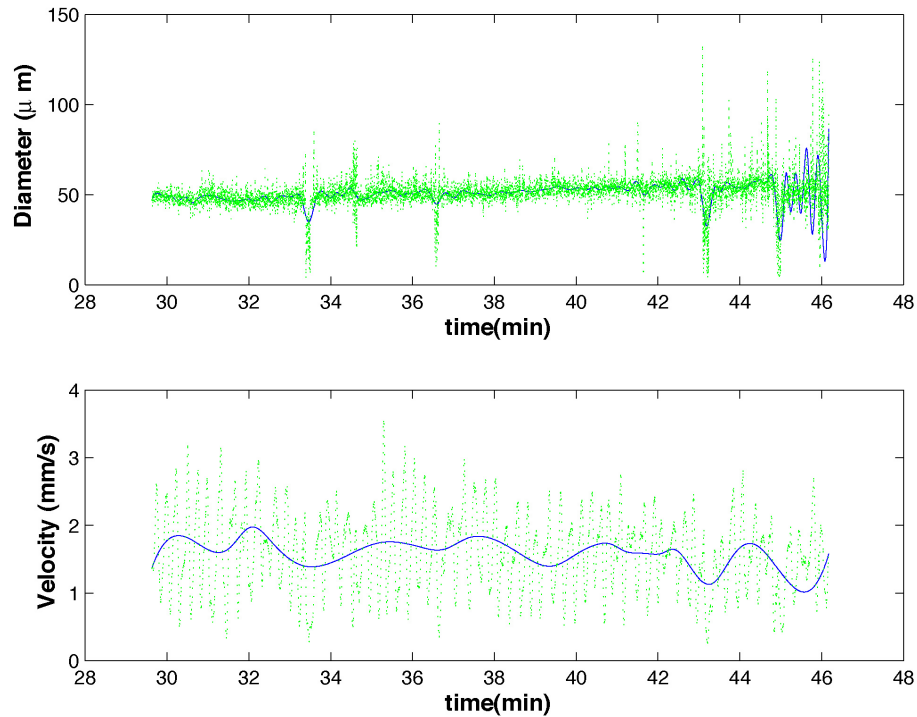


Fig. 31. Arteriole diameter and centerline velocity in the wing during normal ambient conditions (B14, Female, 25.98g). The last part shows a larger variation in diameter due to movement of bat wing and loss of focus in the diameter tracking software.

fairly constant throughout the entire experiment. This indicates that blood flow is not affected at normal ambient conditions. The last portion of the diameter plot (Figure 31 indicates a larger variation due to movement of the animal, which causes a loss of focus in the diameter tracking software.

As expected, the diameter of the observed arterioles increases with time during systemic heating as shown for one bat in Figure 32. Diameter increases at a constant rate up to minute 88 when the heating system is turned OFF; after this point in time, the diameter still increases but at a slower rate. Vessel diameter responds in the

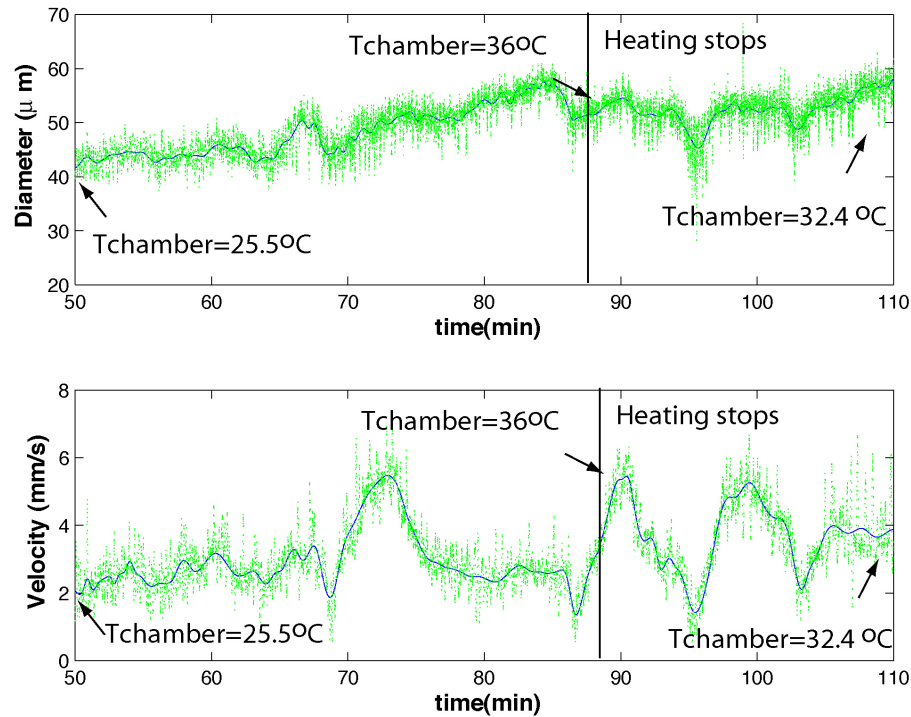


Fig. 32. Changes in arteriole diameter and centerline velocity in the wing during systemic heating (B16, Male, 24.8g). Data shows that diameter increases at a constant rate up to minute 88 which corresponds to the time when the heating stops; the diameter then continues to increase but at a slower rate. Average values of velocity are higher at the end of the experiment when  $T_{chamber}$  is  $32.4^{\circ}C$  than the beginning when  $T_{chamber}$  is  $25.5^{\circ}C$ .

same manner as both  $T_{wing}$  and  $q_{wing}$  which are observed to be affected by changes in  $T_{chamber}$ . Centerline velocity also responds to changes in  $T_{chamber}$  by increasing as  $T_{chamber}$  increases; the average centerline velocity is higher after the metabolic chamber has reached a temperature of  $36^{\circ}C$ .

Blood flow (BF) and wall shear stress (WSS) with respect to time follows the same pattern as changes in diameter (Figure 33). Blood flow was determined by the

relationship

$$BF = \frac{\pi D^2 V}{8}, \quad (5.1)$$

where  $D$  is the vessel diameter and  $V$  is the centerline velocity described previously. This equation shows that blood flow responds more to changes in diameter (vasoconstriction or vasodilation) than to changes in velocity. Blood flow is an important quantity for analysis of heat transfer as heat is delivered from the body to the wing through warm blood. Wall shear stress ( $\tau_w$ ) was determined by

$$\tau_w = \frac{4\mu V}{D}, \quad (5.2)$$

where as in Equation 5.1,  $V$  and  $D$  are velocity and diameter, respectively, and  $\mu$  corresponds to blood viscosity. This quantity is strictly a function of temperature, however, models or experimental relationships that indicate such variation have not been found; in addition, values of  $\mu$  for the blood of bats is not reported, so the value for human blood will be used and set to  $\mu = 3.5 \text{ cP}$ .

Figure 33 indicates BF and WSS calculated for a heating experiment; this figure shows that at the time when heating stops after minute 88, both blood flow and wall shear stress increase. This is due to the fact that the bat is trying to dissipate heat from its body to the environment and the only means available to accomplish that is to increase blood flow to the thermal window (i.e. wing). Initial values show that BF is about 0.1 ml/min and WSS is about 6 dyne/cm<sup>2</sup>; values at the end of the experiment on the same figures show that BF has increased to about 0.3 ml/min and WSS has increased to about 10 dyne/cm<sup>2</sup>. This means that with time, blood flow increased by 300% and wall shear stress increased by 166.6%.

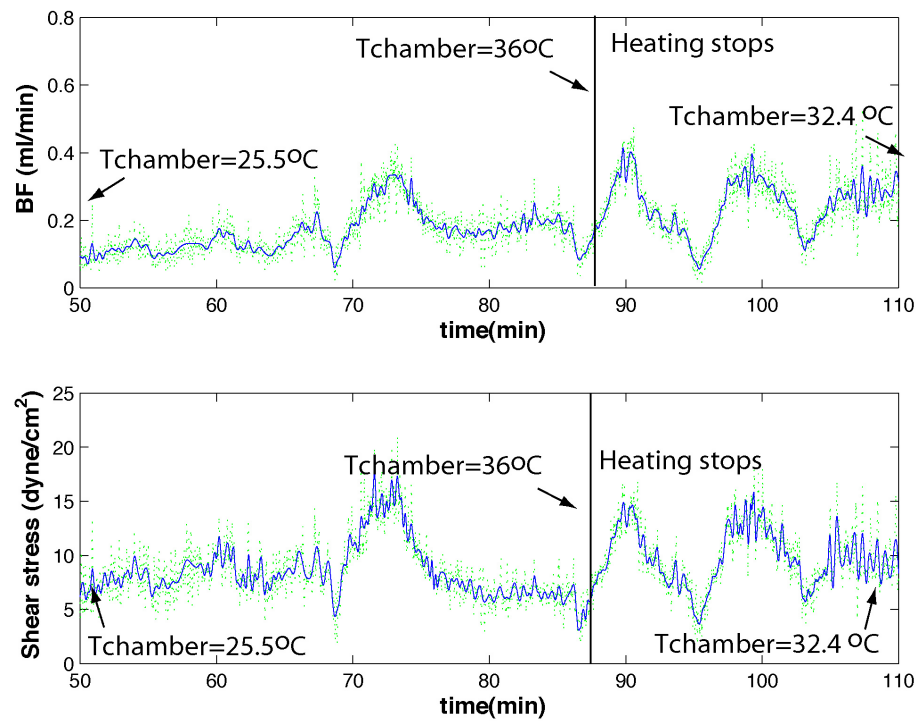


Fig. 33. Blood flow and wall shear stress with respect to time during systemic heating; (B16, Male, 24.8g). After the metabolic chamber has reached a maximum temperature of 36°C blood flow and wall shear stress increase about 0.2 ml/min (300%) and about 4 dyne/cm<sup>2</sup> (166.6%), respectively.

## D. Correlations

The objective of this research was to observe vascular changes in response to systemic heating achieved by alterations in the temperature inside the metabolic chamber ( $T_{chamber}$ ). The purpose of these studies was to determine how much time it takes for the pallid bat to respond to changes in  $T_{chamber}$  as well as estimating the contribution of different factors (metabolism, evaporative water loss and wing heat flux) to achieve an equilibrated body temperature (or thermoneutral condition). In this section we will present correlations between vascular parameters (diameter, centerline velocity, blood flow, wall shear stress) and parameters that characterize the thermal state of the animal such as:  $T_{body}$ ,  $T_{wing}$ ,  $T_{chamber}$  and  $q_{wing}$ . This analysis will help to estimate how blood perfusion to the wing changes in response to systemic and environmental changes. To culminate this analysis, a simple thermoregulatory model for the bat is proposed in the next chapter.

During systemic heating, there are three stages observed as indicated in Figure 26. The three different stages are taken into consideration when analyzing the results with respect to  $T_{chamber}$  and  $T_{body}$ . Figure 26 indicates that the three stages correspond to: **Stage A** ( $T_{body} \geq T_{chamber}$ ), **Stage B** ( $T_{chamber} \geq T_{body}$  and  $T_{body}$  decreases then increases), and **Stage C** ( $T_{chamber} \geq T_{body}$  and  $T_{body}$  decreases). As mentioned in Section B, vessel diameter and centerline velocity data are not available for the entire experiments; initial values are missing because of the time it took to locate and focus on a vessel and values for later times are missing due to movement from the bat and loss of focus in the diameter tracking software. However, for the experiments presented herein, all three different stages (**Stages A, B and C**) are characterized by at least one experiment.

Figures 34 and 35 show that during **Stage A** ( $T_{body} \geq T_{chamber}$ ), there is a positive

correlation between  $T_{body}$  and vessel diameter, velocity and blood flow. When body temperature is increasing, the pallid bat is responding through vasodilation (increase in vessel diameter); thus, there will be a larger volume of blood entering the bat wing and greater blood flow. Figure 34 also shows that diameter and velocity with respect to  $T_{chamber}$  do not show a significant variation. The reason for this is because since body temperature is higher than metabolic chamber temperature,  $T_{chamber}$  does not affect the thermoregulatory responses in the pallid bat.

During **Stage B** ( $T_{chamber} \geq T_{body}$  and  $T_{body}$  is decreasing), Figures 36 and 37 show that after body temperature and metabolic chamber temperature intersect and  $T_{chamber}$  becomes greater than  $T_{body}$ , then  $T_{chamber}$  has a greater effect on the increase of vessel diameter, centerline velocity and blood flow. As  $T_{chamber}$  increases, vessel diameter and centerline velocity respond by increasing (vasodilation); this causes an increase in blood flow and therefore a larger volume of blood in the pallid bat wing where more heat exchange can take place. The vasodilation response then assists  $T_{body}$  to begin to decrease to basal values.

Results for **Stage C** ( $T_{chamber} \geq T_{body}$ ), where body temperature is less than metabolic chamber temperature and body temperature is decreasing, show that the thermoregulatory responses of the pallid bat are in fact helping to dissipate heat from the body to the environment. As a result of an increase in  $T_{chamber}$ , vessel diameter and centerline velocity increase therefore causing blood flow into the wing to increase. This increase of blood volume in the pallid bat's thermal window, signifies more heat exchange can take place as described in Chapter II. When these thermoregulatory responses are in effect, they allow for body temperature to decrease to basal values. The relationships for **Stage C** can be seen in Figures 38 and 39; vessel diameter, centerline velocity and blood flow increase as a result of an increase in  $T_{chamber}$ . These vascular responses are then the stimuli that help reduce body temperature also seen



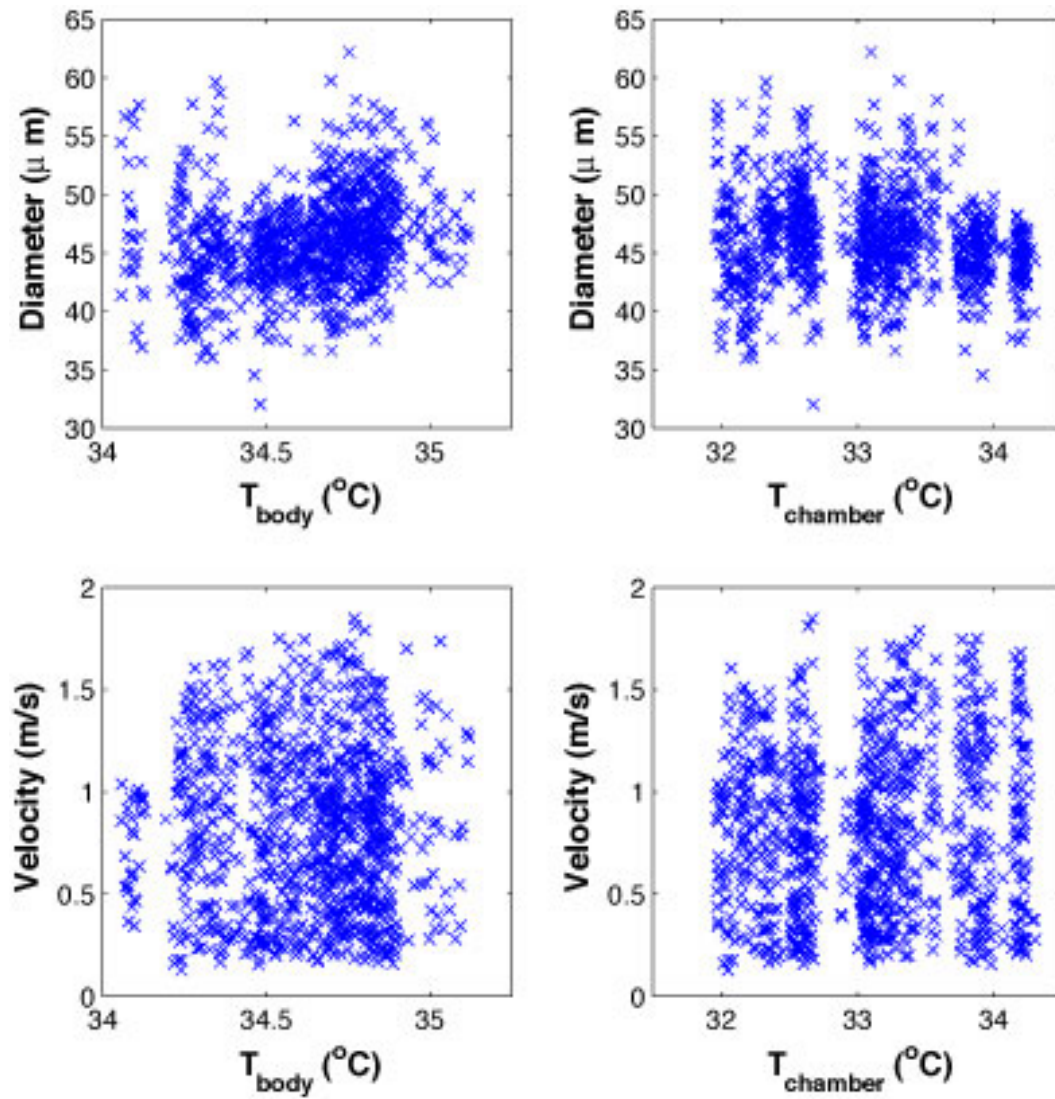


Fig. 34. Results for **Stage A** ( $T_{body} \geq T_{chamber}$ ), shows that as  $T_{body}$  increases the pallid bat responds through vasodilation, indicated by an increase in vessel diameter and centerline velocity (B23, Female, 21.3g).

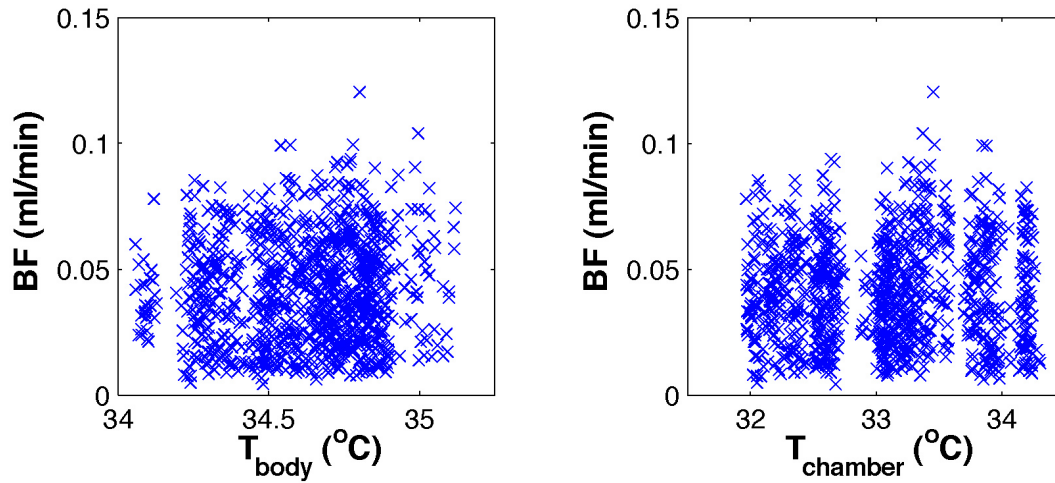


Fig. 35. Results for **Stage A** ( $T_{body} \geq T_{chamber}$ ), shows that as  $T_{body}$  increases blood flow also increases in order for heat exchange to take place in the wing and therefore assist in thermoregulation (B23, Female, 21.3g).

in the same figures (Figures 38 and 39).

In our research, heat flux ( $q_{wing}$ ) is the rate of heat transfer that occurs between the wing and the surrounding environment. Heat flux measurements from the bat wing help determine how the wing assists in dissipating heat from the body to the environment. Heat flux is dependent on the temperature gradient between the wing ( $T_{wing}$ ) and the environment ( $T_{air}$ , outside the box). In our case, we want to study how heat flux varies with changes in  $T_{chamber}$ ,  $T_{body}$  and  $T_{wing}$ .

Results in Figure 40 show that for basal conditions, heat flux remains constant throughout the entire experiment. In this case, there is no increase in  $T_{chamber}$  and therefore no need for the bat to dissipate heat from the body. In the cases during systemic heating (**Stages A, B and C**), when  $T_{chamber}$  increases,  $q_{wing}$  also increases as a need begins for the body to release heat (Figure 41A). One of the sensors (Location #1) shows a slightly higher value of  $q_{wing}$  than the other (Location #2); we believe this may be due to the fact that the sensor at Location #1 is closer to the

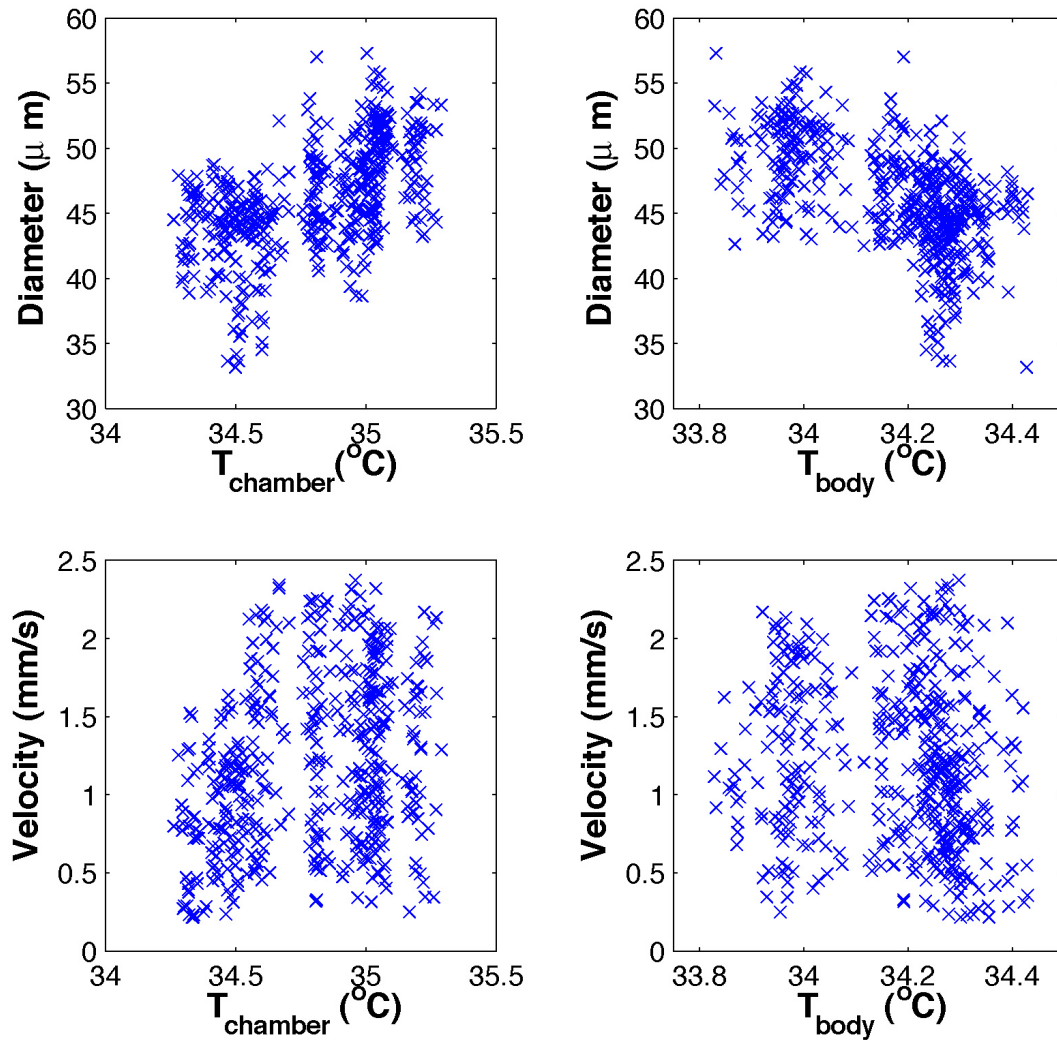


Fig. 36. Results for **Stage B** ( $T_{\text{chamber}} \geq T_{\text{body}}$  and  $T_{\text{body}}$  decreases then increases) show that when  $T_{\text{chamber}}$  increases, the pallid bat responds through vasodilation (increase in vessel diameter and centerline velocity) which then causes  $T_{\text{body}}$  to decrease to basal values (B23, Female, 21.3g).

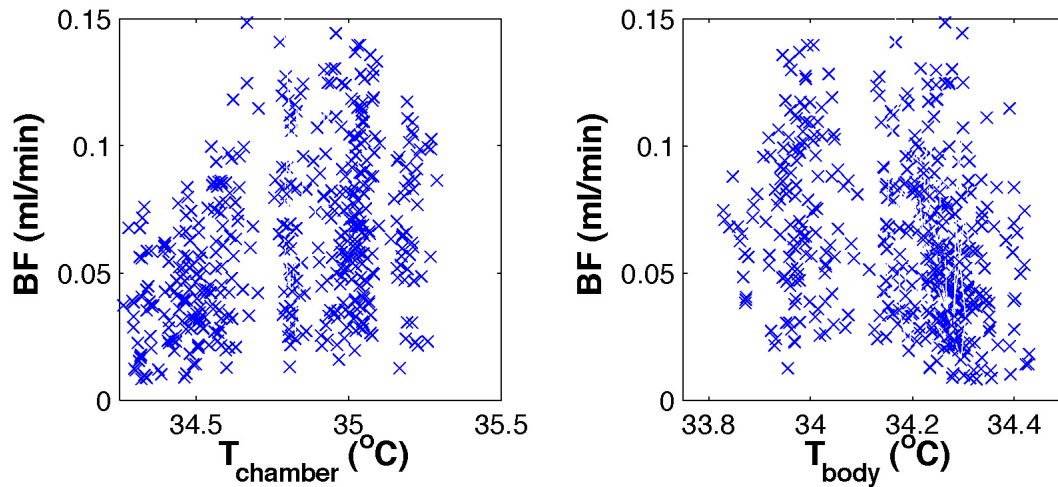


Fig. 37. Results for **Stage B** ( $T_{chamber} \geq T_{body}$  and  $T_{body}$  decreases then increases) show that when  $T_{chamber}$  increases, there is an increase in blood flow which then allows  $T_{body}$  to return to basal values (B23, Female, 21.3g).

body and therefore closer to where warmer blood is entering the wing. The blood at Location #1 does not have enough time to equilibrate its temperature to that of the wing tissue and is therefore able to transfer more heat out of the wing. Even though heat flux at Location #1 is higher than that of Location #2, the percent increase is larger at Location #2. The variation of heat flux with respect to changes in  $T_{body}$  is indicated in Figure 41B and shows that as  $T_{body}$  increases,  $q_{wing}$  follows in the same manner. These responses in  $q_{wing}$  signify that the pallid bat is regulating its body temperature as had been expected.

Heat flux is also positively related to changes in  $T_{wing}$ ; as  $T_{wing}$  increases, observed in Figure 41, heat flux follows in the same manner. At the lowest  $T_{wing}$  shown, heat flux through the wing has a value of about  $-2 \text{ W/m}^2$  ( $T_{chamber} = 32 \text{ }^\circ\text{C}$ ) while at the end of the experiment, when  $T_{chamber} = 34.4 \text{ }^\circ\text{C}$ ,  $q_{wing}$  has a value of about  $6 \text{ W/m}^2$ .

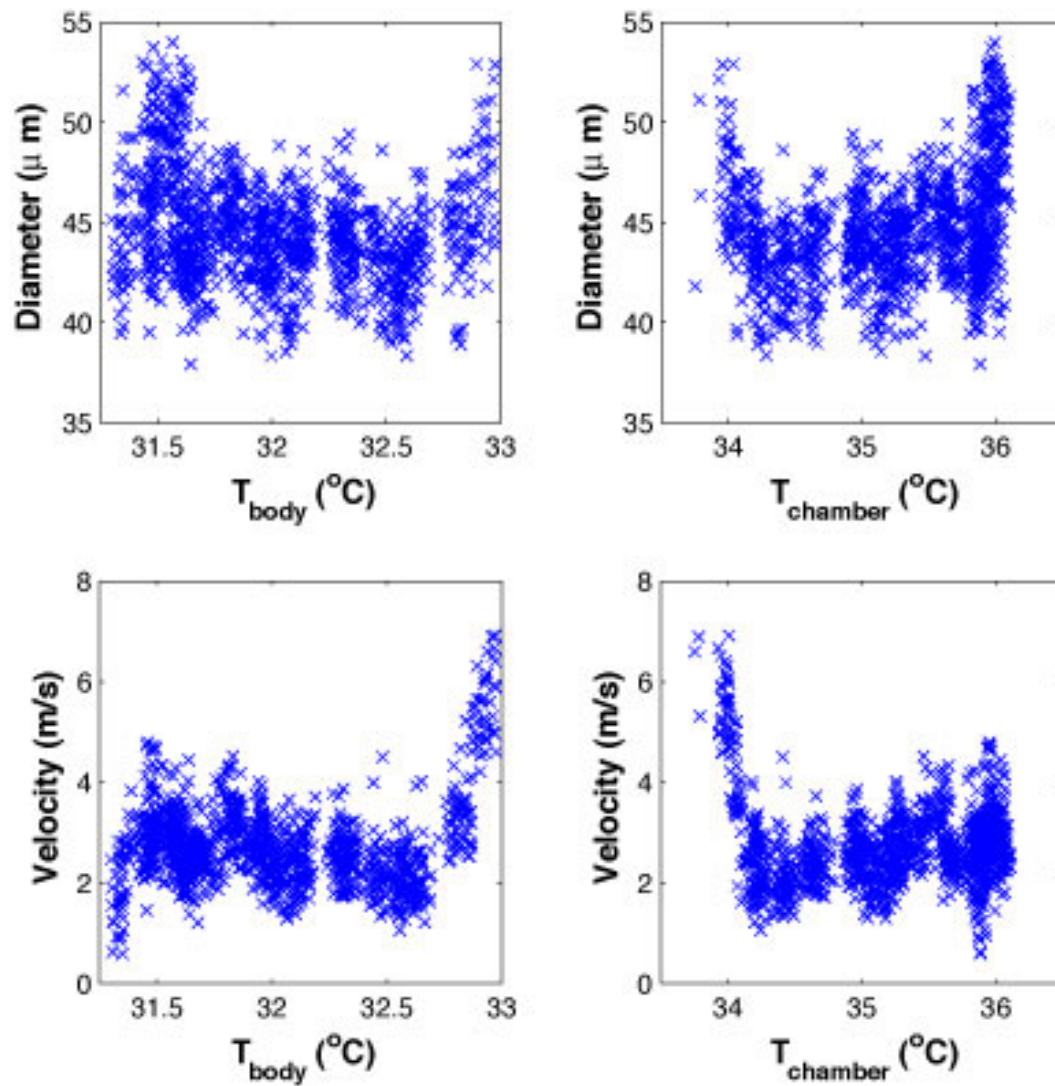


Fig. 38. Results for **Stage C** ( $T_{chamber} \geq T_{body}$  and  $T_{body}$  decreases) show that when  $T_{chamber}$  increases, the pallid bat responds through vasodilation (increase in vessel diameter and centerline velocity) which then causes  $T_{body}$  to decrease to basal values (B16, Male, 24.8g).

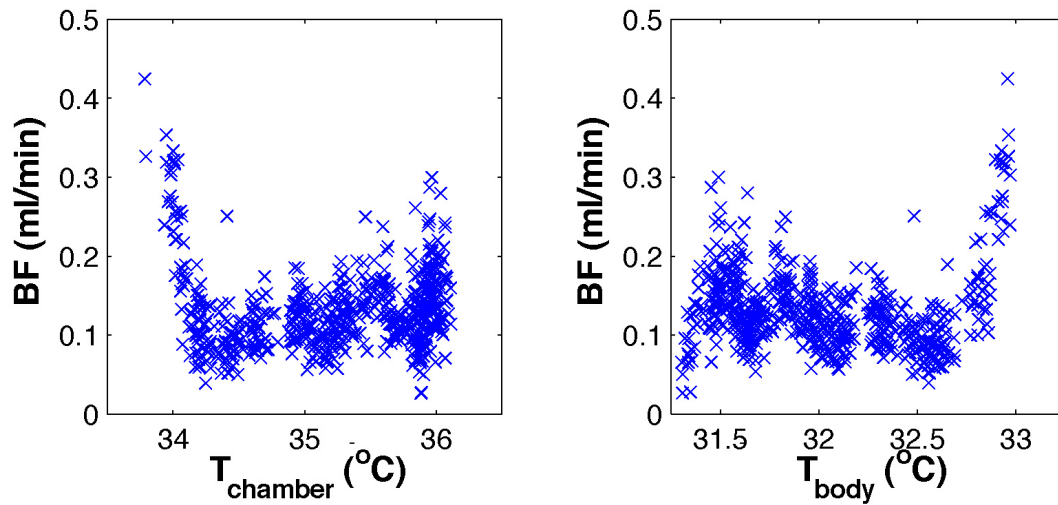


Fig. 39. Results for **Stage C** ( $T_{chamber} \geq T_{body}$  and  $T_{body}$  decreases) show that when  $T_{chamber}$  increases, due to vasodilation, there is an increase in blood flow which then allows  $T_{body}$  to return to basal values because more heat exchange is taking place in the wing (B16, Male, 24.8g).

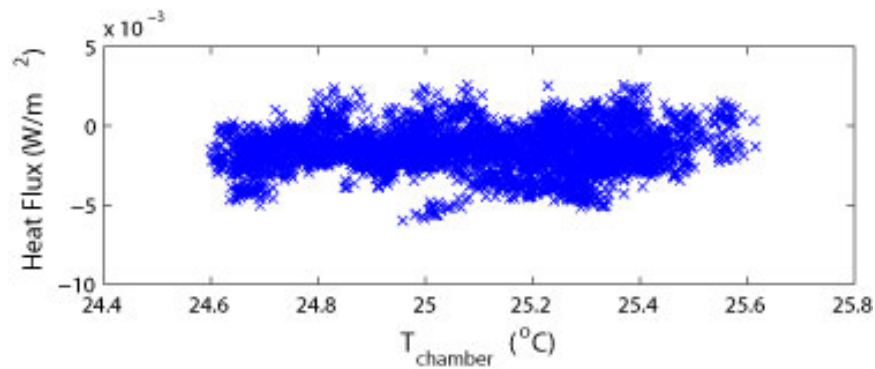


Fig. 40. Heat flux remains constant during experiments at normal ambient conditions; since there is no increase in  $T_{chamber}$ , there is no need for the bat to release heat from the wing to the environment.



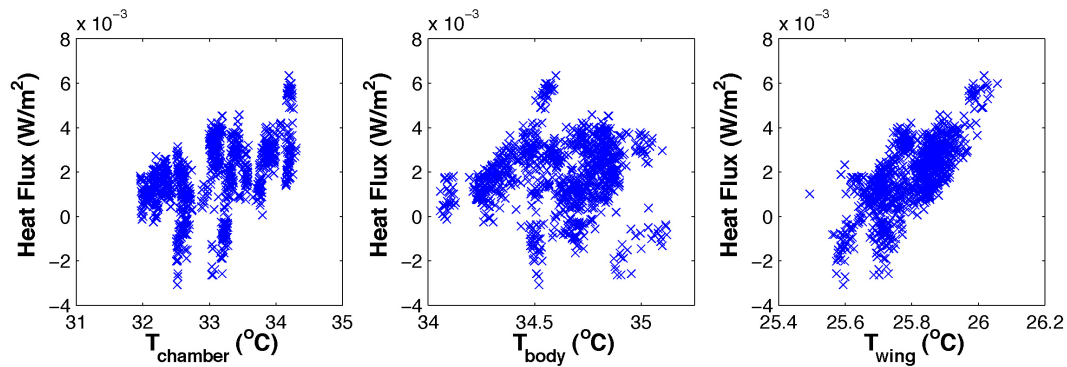


Fig. 41. During systemic heating,  $q_{\text{wing}}$  responds the same during the three different stages (**Stages A, B and C**).  $q_{\text{wing}}$  increases proportional to **A)**  $T_{\text{chamber}}$ , **B)**  $T_{\text{body}}$ , and **C)**  $T_{\text{wing}}$  due to the need for the bat to dissipate heat from to body through the wing.

#### E. Conclusions

The analyses presented previously, summarize data from one baseline experiment and two systemic heating experiments for different bats. During the experiment under normal ambient conditions with the wing extended (Figures 29 and 31), there were no significant variations in  $q_{\text{wing}}$  and vessel diameter; the reason for this being that there was no need for heat to be removed from the body to the environment through the wing. During the experiment under normal ambient conditions, the fact that vessel diameter and centerline velocity were not recorded immediately after the bat was placed in the chamber did not affect the results; however, in the experiments for systemic heating (Figure 25), there was a large piece of information missing with respect to how the pallid bat initially responds to environmental heating. As mentioned in Section B of this chapter, the delay in recording vessel diameter and centerline velocity occurred because of the time it took to locate and focus on a single vessel under the microscope and tracking software.

In order to avoid the same problem, changes were made with respect to when

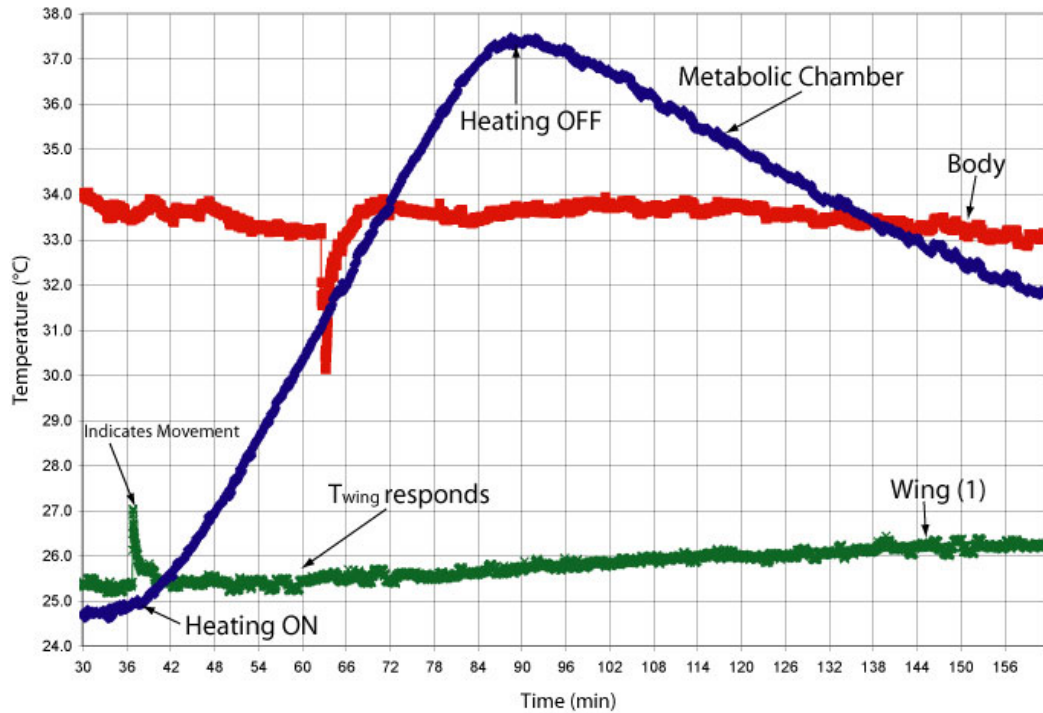


Fig. 42. For the last systemic heating experiment, temperature measurements began before the heating system was turned on.  $T_{wing}$  begins to increase 22 minutes after heating was turned on which indicates a positive response to changes in  $T_{chamber}$  (B14, Female, 25.98g).

heating began; instead of turning on the heating system on when the bat was initially placed inside the metabolic chamber, the heating system was turned on **after** a vessel was located and diameter and centerline velocity recordings began. This procedure was implemented for one last experiment (B14, Female, 25.98g). Results from the last systemic heating experiment show that wing temperature responds differently under different circumstances. Figure 42 shows temperature measurements of a pallid bat where heating was turned on at minute 38. It is observed that  $T_{wing}$  begins to increase at minute 60 which indicates a response to an increase in  $T_{chamber}$ . This thermoregulatory response helped maintain a fairly constant  $T_{body}$ .



An initial increase in body temperature due to stress from handling of the bat and insertion of the rectal probe is not shown in Figure 42. After  $T_{body}$  reaches a maximum value, it then begins to decrease or remain constant (as seen in Figure 42) most likely due to changes in blood flow to the wing which is indicated by an increase in  $T_{wing}$ .  $T_{body}$  in this last experiment does not follow the same trend as the two previous systemic heating experiments presented in Section B; this might be attributed to the weight of the currently used pallid bat as it is one of the heaviest bats in the laboratory. In order to verify this, more experiments with the same bat are needed to reproduce results.

Currently, there is no way of looking at the wing vasculature under the microscope at the time when the rectal probe is inserted to look at the effects of stress on the bat. It has been shown that due to the initial stress of inserting the rectal probe, body temperature increases rapidly; however, vessel diameter and centerline velocity data would be beneficial in that initial vascular changes would be monitored as opposed to obtaining data for an already fully dilated blood vessel.

Results have also shown that in order to determine the efficiency of the wing in terms of dissipating heat from the body, the most important parameter is blood flow. Blood flow is dependent on vessel diameter and centerline velocity as described in Equation 5.1. All results indicate that when vessel diameter and centerline velocity increase, blood flow also decreases which helps reduce  $T_{body}$ . Velocity is not as much a contributor in heat dissipation as blood flow because it does not matter how fast the blood is moving through the wing, but how much volume of blood is in the bat wing at any given point in time. If blood is moving at faster velocities, it does not have much time to interact with the surroundings and therefore does not equilibrate to the wing temperature. If blood flow increases, a larger volume of blood that arrives to the wing at higher temperatures (i.e  $T_{body}$ ) can exchange heat with the surroundings

and return to the core at lower temperatures, therefore assisting in a decrease of body temperature.

This research has focused on vascular response to systemic heating in the pallid bat wing while monitoring  $T_{body}$ ; the trends in body temperature (Figure 25) indicate that after  $T_{chamber}$  becomes greater than  $T_{body}$ , the pallid bat begins to feel the effects of stress from environmental heating and  $T_{body}$  slightly increases. However, once the thermoregulatory mechanisms begin to work (i.e. vasodilation), body temperature begins to decrease to basal values. During the experiments,  $T_{body}$  did not reach basal values as there was a time limit placed on the experiments and complete cooling of the metabolic chamber was not allowed. Vascular responses to systemic heating were indicated by a positive correlation between vessel diameter, centerline velocity and blood flow with  $T_{chamber}$ . The wing of the pallid bat was extended outside the metabolic chamber and was definitely used as a thermal window to dissipate heat from the body to the environment as expected.

## CHAPTER VI

## THEORETICAL ANALYSIS OF THERMOREGULATION IN BATS

Theoretical models of thermoregulation are limited due to the difficulty in achieving model validation [67]. However they are important as they provide a way of testing behaviors under unsafe conditions. In the literature there are two main models of thermoregulation from which all others derive: one for humans first proposed by Stolwijk [68], and one for the squirrel monkey proposed by Spiegel [69] as described in Chapter II. In this study we will use energy balance to establish a simplified model of thermoregulation for the pallid bat based on a simplification of the models indicated above. The main difficulty associated with these models is the lack of anthropometric and thermal data required for its implementation, however they help provide useful insight to factors affecting heat exchange.

Experimental thermoregulatory studies in a few species of bats published in the literature have indicated: **(1)** the need for bats to save energy and how using torpor allows them to survive in colder environments without depleting their metabolic energy [2, 3], **(2)** by using energy conservation and heat transfer, these studies tried to explain why bats are nocturnal animals [88], and **(3)** studies in hot and humid environments have produced correlations between body temperature, metabolic activity, evaporative water loss (EWL) and ambient conditions. Using these studies based on analysis of metabolic energetics in bats, and energy conservation as indicated in Equation 2.2, the following relation is proposed for the analysis of thermoregulation and heat exchange in the pallid bat:

$$Q_{stored} = Q_{met} - Q_{EWL} - Q_{skin}, \quad (6.1)$$

where  $Q_{stored}$  denotes the heat stored in the body of the bat and is related mainly

to the core or body temperature of the animal,  $Q_{met}$  is the metabolic heat produced by the animal,  $Q_{EWL}$  corresponds to the evaporative water loss; finally, the term  $Q_{skin}$  indicates heat loss that takes place at the skin level and is mostly due to the temperature change between the core temperature and the ambient temperature. In the bat, two main contributions need to be considered: **(1)** heat exchange taking place through skin covered with fur, and **(2)** heat exchange taking place through hairless skin, such as the wing and ear membranes; because the wings account for about 80% of the surface area, the skin in the ears can be neglected, and the heat loss through the skin can be given as:

$$Q_{skin} = Q_{fur} + Q_{wing}. \quad (6.2)$$

The different components in the Equation 6.1 are strongly related to ambient temperature ( $T_{air}$ ), body temperature ( $T_{body}$ ), the nature of the boundary layer or air surrounding the animal (i.e. heat transfer coefficient), and more importantly for this work, the volume of blood available in the skin, and how this volume is affected due to vasomotion (vasoconstriction and vasodilation) and its response in the event of environmental temperature alterations or changes in metabolic activity and respiration rate (exercise). The next step in the development of the simplified thermoregulation model for the pallid bat is to write each one of the proposed terms as a function of the appropriate temperature gradients and by incorporating sufficient physical and physiological data available from thermoregulation experiments or other models.

In Equation 6.1, the left-hand side can be written in terms of the body temperature, as follows, by incorporating the specific heat of the tissue:

$$Q_{stored} = \rho CV \frac{dT}{dt}, \quad (6.3)$$

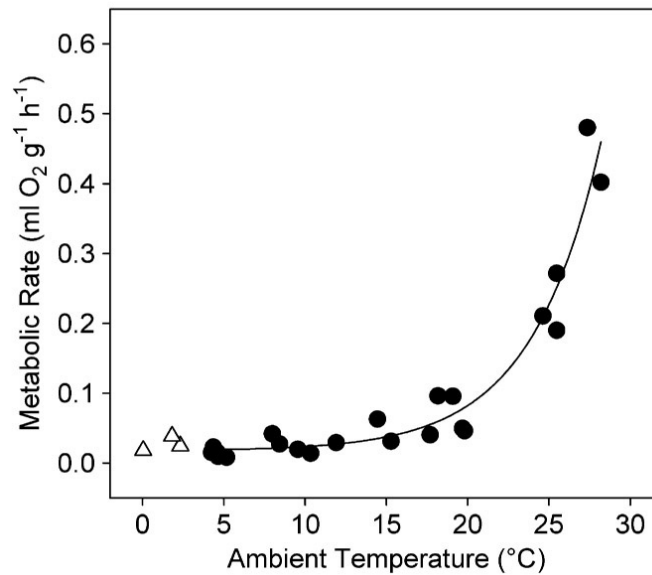


Fig. 43. Relationship between metabolic rate and  $T_a$  for *V. vulturnus*. Values included in the regression analysis are indicated by dark circles, and open triangles are  $T_a$  values below the minimum set-point during which bats increased metabolic rate to maintain body temperature [2].

where  $\rho$  indicates the average density of the bat body as a whole,  $V$  is the volume of the bat body ( $m = \rho V$ ), and  $T$  represents the core or body temperature. The specific heat ( $C$ ) of a bat corresponds to  $C=3200$  J/kg °C [16].

The metabolic heat production term  $Q_{met}$  is a function of body mass and body temperature, and is directly proportional to either the  $\text{CO}_2$  production or the  $\text{O}_2$  consumption of the animal. This term can be related to body temperature by using the  $Q_{10}$  law, which expresses the variation of a property (usually metabolic heat production, oxygen consumption or blood perfusion) in terms of alterations of body temperature from a baseline value  $T_{body,o}$ . This relationship is used to indicate how these physiological parameters change when the temperature that affects the processes (usually body temperature) changes  $10^\circ\text{C}$ . Using the  $Q_{10}$  law, the metabolic heat

production can be expressed as

$$Q_{met} = Q_{met}^o Q_{10}^{\frac{(T-T_o)}{10}}, \quad (6.4)$$

where  $Q_{met}^o$  is the basal metabolic heat production and is measured in W, determined for the bats in this study at thermoneutral conditions<sup>1</sup>; or it has been observed to depend on body mass of the animal ( $m$ ) in the following fashion [16]:

$$Q_{met}^o = \gamma m^{\frac{3}{4}}. \quad (6.5)$$

In this equation, the mass  $m$  is given in kilograms, and the basal metabolic rate is given in W. The value of the  $Q_{10}$  exponent is taken as  $e^1 = 2.71$ , and agrees with observations in bats showing an exponential relationship ( $R^2 = 0.94$ ) between body temperature  $T$  and metabolic rate as indicated in Figure 43.

The evaporative water loss,  $Q_{EWL}$  corresponds to the heat loss that takes place through evaporation during respiration, and through the skin (not covered in fur). The major source of evaporative water loss in the bat is through respiration, as the wing membrane has a composition where evaporative heat loss is minimal; consequently, the contribution of the skin will be neglected. The factors that control  $Q_{EWL}$  are air humidity, water pressure and air temperature but above all, respiration rate, which has been reported to be a function of core and ambient temperature in some species of bats [89]. In this study,  $Q_{EWL}$  will be written as a function of air temperature and body or core temperature, in the following form:

$$Q_{EWL} = \Gamma f_{EWL}(T_{air}) \times Q_{10}^{\frac{(T-T_o)}{10}}, \quad (6.6)$$

where  $\Gamma$  is a constant used to transform the common units used to express evapo-

---

<sup>1</sup>Thermoneutral conditions correspond to basal body temperature, and normal ambient temperature.

rative water loss (ml of water/ grams of tissue/ hour) to *Watts*, the  $Q_{10}$  law is the same as was used in the first contribution and will be taken from experimental thermoregulation studies [89] where the evaporative water loss of bats has been measured by sensing humidity changes while the bat is inside a metabolic chamber. Figure 44 indicates how this quantity varies with ambient temperature  $T_{air}$  in both males and females. Using these data points, an exponential curve is fitted using least squares for both males and females and then an average of both curves is calculated. The corresponding functions associated to the dependence with  $T_{air}$  are as follows:

$$f_{EWL}(T_{air}) = a \exp(bT_{air}) + c. \quad (6.7)$$

In this equation, curve fitting the parameters obtained from Figure 44 were transformed to the appropriate units by using the fact that evaporation of  $1 \text{ g H}_2\text{O min}^{-1} = 40\text{W}$  [16] and with the weight of the animal. It is convenient to mention that this function was established for a different bat species, which is characterized by similar body mass. This relationship is used, as the system built and described in previous chapters is not capable of determining humidity levels of the inlet and outlet air.

In addition, the terms  $Q_{met}$  and  $Q_{EWL}$  can be written using the definition of internal conductance  $C_{int}$  given by

$$C_{int} = \frac{Q_{met} - Q_{EWL}}{T - T_{skin}}.$$

$T_{skin}$  in this case is an average of the skin temperature that should involve both  $T_{wing}$  and  $T_{fur}$  because of the disproportion of skin surface area occupied for each compartment (wing and fur). The  $T_{skin}$  used in the previous equation should be a weighted average of the skin temperature defined as

$$T_{skin} = (A_{fur}T_{fur} + A_{wing}T_{wing})/(A_{fur} + A_{wing}) = 0.2T_{fur} + 0.8T_{wing}, \quad (6.8)$$

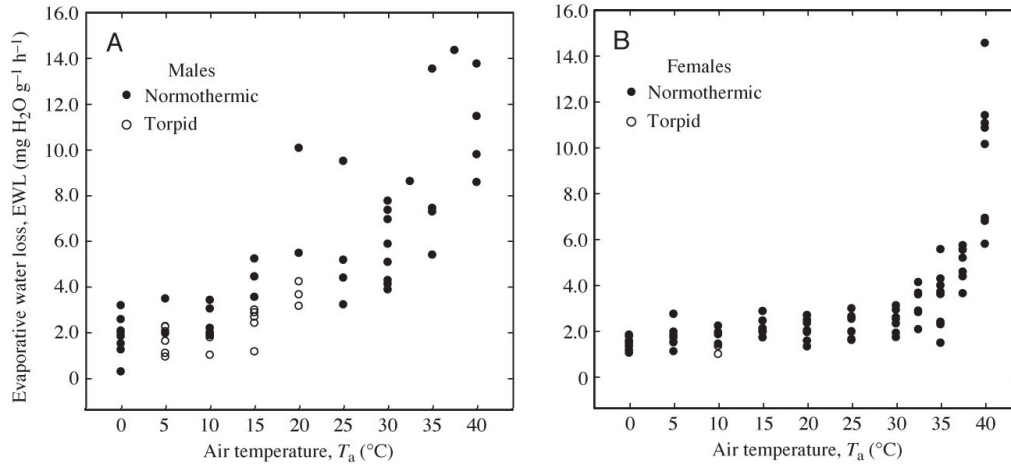


Fig. 44. Mass-specific evaporative water loss of male and female *L. cinereus* as a function of air temperature ( $T_a$ ). Closed symbols represent normothermic individuals, open symbols are torpid bats [89].

where available correlations can be used to determine the area of the wing based on body mass of the bat [88]. From this reference, two main relationships are expressed: **(1)** for bats with body mass ranging from 3 to 130 g,  $A_{wing}=0.18 m^{0.49}$ , and **(2)** for bats with body mass in the range of 16g to 1.4kg,  $A_{wing}=0.23 m^{0.69}$ .

Finally, to write  $Q_{fur}$  and  $Q_{wing}$  in terms of the appropriate temperature gradient, energy conservation at the skin surface needs to be considered, such consideration will provide two more equations that can be used to substitute the skin temperatures  $T_{wing}$  and  $T_{fur}$  in terms of the core temperature  $T$ , the air temperature  $T_{air}$  or ambient temperature outside the chamber and the chamber temperature  $T_{chamber}$ , which is actively varied during the heating protocols. These equations take the following general form during thermoneutral conditions

$$Internal\ heat\ flow\ (H_i) = External\ heat\ flow\ (H_e),\ where \quad (6.9)$$



$$H_e = h_{skin}A_{skin}(T_{skin} - T_{air}), \text{ and } H_i = \beta_{skin}(T_{body} - T_{skin}), \quad (6.10)$$

where  $h_{skin}$  represents the average heat transfer coefficient at the skin level, and it will be different for the skin with fur and the wing;  $\beta_{skin}$  is used to denote internal heat exchange from the core to the surface through alterations in skin blood flow and it represents the energy exchanged by the blood flow measured in  $\text{W}/\text{m}^2\text{°C}$  [90]. Equations 6.9 and 6.10, can be used to estimate the temperature of both the wing tissue ( $T_{wing}$ ) and the skin with fur ( $T_{fur}$ ), for the steady state case.

The heat transfer coefficients  $h_{fur}$  and  $h_{wing}$  can be taken from literature by assuming the bat body as an ellipsoid, a sphere or a finite length cylinder, and the wing as a flat plate. In this study, we will consider natural convection because the bat is at rest, the wing is restrained and fully extended. In addition, the body is inside a chamber where minimal air currents are present. For natural convection of air, the typical values for the heat transfer coefficient are from 3 - 25  $\text{W}/\text{m}^2\text{°C}$  [39]. Particularly, for flat plates, the following relationship can be used to estimate the heat transfer coefficient due to natural convection

$$h_{wing} = \frac{\rho_{air}C_{p,air}}{r_{free}}, \quad (6.11)$$

where  $r_{free}$  represents the thermal resistance and is expressed in terms of the dimensions of the wing  $d$  or wing span

$$r_{free} = 820(d/(T_{wing} - T_{air}))^{0.25}. \quad (6.12)$$

The wing span  $d$  is defined as the distance between the tips of the wings, which can be between 28 to 32 cm for bats of the size of the pallid bat. In the calculations presented here, we use the value of  $d/2$ , as only a single wing is extended outside the

chamber.

During active thermoregulation, or while body temperature and wing temperature are changing in response to alterations in ambient temperature, Equations 6.9 and 6.10, need to be modified to introduce the dynamic behavior; this is done by assuming that the changes in skin temperature (wing or skin with fur) are described by the general equation:

$$\rho_{skin} C_p V_{skin} \frac{dT_{skin}}{dt} = h_{skin} A_{skin} (T_{air} - T_{skin}) + \rho_b C_{pb} \beta_{skin} (T_{body} - T_{skin}), \quad (6.13)$$

where,  $\rho$  indicates the tissue density,  $C_p$  is the tissue specific heat,  $V$  represents the tissue volume,  $A$  is the surface area,  $\rho_b$  and  $C_{pb}$  indicate the density and specific heat of blood, and  $\beta_{wing}$  indicates the volumetric blood flow or perfusion to the tissue.  $T_{body}$  is the body or core temperature,  $h_{skin}$  is the heat transfer coefficient at the wing surface, which dominates the environmental heat exchange; finally  $T_{air}$  represents the temperature of the surrounding air. This equation separates the factors that contribute to tissue temperature in environmental and blood perfusion. Using the model of Equation 6.13, equations for the temperature of the wing and the skin with fur can be written.

The term  $\beta_{skin}$  is associated to heat exchange by internal convection, as the blood permeates the tissue entering through the arteries, passing through the capillaries and leaving through the veins. To estimate such heat exchange, detailed description of vascular structure, as well as blood flow in the different arteries is required. Completion of this task is complicated even in a tissue containing only two main arterial branches, like the bat wing. A common technique of still capture heat exchange by the circulation without the need of detailed analysis of the vascular structure and blood flow in every location of the arterial tree involves using a volumetric perfusion term  $\omega_b$ , commonly expressed in ml of blood entering a volume of mass  $m$  per unit

time (ml blood/g of tissue/minute) or in units of volume per unit time ( $\text{m}^3/\text{s}$ ). The amount of heat exchanged by the circulation ( $\beta_{skin}$ ) as it moves blood from core to surface is defined as:

$$\beta = \rho_b C_b \omega_b,$$

where  $\rho_b$  and  $C_b$  correspond to density and specific heat of blood and have the values of  $1050 \text{ kg/m}^3$  and  $3800 \text{ J/kg } ^\circ\text{C}$ , respectively [91], and  $\omega_b$  is a function that will depend on skin temperature and body temperature and will increase as skin temperature or body temperature increases (vasodilatation response) and its magnitude will be reduced as skin temperature is reduced. If  $\beta_{skin}$  can be estimated from measurements of blood flow at the wing, then Equation 6.9 can be used to write equations for  $T_{wing}$  and  $T_{fur}$  and complete a system of 3 equations with 3 unknowns ( $T$ ,  $T_{wing}$ , and  $T_{fur}$ ).

$$\rho C V \frac{dT_{body}}{dt} = (Q_{met,o} - f_{EWL}(T_{chamber})) Q_{10}^{\frac{\Delta T_{body}}{10}} - \quad (6.14)$$

$$h_{wing} A_{wing} (T_{wing} - T_{air}) - h_{fur} A_{fur} (T_{fur} - T_{air}),$$

$$\rho_{fur} C_p V_{fur} \frac{dT_{fur}}{dt} = h_{fur} A_{fur} (T_{air} - T_{fur}) + \rho_b C_{pb} \beta_{fur} (T_{body} - T_{fur}), \quad (6.15)$$

$$\rho_{wing} C_p V_{wing} \frac{dT_{wing}}{dt} = h_{wing} A_{wing} (T_{air} - T_{wing}) + \rho_b C_{pb} \beta_{wing} (T_{body} - T_{wing}). \quad (6.16)$$

The set of ordinary differential equations given above requires the initial temperature values, the temporal variation of the air outside the chamber ( $T_{air}$ ) and the temperature of the chamber  $T_{chamber}$ ; as well as the functions describing the relationship between the different temperatures ( $T_{fur}$ ,  $T_{wing}$  and  $T_{body}$ ) and the perfusion terms  $\beta_{wing}$  and  $\beta_{fur}$ . Such functional relationship can be estimated from the observations presented in the previous chapter where the changes in blood flow in response to alterations in  $T_{chamber}$  and  $T_{body}$  were presented.

The set of equations 6.14-6.16 will be solved using the fourth order Runge-Kutta

method with variable time step, this algorithm was implemented in MATLAB. In the experiments performed and discussed in the previous chapter, the temperature at the skin with fur was not recorded systematically or throughout the experiments; given the lack of information regarding  $T_{fur}$ . For the analysis presented next, we will neglect the contribution of  $T_{fur}$  and the variation in the skin blood in the regions with fur. This assumption is justified because of two main reasons: **(1)** the presence of fur reduced considerably the heat loss due to the quiescent layer of air trapped in the fur, and **(2)** most of the heat exchange takes place through the wing because of its large surface area, and small volume, which makes it a thermal window. Until a safe and efficient way of recording skin temperature in the skin with fur is devised in our experiments, we will not be able to estimate the contribution of this term.

#### A. Model Implementation

The simplified model of equations 6.14 to 6.16 will be used to analyze how alterations in the environmental conditions, particularly heating, affect the body and wing temperatures. To solve the set of equations that describe the thermoregulatory capacity of the bat, the parameters described in Table III are used. An important parameter involved in this model, is the perfusion term  $\beta_{wing}$ , as it is able to combine vascular response, or alterations in centerline velocity, blood flow and vessel diameter to systemic parameters such as body temperature, wing temperature and ambient or chamber temperature.

The perfusion term introduced in the equations should vary proportional to the blood flow. Variations of blood flow and chamber and body temperatures have been discussed in the previous chapter, in Figures 35 and 37. From these figures, it is observed that the relationship between perfusion and the discussed temperatures can

Table III. Table Indicating Parameters Involved in the Thermoregulation Model Described by Equations 6.14 to 6.16

$\rho, (kg/m^3)$	1, 075	Ref. [16]
$C_p, (J/kg.^{\circ}K)$	2, 700 – 3, 200	Ref. [16]
$\rho_b, (kg/m^3)$	1, 069	Ref. [91]
$C_b, (J/kg.^{\circ}K)$	3, 650	Ref. [91]
$\rho_{air}, (kg/m^3)$	1.2	Ref. [88]
$C_{p,air}, (J/kg.^{\circ}K)$	1, 000	Ref. [88]
$Q_{met}, (Watts)$	$\gamma m^{\frac{3}{4}} Q_{10}^{\frac{(T-T_o)}{10}}$ $\gamma = 3.4$ $T_o = \text{basal body temperature}$	Eqs. 6.4 -6.5
$f_{EWL}, (mgH_2O/gh)$	$(a \exp(bT_{air}) + c) Q_{10}^{\frac{(T-T_o)}{10}}$ $a = 1.5763, b = 0.0331, c = 0.0$	Eq. 6.7
$A_{wing}, (m^2)$	$0.18m^{0.49}$	Ref. [88]
$h_{wing}, (W/m^2.^{\circ}C)$	$\frac{\rho_{air} C_{p,air}}{r_{free}}$ $r_{free} = 820(d/(T_{wing} - T_{air}))^{0.25}$ $d = \text{wing span}/2$	Ref. [88] Eq. 6.12
$\beta_{wing}, (m^3/s)$	$\beta_o \left( A Q_{10}^{\frac{\Delta T_{body}}{10}} + B Q_{10}^{\frac{\Delta T_{chamber}}{10}} \right)$	Eq. 6.17.

be approximated by a straight line. So far, we have been able to estimate trends and correlations between body temperature, chamber temperature and blood flow; but data to develop a functional relationship between these parameters will only be available until more experiments are conducted.

To establish a mathematical relationship or model for the perfusion function in terms of  $T_{chamber}$  and body temperature  $T$ , we will focus on the following observations:

- Models dealing with estimation of tissue temperature use the  $Q_{10}$  law to estimate how blood perfusion and metabolic activity change as body or tissue temperature is changed.
- Published studies in thermoregulation and analysis of vasodilation have established that there are two main temperature signals controlling the level or percent of vasodilation (VD). These two temperature signals correspond to: **(1)** body temperature,  $T$  and **(2)** skin temperature,  $T_{skin}$ , which as discussed in previous chapters its value depends on both body temperature and ambient temperature. Finally
- Our experimental observations indicate that there are strong correlations between blood flow and both body temperature and chamber temperature.

Due to the reasons mentioned before, the perfusion  $\beta_{wing}$  will be approximated with the following relationship:

$$\beta_{wing} = \beta_o \left( A Q_{10}^{\frac{\Delta T_{body}}{10}} + B Q_{10}^{\frac{\Delta T_{chamber}}{10}} \right), \quad (6.17)$$

where  $\Delta T_{body} = T_{body} - T_{body}^o$ , and  $T_{body}^o$  is the basal body temperature,  $\Delta T_{chamber} = T_{chamber} - T_{chamber}^o$ , and  $T_{chamber}^o$  correspond to the normal ambient temperature. Finally, the coefficients  $A$  and  $B$  indicate the contribution of each one of temperature sig-

nals to the perfusion, and it is assumed that  $A + B = 1$ . At this stage, we are not certain about the contribution of each term to the perfusion function, this can be tested experimentally by fixing the wing temperature for instance using a heating plate or a cooling device. What we hypothesize is that the contribution of the body temperature signal ( $Q_{10}^{\frac{\Delta T_{body}}{10}}$ ) and the chamber temperature signal ( $Q_{10}^{\frac{\Delta T_{chamber}}{10}}$ ) should depend on both: **(1)** heating stage as described in the previous chapter ( $T_{body} > T_{chamber}$  or  $T_{body} < T_{chamber}$ ) and **(2)** the rate at which body temperature and/or  $T_{chamber}$  change.

Finally, as observed in Equation 6.17, the coefficient  $\beta_o$  needs to be determined, this coefficient represents the basal perfusion, and can be estimated considering that the basal conditions occur at the thermoneutral state, and therefore, the system of equations for the thermoregulation model 6.14-6.16 can be used to obtain the following relationship for  $\beta_o$ :

$$\beta_o = \frac{Q_{met,o} - Q_{EWL,o}}{\rho_b C_{p,b} (T_o - T_{wing,o})} \quad (6.18)$$

## B. Numerical Results

To solve the system of equations formed by Equations (6.14) and (6.16), the dynamic variation of both  $T_{chamber}$  and  $T_{air}$  are necessary, as well as two initial conditions, one for the body temperature and the other for the wing temperature as follows:

$$T(t = 0) = T^o, \quad \text{and} \quad T_{wing}(t = 0) = T_{wing}^o. \quad (6.19)$$

For the calculations it is assumed that the room temperature  $T_{air}$  remained constant throughout the experiments, and  $T_{chamber}$  varied from  $T_{chamber} = 24^\circ\text{C}$  to the maximum allowed chamber temperature of  $36^\circ\text{C}$  according to our animal use protocol. The time variation for the chamber temperature  $T_{chamber}$  is assumed to follow a linear trend, where the heating rate can be varied.

The model will be used to analyze the effect of different factors such as:

- initial condition,
- metabolic heat production,
- wing perfusion,
- heating rate.

For the calculations, the mass of the bat is assumed to be 22 grams, the values of densities, and specific heats for tissues and air are given in Table III together with the relationships for the convective heat transfer coefficient at the wing surface  $h_{air}$  given in Equation 6.11. Figure 45 shows the general trend observed in the calculations of body and wing temperature. The upper lines correspond to the body temperature calculated using the thermoregulation model for the case of different initial conditions  $T^o=35, 33, 31$  and  $29^\circ\text{C}$ . Some of these conditions correspond to the case of body temperature greater than basal body temperature. The bottom lines correspond to the time variation of the wing temperature; in these calculations the initial wing temperature  $T_{wing}^o$  is considered constant in all the cases. This assumption is made because a clear relationship between body temperature and wing temperature was not observed during the experiments performed, however more trials are necessary to fully discard a correlation between body temperature and wing temperature.

It is seen in Figure 45 that the model phenomenologically reproduces the behavior observed during heating; however, we do not observe the characteristic behavior observed in **Stage B** of some of the heating experiments shown in Figure 25; we believe that this behavior is reproduced by the fact that the coefficients  $A$  and  $B$  associated to the wing perfusion function  $\beta_{wing}$  are not constant in time, and they might depend on the time variation or time derivative of both temperature signals.



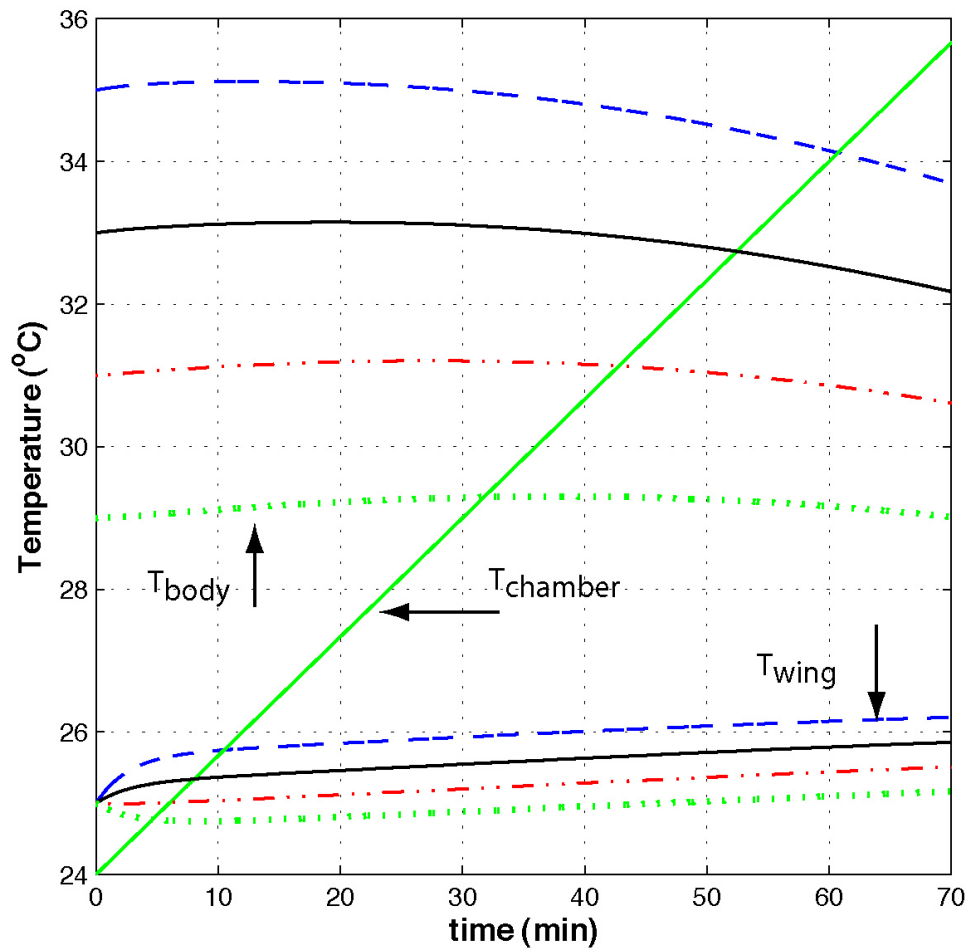


Fig. 45. Calculated time variation of both body temperature and wing temperature during a heating experiment for the case of different values of the initial body temperature. The initial wing temperature  $T_{wing}^o$  is considered constant in all the cases.

For the calculations presented in this figure, as well as in most of the figures presented, it is assumed that the coefficients  $A$  and  $B$  indicated in Equation 6.17 for the wing perfusion  $\beta_{wing}$  have the value of:  $A = B = 0.5$ , which indicates that the contribution of the body temperature and chamber temperature to the blood perfusion function is the same.

Figure 46 shows how different linear combinations of the contribution of body temperature and chamber temperature to the wing perfusion affects the calculated temperatures. Three cases are considered that correspond to: **Case A:**  $A = B = 0.5$  or equal contribution; **Case B:** where  $A = 0.75$  and  $B = 0.25$ , that represents the case where the body temperature signal dominates blood perfusion; and finally, **Case C:** where the chamber temperature signal dominates the perfusion function as the coefficients  $A$  and  $B$  are selected as  $A = 0.25$  and  $B = 0.75$ . In this case it is observed that the variation in both body and wing temperature start as the chamber temperature increases, the variation in the response is observed first in the wing and then on the body temperature signal. It is seen that when the chamber temperature dominates the perfusion function (Case C), then the wing temperature increases and the body temperature is reduced; the opposite effect is observed in Case B.

Figure 47 shows the variation in the thermal response when the basal metabolic heat  $Q_{met,o}$  is varied. Three different values: corresponding to:  $2Q_{met,o}$ ,  $Q_{met,o}$  and  $Q_{met,o}/2$ , where  $Q_{met,o}$  is calculated at baseline body temperature and for a mass of 22g using Equation 6.5. As before, it is assumed that the contribution of the body temperature and chamber temperature to the blood perfusion function is the same ( $A = B = 0.5$ ). This figure shows that the basal metabolic heat has a significant effect on both: body temperature and wing temperature; in addition, the way that the wing responds in the first few minutes of heating is strongly characterized by this quantity.

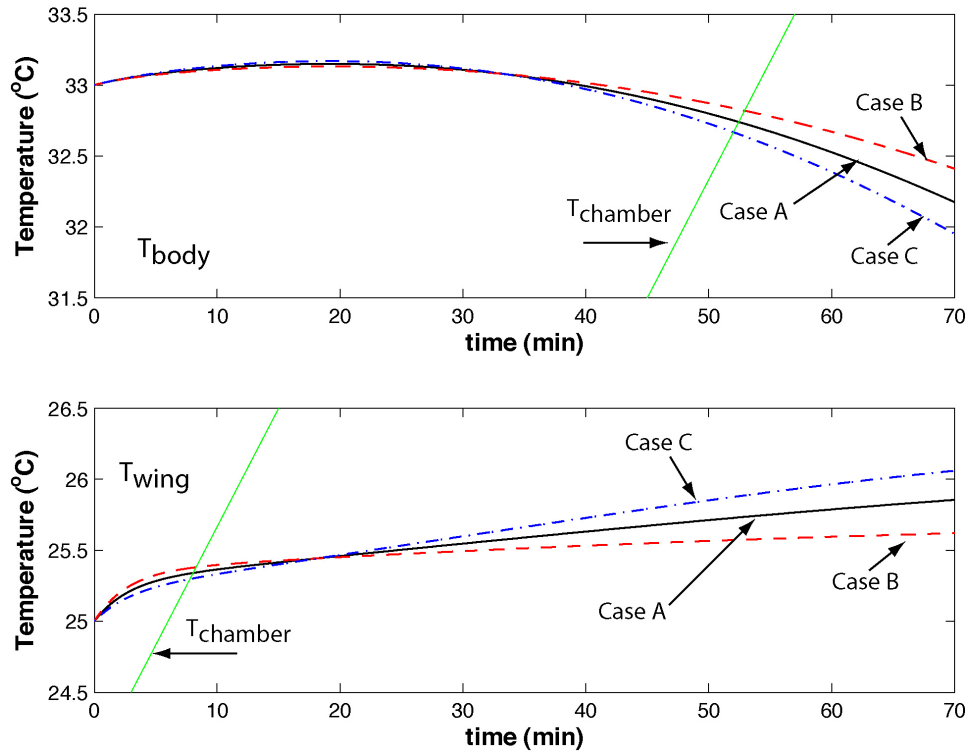


Fig. 46. Calculated time variation of both body temperature and wing temperature during a heating experiment for the case of different combinations of the values associated to coefficients  $A$  and  $B$  used in Equation 6.17 to estimate the contribution of body temperature and wing temperature signals to the wing perfusion  $\beta_{wing}$ .

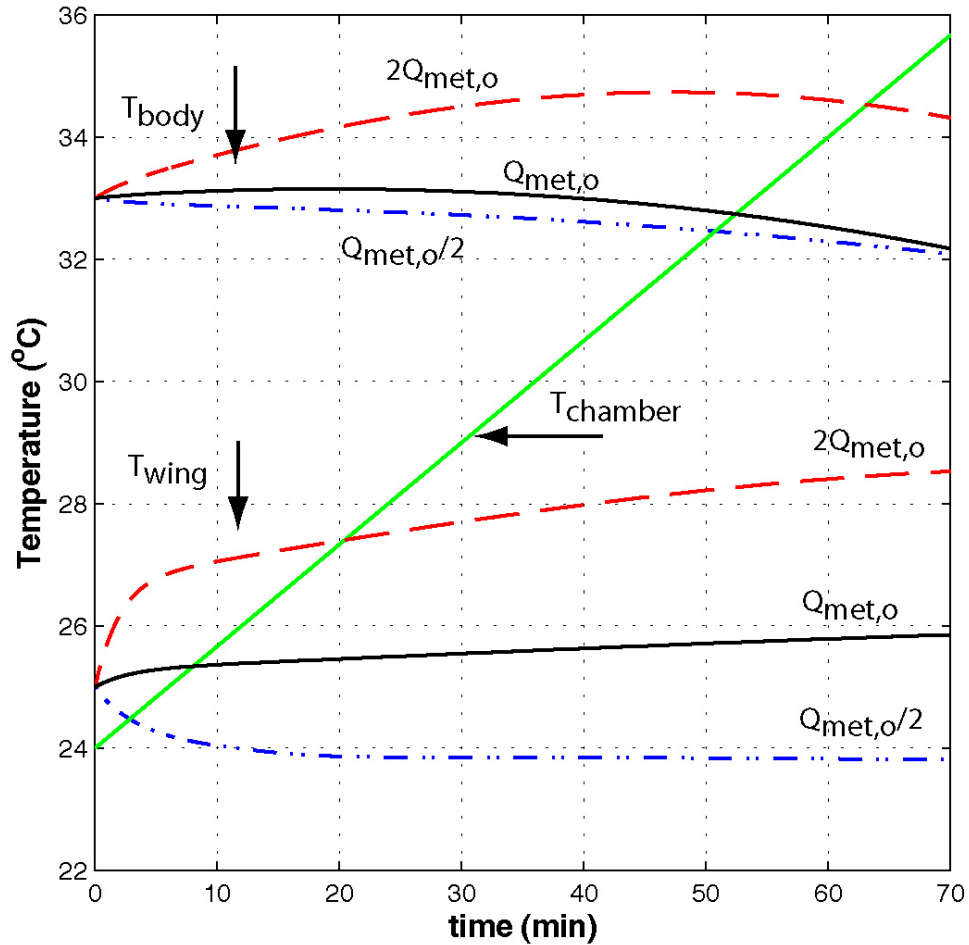


Fig. 47. Calculated time variation of both body temperature and wing temperature during a heating experiment for the case of different value of basal metabolic heat production. The plot shows three different values: corresponding to:  $2Q_{met,o}$ ,  $Q_{met,o}$  and  $Q_{met,o}/2$ , where  $Q_{met,o}$  is calculated at baseline body temperature and for a mass of 22g using Equation 6.5. In the figure, the time variation of  $T_{chamber}$  is presented as reference.

Finally, Figure 48 shows variations in the heating rate, and considers two cases, one referred to as *slow heating* where  $T_{chamber}$  changes from 24°C to 36°C in 72 minutes as performed during the experiments; and the other heating protocol where the heating time is reduced to 36 minutes and is denoted as *rapid heating*. While varying heating rate, it is observed that the values of both body temperature and wing temperature when they cross the  $T_{chamber}$  line are the same independently of the heating rate; this result indicates two issues: **1)** Experiments need to be performed where the heating rate is altered, and **2)** the current thermoregulation model is unable to show the dynamic responses that characterize how fast or slow an animal can react to alterations in its ambient conditions. As mentioned before, this can be introduced in the model by considering the effect of  $dT/dt$ ,  $dT_{wing}/dt$  and  $dT_{chamber}/dt$ .

### C. Conclusions

Developing a thermoregulation model was beneficial in that we can study unsafe conditions for the animal that otherwise could not be studied experimentally. The model developed was able to reproduce general trends observed for  $T_{wing}$  and  $T_{body}$  during heating experiments, indicating that it is a good starting point in describing the parameters that affect temperature changes in the pallid bat.

Results from varying the perfusion function described in this chapter which combines contributions of  $T_{body}$  and  $T_{chamber}$  needs to be improved to consider the time derivatives of these temperature signals. By introducing these time derivatives then the dynamic response of the animal will be observed.

Also, the thermoregulation model showed the need of improving the experimental set-up to estimate evaporative water loss; mathematical results show that metabolic heat production is the most important parameter affecting changes in  $T_{body}$  and  $T_{wing}$

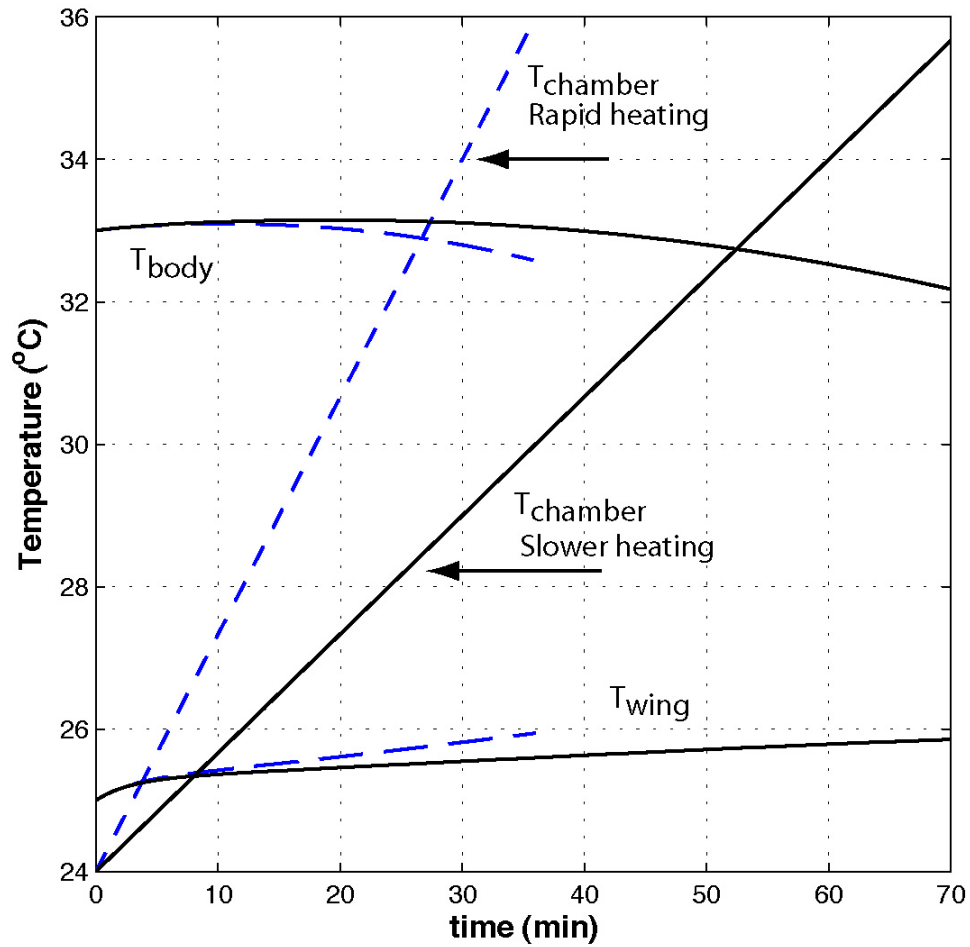


Fig. 48. Calculated time variation of both body temperature and wing temperature during two heating experiment where two different heating rates are considered: *slow heating* and *rapid heating*.

which might be due to the fact that there is a limited description of evaporative water loss. By improving the experimental set-up, we can have a better understanding of the parameters involved in temperature regulation.

## CHAPTER VII

## CONCLUSIONS

This research has focused on vascular response to systemic heating in the pallid bat wing while monitoring  $T_{body}$ ; the trends in body temperature indicate that after  $T_{chamber}$  becomes greater than  $T_{body}$ , the pallid bat begins to feel the effects of stress from environmental heating and  $T_{body}$  slightly increases. However, once the thermoregulatory mechanisms begin to work (i.e. vasodilation), body temperature begins to decrease to basal values. During the experiments,  $T_{body}$  did not reach basal values as there was a time limit placed on the experiments and complete cooling of the metabolic chamber was not allowed. Vascular responses to systemic heating were indicated by a positive correlation between vessel diameter, centerline velocity and blood flow with  $T_{chamber}$ . The wing of the pallid bat was extended outside the metabolic chamber and was definitely used as a thermal window to dissipate heat from the body to the environment as expected.

Developing a thermoregulation model was beneficial in that we can study unsafe conditions for the animal that otherwise could not be studied experimentally. The model developed was able to reproduce general trends observed for  $T_{wing}$  and  $T_{body}$  during heating experiments, indicating that it is a good starting point in describing the parameters that affect temperature changes in the pallid bat.

Results from varying the perfusion function described in this chapter which combines contributions of  $T_{body}$  and  $T_{chamber}$  needs to be improved to consider the time derivatives of these temperature signals. By introducing these time derivatives then the dynamic response of the animal will be observed. The thermoregulation model served to show the need of improving the experimental set-up to estimate evaporative water loss.



## REFERENCES

- [1] R.J. Widmer, J.E. Laurinec, M.F. Young, G.A. Laine, and C.M. Quick, “Local heat produces a shear-mediated biphasic response in the thermoregulatory microcirculation of the pallid bat wing,” *Am J Physiol Regul Integr Comp Physiol*, vol. 291, pp. 625–632, 2006.
- [2] C.K.R. Willis, C. Turbill, and F. Geiser, “Torpor and thermal energetics in a tiny Australian vespertilionid, the little forest bat (*Vespadelus vulturnus*),” *J Comp Physiol B*, pp. 479–486, 2005.
- [3] D.J. Hosken and P.C. Withers, “Temperature regulation and metabolism of an Australian bat, *Chalinolobus gouldii* (Chiroptera: Vespertilionidae) when euthermic and torpid,” *J Comp Physiol B*, pp. 71–80, 1997.
- [4] S.P. Thomas, D.B. Follette, and A.T. Farabaugh, “Influence of air temperature on ventilation rates and thermoregulation of a flying bat,” *Am J Physiol Regul Integr Comp Physiol*, vol. 260, pp. 960–968, 1991.
- [5] C.L. Lausen and R.M.R. Barclay, “Thermoregulation and roost selection by reproductive female big brown bats (*Eptesicus fuscus*) roosting in rock crevices,” *J Zool, Lond.*, vol. 260, pp. 235–244, 2003.
- [6] M.A. Chappell and R.C. Roverud, “Temperature effects on metabolism, ventilation, and oxygen extraction in a neotropical bat,” *Respiration Physiology*, vol. 81, pp. 401–412, 1990.
- [7] F. Geiser and R.M. Brigham, “Torpor, thermal biology, and energetics in Australian long-eared bats (*Nyctophilus*),” *J Comp Physiol B*, vol. 170, no. 2, pp. 153–162, 2000.

- [8] R.V. Baudinette, S.K. Churchill, K.A. Christian, J.E. Nelson, and P.J. Hudson, "Energy, water balance and the roost microenvironment in three australian cave-dwelling bats (*Microchiroptera*)," *J Comp Physiol B*, vol. 170, no. 2, pp. 439–446, 2000.
- [9] P. Libby, "Inflammation and cardiovascular disease mechanisms," *American Journal of Clinical Nutrition*, vol. 83, no. 2, pp. 456S–460S, 2006.
- [10] M. Shechter, I. Marai, S. Marai, Y. Sherer, B.A. Sela, M.S. Feinberg, A. Rubinstein, and Y. Shoenfeld, "The association of endothelial dysfunction and cardiovascular events in healthy subjects and patients with cardiovascular disease," *The Israel Medical Association Journal*, vol. 9, no. 4, pp. 271–276, 2007.
- [11] P. Valensi, O. Smagghue, J. Paries, P. Velayoudon, T.N. Nguyen, and J.R. Attali, "Peripheral vasoconstrictor responses to sympathetic activation in diabetic patients: Relationship with rheological disorders," *Metabolism*, vol. 46, no. 3, pp. 235–241, 1997.
- [12] B.T. Ngo, K.D. Hayes, D.J. DiMiao, S.K. Srinivasan, C.J. Huerter, and M.S. Rendell, "Manifestations of cutaneous diabetic microangiopathy," *American Journal Clinical Dermatology*, vol. 6, no. 4, pp. 225–237, 2005.
- [13] N. Charkoudian, "Skin blood flow in adult human thermoregulation: How it works, when it does not, and why," *Mayo Clinic Proc.*, pp. 603–612, 2003.
- [14] A.L. Herrick, "Pathogenesis of Raynaud's phenomenon," *Rheumatology*, vol. 44, no. 5, pp. 587–596, 2005.
- [15] A.H. Mawdsley and S.J. Brown, "Raising awareness of Raynaud's phenomenon and scleroderma," *Nursing Times*, vol. 101, no. 8, pp. 30–31, 2005.

- [16] C. Jessen, *Temperature Regulation in Humans and Other Mammals*, Springer, New York, NY.
- [17] M.E. Hernando, E.J. Gomez, A. Gili, M. Gomez, G. Garcia, and F. del Pozo, “New trends in diabetes management: mobile telemedicine closed-loop system,” *Stud Health Technol Inform*, vol. 105, pp. 70–9, 2004.
- [18] H. Kitaoka, M. Majima, A. Kitazawa, S. Sakane, K. Takeda, J. Takamatsu, and N. Ohsawa, “Impaired regulation of skin temperature in patients with diabetes mellitus evaluated by the cold exposure test,” *Bull Osaka Med Coll*, vol. 35, no. 1-2, pp. 99–105, 1989.
- [19] M.F. Meyer, C.J. Rose, J.O. Hulsmann, H. Schatz, and M. Pfohl, “Impairment of cutaneous arteriolar 0.1 hz vasomotion in diabetes,” *Exp Clin Endocrinol Diabetes*, vol. 111, no. 2, pp. 104–110, 2003.
- [20] H.T. Hammel, “Regulation of internal body temperature,” *Annual Review of Physiology*, pp. 641–710, 1968.
- [21] M. Cabanac, “Temperature regulation,” *Annual Review of Physiology*, pp. 415–439, 1975.
- [22] A. Hemingway and W.M. Price, “The autonomic nervous system and regulation of body temperature,” *Anesthesiology*, vol. 29, no. 4, pp. 693–701, 1968.
- [23] W. Yang, *Biothermal-Fluid Sciences: Principles and Applications*, Hemisphere Publishing Corporation, New York, NY, 1989.
- [24] T.L. Smith, L.A. Koman, E.S. Gordon, M.B. Holden, and B.P. Smith, “Effects of peripheral sympathectomy on thermoregulatory vascular control in the rabbit ear,” *Microsurgery*, vol. 18, pp. 129–136, 1998.

- [25] M.J. Mullen, R.K. Kharbanda, J. Cross, A.E. Donald, M. Taylor, P. Vallance, J.E. Deanfield, and R.J. MacAllister, "Heterogenous nature of flow-mediated dilatation in human conduit arteries in vivo: relevance to endothelial dysfunction in hypercholesterolemia," *Circulation Research*, vol. 88, pp. 145–151, 2001.
- [26] Y. Higashi and M. Yoshizumi, "New methods to evaluate endothelial function: method for assessing endothelial function in humans using a strain-gauge plethysmography: nitric oxide-dependent and -independent vasodilation," *Journal of Pharmacological Sciences*, vol. 93, pp. 399–404, 2003.
- [27] S. Tandon, K. Bhargava, H. Gupta, M. Bansal, and R.R. Kasliwal, "Non-invasive assessment of endothelial function by brachial artery flow mediated vasodilatation and its association with coronary artery disease: an Indian perspective," *Journal of the Indian Medical Association*, vol. 102, pp. 243–246, 251–252, 2004.
- [28] H.A. Hadi, C.S. Carr, and J. Al Suwaidi, "Endothelial dysfunction: cardiovascular risk factors, therapy, and outcome," *Vascular Health and Risk Management*, vol. 1, no. 3, pp. 183–198, 2005.
- [29] P.M. Netten, H. Wollersheim, T. Thien, and J.A. Lutterman, "Skin microcirculation of the foot in diabetic neuropathy," *Clinical Science*, vol. 91, no. 5, pp. 559–565, 1996.
- [30] R. Vanholder, W. Van Biesen, F. Verbeke, and N. Lameire, "The epidemic of cardio-vascular disease in renal failure: where does it come from, where do we go," *Acta Clinica Belgica*, vol. 61, no. 5, pp. 205–211, 2006.
- [31] J. Schattschneider, K. Hartung, M. Stengel, J. Ludwig, A. Binder, G. Wasner, and R. Baron, "Endothelial dysfunction in cold type complex regional pain syndrome," *Neurology*, vol. 67, no. 4, pp. 673–675, 2006.

- [32] C.I. Wright, C.I. Kroner, and R. Draijer, “Non-invasive methods and stimuli for evaluating the skin’s microcirculation,” *Journal of Pharmacological and Toxicological Methods*, vol. 54, pp. 1–25, 2006.
- [33] D.L. Kellogg, “In vivo mechanisms of cutaneous vasodilation and vasoconstriction in humans during thermoregulatory challenges,” *Journal of Applied Physiology*, vol. 100, pp. 1709–1718, 2006.
- [34] R.C. Littleford, F. Khan, and J.J. Belch, “Impaired skin vasomotor reflexes in patients with erythromelalgia,” *Clinical Science*, vol. 96, no. 5, pp. 507–512, 1999.
- [35] M. Berghoff, M. Kathpal, S. Kilo, M.J. Hilz, and R. Freeman, “Vascular and neural mechanisms of ach-mediated vasodilation in the forearm cutaneous microcirculation,” *Journal of Applied Physiology*, vol. 92, no. 2, pp. 780–788, 2002.
- [36] C. Lemne, U. de Faire, and B. Fagrell, “Mental stress induces different reactions in nutritional and thermoregulatory skin microcirculation: a study in borderline hypertensives and normotensives,” *Journal of Human Hypertension*, vol. 8, no. 8, pp. 559–563, 1994.
- [37] M.M. Chen, *Heat Transfer in Medicine and Biology: Analysis and Applications*, vol. 1, pp. 153–164, Plenum Press, New York, NY, 1985.
- [38] M.M. Chen and K.R. Holmes, *Microvascular Contributions in Tissue Heat Transfer*, *Annals New York Academy of Sciences*, vol. 335, pp. 98–106, 1980.
- [39] Y.A. Cengel, *Heat Transfer: A practical approach*, The McGraw-Hill Companies, Columbus, OH, 2002.

- [40] A. Shitzer and R.C. Eberhart, *Heat Transfer in Medicine and Biology: Analysis and Applications*, vol. 1, pp. 137–152, Plenum Press, New York, NY, 1985.
- [41] A. Hsu, S. Heshka, I. Janumala, M.Y. Song, M. Horlick, N. Krasnow, and D. Gallagher, “Larger mass of high-metabolic-rate organs does not explain higher resting energy expenditure in children,” *The American Journal of Clinical Nutrition*, vol. 77, no. 6, pp. 1506–1511, 2003.
- [42] L.M. Jiji, S. Weinbaum, and D.E. Lemons, “Theory and experiment for the effect of vascular microstructure on surface tissue heat transfer - Part II: Model formulation and solution,” *Journal of Biomechanical Engineering*, vol. 106, pp. 331–341, November 1984.
- [43] D.D. Heistad and F.M. Abboud, “Factors that influence blood flow in skeletal muscle and skin,” *Anesthesiology*, vol. 41, no. 2, pp. 139–156, 1974.
- [44] T.K. Bergersen, M. Eriksen, and L. Walloe, “Effect of local warming on hand and finger artery blood velocities,” *Am J Physiol Regulatory Integrative Comp Physiol*, vol. 269, pp. 325–330, 1995.
- [45] T.K. Bergersen, J. Hisdal, and L. Walloe, “Perfusion of the human finger during cold-induced vasodilation,” *Am J Physiol Regulatory Integrative Comp Physiol*, vol. 276, pp. 731–737, 1999.
- [46] F. Holmlund, C. Freccero, S. Bornmyr, J. Castenfors, A.M. Johansson, J. Nordquist, G. Sundkvist, H. Svensson, and P. Wollmer, “Sympathetic skin vasoconstriction—further evaluation using laser doppler techniques,” *Clinical Physiology*, vol. 21, no. 3, pp. 287–291, 2001.
- [47] T.K. Bergersen, M. Eriksen, and L. Walloe, “Local constriction of arteriovenous

- anastomoses in the cooled finger,” *American Journal of Physiology*, vol. 273, no. 3, pp. 880–886, 1997.
- [48] A. Kurz, D.I. Sessler, R. Christensen, D. Clough, O. Plattner, and J. Xiong, “Thermoregulatory vasoconstriction and perianesthetic heat transfer,” *Acta Anaesthesiol Scand Suppl.*, vol. 109, pp. 30–33, 1996.
- [49] D. Richardson, H. Qing-Fu, and S. Shepherd, “Effects of invariant sympathetic activity on cutaneous circulatory responses to heat stress,” *American Physiological Society*, pp. 521–529, 1991.
- [50] J.R.S. Hales, C. Jessen, A.A. Fawcett, and R.B. King, “Skin area and capillary dilatation and constriction induced by local skin heating,” *Pflügers Arch*, vol. 404, pp. 203–207, 1985.
- [51] J. R. S. Hales, M. Iriki, K. Tsuchiya, and E. Kozawa, “Thermally-induced cutaneous sympathetic activity related to blood flow through capillaries and arteriovenous anastomoses,” *Pflügers Arch.*, vol. 375, pp. 17–24, 1978.
- [52] S. Weinbaum, L. M. Jiji, and D. E. Lemons, “Theory and experiment for the effect of vascular microstructure on surface tissue heat transfer - part i: Anatomical foundation and model conceptualization,” *Journal of Biomechanical Engineering*, vol. 106, pp. 321–330, November 1984.
- [53] M. Ursino, A. Colantuoni, and S. Bertuglia, “Vasomotion and blood flow regulation in hamster skeletal muscle microcirculation: A theoretical and experimental study,” *Microvascular Research*, vol. 56, pp. 233–252, 1998.
- [54] A.L. Krogstad, M. Elam, T. Karlsson, and B.G. Wallin, “Arteriovenous anastomoses and the thermoregulatory shift between cutaneous vasoconstrictor and

- vasodilator reflexes,” *Journal of the Autonomic Nervous System*, vol. 53, pp. 215–222, 1995.
- [55] H. V. Sparks, *Peripheral Circulation*, pp. 193–230, John Wiley & Sons, New York, NY, 1978.
- [56] E.R. Raman, M.F. Roberts, and V.J. Vanhuyse, “Body temperature control of rat tail blood flow,” *Am J Physiol Regul Integr Comp Physiol*, vol. 245, pp. 426–432, 1983.
- [57] Y. Wang, K. Kimura, K. Inokuma, M. Saito, Y. Kontani, Y. Kobayashi, N. Mori, and H. Yamashita, “Potential contribution of vasoconstriction to suppression of heat loss and homeothermic regulation in ucp1-deficient mice,” *Pflügers Archiv, European Journal of Physiology*, vol. 452, no. 3, pp. 363–369, 2006.
- [58] T. Mundel, S.J. Bunn, P.L. Hooper, and D.A. Jones, “The effects of face cooling during hyperthermic exercise in man: evidence for an integrated thermal, neuroendocrine and behavioural response,” *Experimental Physiology*, vol. 92, no. 1, pp. 187–195, 2007.
- [59] A.M. Rivera-Brown, T.W. Rowland, F.A. Ramirez-Marrero, G. Santacana, and A. Vann, “Exercise tolerance in a hot and humid climate in heat-acclimatized girls and women,” *International Journal of Sports Medicine*, vol. 27, no. 12, pp. 943–950, 2006.
- [60] X. Zhang and D. Wang, “Energy metabolism, thermogenesis and body mass regulation in brandt’s voles (*lasiodromys brandtii*) during cold acclimation and rewarming,” *Hormones & Behavior*, vol. 50, no. 1, pp. 61–69, 2006.
- [61] J.M. Hynson, D.I. Sessler, A. Moayeri, and J. McGuire, “Absence of nonshivering



- thermogenesis in anesthetized adult humans,” *Anesthesiology*, vol. 79, no. 4, pp. 695–703, 1993.
- [62] T. Matsukawa, D.I. Sessler, R. Christensen, M. Ozaki, and M. Schroeder, “Heat flow and distribution during epidural anesthesia,” *Anesthesiology*, vol. 83, no. 5, pp. 961–967, 1995.
- [63] J.W. Baish, “Formulation of a statistical model of heat transfer in a perfused tissue,” *Journal of Biomechanical Engineering*, vol. 116, pp. 521–527, 1994.
- [64] R.P. Clark and O.G. Edholm, *Man and His Thermal Environment*, Edward Arnold, London, UK, 1985.
- [65] Y. Shoji, T. Takemori, H. Matsunami, and T. Nakajima, “Three-dimensional, clothed human thermal model,” *Scripta Technica Inc*, vol. 26, no. 8, pp. 554–566, 1997.
- [66] T.K. Bergersen, M. Eriksen, and L. Walloe, “Relative contribution of core and cutaneous temperatures to thermal comfort and autonomic responses in humans,” *J Appl Physiol*, vol. 86, no. 5, pp. 1588–1593, 1999.
- [67] D.A. Nelson, A.R. Curran, E.A. Martilla, S. Charbonnel, and D. Fiala, “Thermoregulation in humans: results from an anatomically-based, high resolution voxelized model,” in *2007 Summer Bioengineering Conference*, Keystone, CO, 2007, ASME.
- [68] J.A.J. Stolwijk, “A mathematical model of physiological temperature regulation in man,” in *NTIS N71-33401*, Washington, DC, 1971, NASA.
- [69] R.J. Spiegel and M.B.E. Fatmi, “A three-dimensional finite difference thermoregulatory model of a squirrel monkey,” *Int. J. Radiation Oncology Biol. Phys*, vol.

- 12, pp. 983–992, 1986.
- [70] G.A Brooks, T.D. Fahey, T.P White, and K.M. Baldwin, *Exercise physiology: Human bioenergetics and its applications*, Mayfield Publishing Company, 2000.
- [71] J.A.J. Stolwijk, “Expansion of a mathematical model of thermoregulation to include high metabolic rates,” in *NTIS NTD-19831*, Washington, DC, 1969, NASA.
- [72] H.H. Pennes, “Analysis of tissue and arterial blood temperatures in the resting human forearm,” *J Appl Phys*, vol. 1, no. 2, pp. 93–122, 1948.
- [73] J. Stolwijk, “Mathematical models of thermal regulation,” *Annals of the New York Academy of Sciences*, vol. 335, pp. 98–106, 1980.
- [74] W. Wulff, “The energy conservation equation for living tissue,” *IEEE Transactions on Biomedical Engineering*, vol. 21, pp. 494 – 495, 1974.
- [75] W. Wulff, “Alternatives to the bio-heat transfer equation,” *The New York Academy of Science*, vol. 335, pp. 151–154, 1980.
- [76] S. Weinbaum and L. M. Jiji, “A new simplified bioheat equation for the effect of blood flow on local average tissue temperature,” *Journal of Biomechanical Engineering*, vol. 107, pp. 131–139, May 1985.
- [77] C. Charny, S. Weinbaum, and R. Levin, “An evaluation of the Weinbaum-Jiji bioheat transfer model for simulations of hyperthermia,” *Advances in Heat and Mass Transfer in Biotechnology-ASME*, pp. 1–10, 1999.
- [78] S. Weinbaum, L. Xu, and L. Zhu, “A new fundamental equation for muscle tissue: Part I blood perfusion term,” *Journal of Biomechanical Engineering*, vol. 19, pp. 278–288, 1997.

- [79] H. Arkin, L.X. Xu, and K.R. Holmes, “Recent developments in modeling heat transfer in blood perfused tissues,” *IEEE Transactions on Biomedical Engineering*, vol. 41, no. 2, pp. 97–107, 1994.
- [80] G. Neuweiler, *The Biology of Bats*, Oxford University Press, Oxford, UK, 2000.
- [81] D.J. Schmidly, *The Bats of Texas*, Texas A&M University Press, College Station, TX, 2000.
- [82] J.N. Maina, “What it takes to fly: The structural and functional respiratory refinements in birds and bats,” *The Journal of Experimental Biology*, vol. 203, pp. 3045–3064, 2000.
- [83] F.C. Kallen, “The active venous pulse in the wing circulation of bats (*chiroptera*). overview of circulation in the wing membrane.,” *Experientia.*, vol. 34, no. 11, pp. 1398–1400, 1978.
- [84] I.I.H. Chen, B.P. Fleming, and R.L. Prewitt, “A mathematical representation of the microvascular network in the bat’s wing,” *Microcirculation, Endothelium, and Lymphatics*, vol. 1, pp. 57–70, 1984.
- [85] S. Assous, A. Humeau, and J.P. L’huillier, “Empirical mode decomposition applied to laser doppler flowmetry signals: diagnosis approach,” in *27th Annual International Conference of the IEEE Engineering in Medicine and Biology Society*. 2005, IEEE Cat. No.05CH37611C.
- [86] W. Binwei, M. Blanco-Velasco, and K.E. Earner, “Ecg denoising based on the empirical mode decomposition,” in *Annual International Conference of the IEEE Engineering in Medicine and Biology Society*. 2006, IEEE Cat. No.06CH37748.

- [87] A.O. Andrade, “Emg signal filtering based on empirical mode decomposition,” *Biomedical Signal Processing and Control*, vol. 1, no. 1, pp. 44–55, 2006.
- [88] J.R. Speakman, G.C. Hays, and P.I. Webb, “Is hyperthermia a constraint of the diurnal activity of bats?,” *J. Theor. Biol.*, vol. 171, pp. 325–341, 1994.
- [89] P.M. Cryan and B.O. Wolf, “Sex differences in the thermoregulation and evaporative water loss of a heterothermic bat, *Lasiurus cinereus*, during its spring migration,” *Journal of Experimental Biology*, vol. 206, pp. 3381–3390, 2003.
- [90] D. Fiala, K.J. Lomas, and M. Stohrer, “Computer prediction of human thermoregulatory and temperature responses to a wide range of environmental conditions,” *Int. J. Biometeorol.*, vol. 45, no. 3, pp. 143–159, 2001.
- [91] M.H. Tawhai and P.J. Hunter, “Modeling water vapor and heat transfer in the normal and the intubated airways,” *Ann. Biomed. Eng.*, vol. 32, no. 4, pp. 609–622, 2004.

## VITA

Name: Tanya Mendez

Permanent Address: 2416 Biola Ave San Diego, California 92154

E-mail: tmvision5@yahoo.com

Educational Background:

**B.S.**, Mechanical Engineering, University of California at Davis, 2005

**M.S.**, Mechanical Engineering, Texas A&M University, 2007